MODELLING THE HOLOCENE SEDIMENT BUDGET OF THE RHINE SYSTEM

DISSERTATION

zur
Erlangung des Doktorgrades (Dr. rer. nat.)
der
Mathematisch-Naturwissenschaftlichen Fakultät
der
Rheinischen Friedrich-Wilhelms-Universität Bonn

vorgelegt von

THOMAS HOFFMANN

aus
Witten a.d. Ruhr

Bonn 2006

Angefertigt mit Genehmigung der Mathematisch-Naturwissenschaftlichen
Fakultät der Rheinischen Friedrich-Wilhelms-Universität Bonn

1. Referent: Richard Dikau
2. Referent: Lothar Schrott

Tag der Promotion: 13. Februar 2007

Diese Dissertation ist auf dem Hochschulschriftenserver der ULB Bonn
http://hss.ulb.uni-bonn.de/diss_online elektronisch publiziert

Abstract

Rivers transport large amounts of water, sediments, nutrients and carbon from the continents to the oceans. Thus, they are important links within the global biogeochemical cycle. To understand biogeochemical fluxes in river channels, holistic system-based approaches are needed that consider river channels and their corresponding catchments. Sediment fluxes in fluvial systems change in consequence of changing external controls (land use and climate). However, the system's response to land use and climate change varies depending on internal controls (e.g. catchment size and structure). While forcing-response mechanisms of small catchments are reasonably well understood, the response of larger drainage basins is less clear. In particular, the impact of land use and climate change on the Rhine system is poorly known owing to the catchment size (185 000 km^2) and the long history of human cultivation, which started approx. 7500 years ago.

A sediment budget is calculated to specify the amount of alluvial sediment and total organic carbon that deposited during the Holocene and to estimate long term soil erosion rates. The focus was driven to floodplains because they act as important sinks in terms of sediment and carbon flux and therefore, provide a range of potential sites of palaeoecological data. To obtain information on the temporal development of the Rhine system, a database of ^{14}C-ages taken from colluvial and alluvial deposits was compiled and analysed in terms of i) cumulative frequency distributions of the ages and ii) changing sedimentation rates on floodplains and in palaeochannels.

The results of the sediment budget suggest that $59 \pm 14 \times 10^9$ t of Holocene alluvial sediment is stored in the non-alpine part of the Rhine catchment (South and Central Germany, Eastern France, The Netherlands). About 50 % of Holocene alluvial sediment is deposited along the trunk valley and the delta (Upper Rhine, Lower Rhine, coastal plain), while the rest is stored along the tributary valleys. The floodplain sediment storage corresponds to a mean erosion rate of 0.55 ± 0.16 t $ha^{-1}year^{-1}$ (38.5 ± 10.7 mm kyr^{-1}) across the Rhine catchment outside the Alps. This Holocene-averaged estimate amounts for sediments that were delivered to the channel network and is at

the lower limit of erosion rates from other studies of different methodology.

The statistical analysis of 1948 organic carbon measurements in different parts of the Rhine catchment suggest a strong influence of the sedimentary facies on the organic carbon content. The analysis allowed the development of a conceptual carbon budget model of fluvial systems, which was coupled with the alluvial sediment storage, to estimate the Holocene sequestration rates of carbon storage in floodplains. Averaged over the Rhine catchment the sedimentary carbon sequestration ranges between 3.4 to 25.4 g m^{-2} $year^{-1}$ with more reasonable values between 5.3 to 17.7 g m^{-2} $year^{-1}$. Compared to the recent particulate carbon export, these values are in the same order of magnitude but somewhat smaller indicating that approximately the same amount of the exported carbon may be stored in floodplains. However, compared to sedimentary carbon sequestration rates obtained elsewhere, the presented values are at the lower limit, corresponding to the lower mean Holocene soil erosion and floodplain accumulation rates.

Based on the cumulative frequency distributions of the ^{14}C-ages eight periods of geomorphic activity are identified (peaking at 8.2 kyr, 7.54 kyr, 5.6 kyr, 4.2 kyr, 3.3 kyr, 2.8 kyr, 2.3 kyr and since 1075 years BP). These periods were compared with climatic, palaeohydrological and human impact proxy data. Until 4200 years BP, events of geomorphic activity are mainly coupled to wetter and/or cooler climatic phases. Between 3300 and 2770 years BP, the increased geomorphic activity cannot unequivocally be related to climate. The growing population and the intensification of agricultural activities must be considered as an additional control during the Bronze age. Since 1075 years BP the growing population density is considered as the major external forcing. Additionally, it could be shown that the newly developed approach has major advantages compared to the approach used to analyse the ^{14}C-database of Great Britain, Spain and Poland.

Concerning the changing sedimentation rates on floodplains and in palaeochannels, three phases were identified, during the last 14 000 years: i) the Late Glacial-Holocene with medium sedimentation rates, ii) the Holocene Climatic Optimum with slightly decreasing rates and iii) the last 4000 years, which are characterised by increasing sedimentation rates. The results are in good correspondence with a conceptual model of the Holocene floodplain development in Europe.

Until now, the spatially distributed sediment and carbon budgets and the temporal analysis of the ^{14}C-database are analysed based on linear relationships of causes and effects. However, to understand the nonlinear response of the Rhine system to changes of land use and climate impacts during the Holocene, it is necessary to couple the temporal and spatial approaches that were developed in this thesis.

Vorwort

Die vorliegenden Dissertation entstand im Rahmen des Projektes "Modellierung des holozänen Sedimenthaushalts fluvialer Systeme", welches Teil des DFG-Projektbündels "Mensch-Umwelt-Einflüsse auf das fluviale System des Rheins seit Beginn der landwirtschaftlichen Nutzung (RheinLUCIFS)" war. Das RheinLUCIFS Bündel bot einen wunderbaren interdisziplinären Rahmen, in dem lebhaft die Fragestellungen der Geomorphologie, Archäologie, Paläobotanik und historischen Geographie mit den Kollegen des Bündels diskutiert werden konnten. Ich möchte allen Teilnehmern des Bündels danken, die zum Gelingen der Arbeit in diesem Bündel beigetragen haben.

Allen voran möchte ich mich bei Prof. Richard Dikau für die Finanzierung, die vielseitige Betreuung und sein Interesse bedanken. Erst durch Ihn und sein Vertrauen in meine Arbeit wurde diese Dissertation ermöglicht. Die lebhaften und offenen Diskussionen zur Thematik des fluvialen Sedimenttransportes und der Komplexität und Nicht-Linearität geomorphologischer Systeme waren wichtige Inspirationsquellen meiner Arbeit.

Meinen Kollegen der Arbeitsguppe Dikau möchte ich für den guten Zusammenhalt und den offenen Umgang innerhalb der Gruppe danken. Ihre Hilfsbereitschaft und die vielen kreativen Diskussionen zur Thematik und anderen Dingen des Lebens und der Wissenschaft haben meine Motivation zur Arbeit stets positiv beeinflußt. Jan, Frank, Michael + Michael und Rainer ihr seid super Jungs!!!!! Meinen Helferinnen Manuela Schlummer und Julia Gerz danke ich für ihr unendliches Leidenspotential, die fehlende Langeweile ;-) und das Ertragen der vielen, oft monotonen Arbeiten. Ich weiß gar nicht, was ich ohne Euch hätte machen sollen.

Für die Datenbereitstellung, vielseitigen Hilfestellungen und Einblicke in den Umgang mit ^{14}C-Datierungen, Kohlenstoff-Analysen und archäologischen Daten danke ich Andreas Lang (Liverpool), Peter Houben und Jürgen Wunderlich (beide Uni Frankfurt), Stefan Glatzel (Uni Rostock), Jochen Seidel (Uni Freiburg) sowie Andreas Zimmermann und Karl Peter Wendt (beide Uni Köln).

Meinen niederländischen Kollegen, Gilles Erkens, Kim Cohen, freaky Freek Buschers und Hans Middelkoop (Uni Utrecht) danke ich für die kreativen Diskussionen und die unkonventionellen Gedanken zur holozänen Sedimentbilanzierung. Ich hoffe, dass noch ganz viel Wasser den Rhein herunter fliesen wird und die begonnen Kooperationen nicht versiegen lässt.

Erik Sprokkereef (International Commission fort he Hydrology of the Rhine basin, CHR/KHR) stellte dankenswerterweise Daten aus dem Rheineinzugsgebiet zur Verfügung.

Last but not least, danke ich Mr. Andrews (alias Herr Mister) für die Durchsicht des Manuskripts und der Nachsicht mit meinem englischen Schreibstil.

Bonn im Dezember 2006
Thomas Hoffmann

Contents

1 Introduction **1**

2 Scientific framework **7**
2.1 Fluvial Systems 9
2.1.1 The Hillslope System 10
2.1.2 Sediment transport in river channels 12
2.1.3 Floodplains 15
2.1.4 Importance of carbon flux in fluvial systems 19
2.2 Holocene environmental change 21
2.2.1 Climate change 21
2.2.2 Human Impact 24
2.3 Fluvial response 28
2.3.1 Climate impacts on fluvial systems 28
2.3.2 Human impact on fluvial systems 32
2.3.3 The internal configurational state 35
2.3.4 Relative importance of land use and climate impact . . 44

3 Study site: Rhine catchment **47**
3.1 General geographical setting 49
3.2 Geological and geomorphological setting 49
3.3 Climate, hydrology and modern sediment flux 51
3.4 Human Impact 55
3.5 Holocene valley development 57
3.6 Human impact on sediment fluxes 59

4 Concept and methods **61**
4.1 Problems, needs and aims 63
4.2 Holocene fluvial sediment budget 67
4.2.1 Estimation of Holocene floodplain volumes 67
4.2.2 Calculation of hinterland volume 68
4.2.3 Calculation of the delta volume 71

4.2.4 Erosion rate calculations . . . 73
4.3 Holocene fluvial *TOC* budget . . . 75
4.3.1 Data analysis . . . 75
4.3.2 Conceptual carbon budget model . . . 78
4.4 ^{14}C-database analysis . . . 80
4.4.1 Cumulative frequency distributions . . . 81
4.4.2 Sedimentation rates . . . 85

5 Results 87
5.1 Holocene fluvial sediment budget . . . 89
5.1.1 Alluvial sediment storage . . . 89
5.1.2 Holocene erosion rates . . . 91
5.2 *TOC* storage in floodplains . . . 93
5.2.1 Sample depth and clay content . . . 93
5.2.2 Depositional environment and sedimentary facies . . . 93
5.3 Holocene alluvial *TOC* budget . . . 101
5.3.1 *TOC* flux related to channel bed erosion and deposition 101
5.3.2 *TOC* storage related to overbank deposition . . . 102
5.4 ^{14}C-database analysis . . . 104
5.4.1 Cumulative frequency distributions . . . 104
5.4.2 Sedimentation rates . . . 108

6 Discussion 111
6.1 Holocene fluvial sediment budget . . . 113
6.1.1 Quantification of sediment storage . . . 113
6.1.2 Quantification of mean Holocene erosion rate . . . 114
6.1.3 Comparison of the erosion rate with other studies . . . 116
6.2 Holocene alluvial carbon budget . . . 118
6.2.1 Limitations and uncertainties . . . 118
6.2.2 Significance and perspective . . . 119
6.3 ^{14}C-database analysis . . . 120
6.3.1 Cumulative frequency distributions . . . 120
6.3.2 Sedimentation rates . . . 125

7 Conclusion and Perspectives 129
7.1 Holocene fluvial sediment budget . . . 131
7.2 Holocene alluvial *TOC* budget . . . 131
7.3 ^{14}C-database analysis . . . 132
7.4 Concluding summary and perspectives . . . 132

List of Figures

1.1 Greenhouse gas concentrations during the last 400 ka BP. . . . 2
1.2 Coupling sediment budgets and geoarchives. 3

2.1 Zones of erosion, transportation and deposition within the fluvial system. 9
2.2 Simplified sediment budget of fluvial systems. 10
2.3 Hysteresis in sediment concentration curves. 13
2.4 Floodplain landorms associated with meandering rivers 16
2.5 Channel patterns, taken from Berendsen & Stouthamer (2001). 17
2.6 Quaternary temperature variability at different time scales . . 22
2.7 Holocene temperature variability 24
2.8 Chronology of cultural periods in various regions of Europe . . 25
2.9 Population growth during the last 14 000 years in Central Europe 26
2.10 Upstream, local and downstream controls of fluvial response . 29
2.11 Spatial and temporal scales of forms and components of fluvial systems 29
2.12 Phases of increased deposition during the Holocene 31
2.13 Floodplain sedimentation rates of the Mississippi and Yellow River 36
2.14 Simplified representation of unbalanced response of fluvial systems 37
2.15 Influence of drainage basin area on the relative magnitude (S_{max}/S_{min}) of change in response to human impact 38
2.16 Conceptual model of external impact and scaled dependent response of fluvial system. 40
2.17 Spatial scaling of landscape connectivity in fluvial systems . . 41
2.18 Scale linkages in the hierarchy of catchments 43
2.19 Soil erosion and land use in Central Europe during the last 1400 years 45

3.1 The Rhine catchment and its main tributaries 50

3.2 Long profile of the River Rhine 52
3.3 Mean annual precipitation in the Rhine catchment 53
3.4 Seasonal variation of daily discharge at different gauging stations 54
3.5 Rectification of the Upper Rhine valley near Breisach 56
3.6 Valley bottom architecture in Central Europe 58
3.7 Conceptual model of hillslope-channel coupling during the period of agriculture in Central Europe 60

4.1 The component of historical explanation required to explain geomorphological systems 65
4.2 Simplified flowchart of the RheinLUCIFS concept 65
4.3 Schematic representation of the applied sediment budget approach 68
4.4 Flowchart for calculations yielding the Holocene floodplain fines volume of the Hinterland 69
4.5 Floodplain width (w) vs. upstream catchment area (A_d) . . . 70
4.6 Catchment-wide Holocene thickness of floodplain fines 72
4.7 Shaded relief map of Germany with TOC sampling locations indicated. 76
4.8 C-cycle with focus on the sediment transfer in fluvial systems 79
4.9 Shaded relief map of Germany with ^{14}C sampling locations indicated 82
4.10 Example of ^{14}C-calibration 84

5.1 TOC content versus depth. 95
5.2 Clay content versus TOC content. 96
5.3 TOC versus depositional environment. 98
5.4 TOC versus sedimentary facies 98
5.5 Comparison of TOC content of sedimentary facies 99
5.6 CPF of activity, stability and transitional ages 105
5.7 Phases of increased activity and stability. 106
5.8 Sensitivity analysis of activity and stability CPFs 107
5.9 Sedimentation rates of floodplains and palaeochannels 109

6.1 Size of Holocene alluvial sediment storages vs. subcatchment area 114
6.2 Comparison of estimates of long-term erosion rates. 117
6.3 Activity and stability CPFs plotted alongside independent palaeohydrological indicators and population data 121
6.4 Comparing CPF of equally distributed ^{14}C-ages and reanalysed CPDFs of 'change dates' from Europe 124

List of Tables

2.1 Six chronological phases of river use and the management methods 33

3.1 Areas of the Rhine catchment shared by different states and of major tributaries 51

4.1 Studied region, number of TOC measurements and drill locations and used TOC estimation method of analysed publications. 75
4.2 English and German names and abbreviations of sedimentary facies used for the classification of TOC measurements. 77
4.3 Number of ^{14}C data taken from different depositional environments and sedimentary facies 83

5.1 Holocene alluvial sediment storage within the Rhine catchment and its tributaries 90
5.2 Total Holocene alluvial sediment storage for different time scenarios. 91
5.3 Quantification of erosion and erosion rates based of different scenarios for the input parameters. 92
5.4 Number of TOC measurements taken from different publications and sedimentary facies 94
5.5 Results of Kruskal-Wallis test of TOC in different sedimentary facies and depositional environments 97
5.6 Comparison of TOC-means in different sedimentary facies . . 100
5.7 Wilcox test on NT and CBS facies 103
5.8 TOC budget of the Rhine catchment based on floodplain deposition 103

Abbreviations

AD	Anno Domini
BP	Before Present (reference year = 1950 AD)
C	Carbon
CND	Complex Nonlinear Dynamics
CPDF	Cumulative Probability Difference Function
CPF	Cumulative Probability Function
CSDR	Channel Sediment Delivery Ratio
DEM	Digital Elevation Model
DFG	Deutsche Forschungs Gesellschaft
ER	Erosion Rate
GIS	Geographical Information System
GK	Geological Map
GK25	Geological Map (mapscale 1:25 000)
GK200	Geological Map (mapscale 1:200 000)
HSDR	Hillslope Sediment Delivery Ratio
IGBP	International Global Geosphere-Biosphere Programme
IRD	Ice Rafted Debris
kyr BP	years Before Present (in thousand years)
LUCIFS	Land Use and Climate Impacts on Fluvial Systems during the period of agriculture
PAGES	Past Global changES
SDR	Sediment Delivery Ratio
SRTM	Shuttle Radar Topography Mission
SR	Sedimentation Rate
SY	Sediment Yield
SSY	Specific Sediment Yield
TOC	Total Organic Carbon

Chapter 1

Introduction

Rivers are major transport agents of water, sediments, nutrients and carbon (Hay, 1998; Meybeck *et al.*, 2003; Meybeck, 2003; Milliman & Syvistki, 1992; Syvitski, 2003). Many landscapes are predominantly formed by running water in rivers. The holistic explanation of landform evolution must therefore involve a description of fluvial systems as an important component of the geomorphological system. Besides their geomorphological significance, rivers perform many essential functions in societal and ecosystem terms, including water consumption, energy production, agricultural, navigational and, industrial uses. Rivers have always played an important role in human affairs. Due to the availability of water and their function as transport agent, all of the early great civilizations arose on the banks of large rivers. Thus rivers are important links within the global biogeochemical cycle (Slaymaker & Spencer, 1998).

During the last 7500 years, human impact has profoundly altered the natural functioning of rivers. While natural Earth system drivers, such as lithology, relief, climate and vegetation had a major impact on Earth's rivers before the Holocene, it is now believed that anthropogenic forcing is the dominant agent of environmental change (Meybeck, 2003). However, the increasing human pressure is not limited to fluvial systems but can be attributed to the Earth's environment as a whole, causing Crutzen & Stroemer (2000) to call the time during which human activities have altered the greenhouse gas concentration in the atmosphere (last 200 years) the "Anthropocene". As shown in Fig. 1.1 the Anthropocene is marked by an extreme rise in mean annual Northern Hemisphere temperature and by greenhouse gas levels well outside the range of at least the last 400 000 years (Oldfield & Alverson, 2003).

Due to the increasing population density, land use pressure and climate change the vulnerability of societies and economies to extreme events and

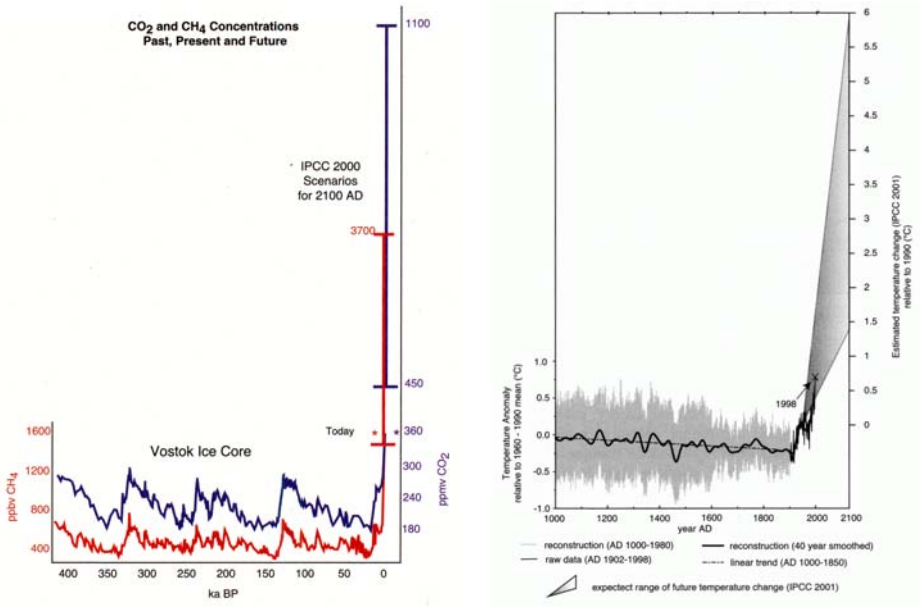

Figure 1.1: Left: Greenhouse gas concentrations measured at the the Vostok Ice Core and extrapolated to present day compared with the IPCC scenarios for the year 2001. Right: Multiproxy reconstruction of mean annual Northern Hemisphere temperature and extrapolated ranges of the IPCC 2001 report. Both Figures taken from Oldfield & Alverson (2003).

natural variability increases (Messerli *et al.*, 2000). The human quest for security and stability in the direct neighbourhood of rivers is only possible if we are able to manage river systems in a sustainable way. The sustainable management of rivers systems, however, requires the understanding of river behaviour and the prediction of river-borne fluxes in a changing environment and therefore the links between environmental changes and fluvial processes (Wasson, 1996; Slaymaker & Spencer, 1998; Walling & Fang, 2003; Meybeck *et al.*, 2003). Due to the fact that environmental change takes place at a variety of temporal scales (Chapters 2.2 and 2.3), future developments can only be predicted if the past and present status of the Earth system is known. Therefore, to predict future changes of fluvial systems it is necessary to understand the present and past status concerning the sediment production and transfer as well as of the formation and degradation of corresponding landforms (e.g. gullies and colluvial and alluvial landforms).

In this context the scaled dependent interaction between "*Land Use and Climate Impacts on Fluvial Systems during the period of agriculture*" (LU-

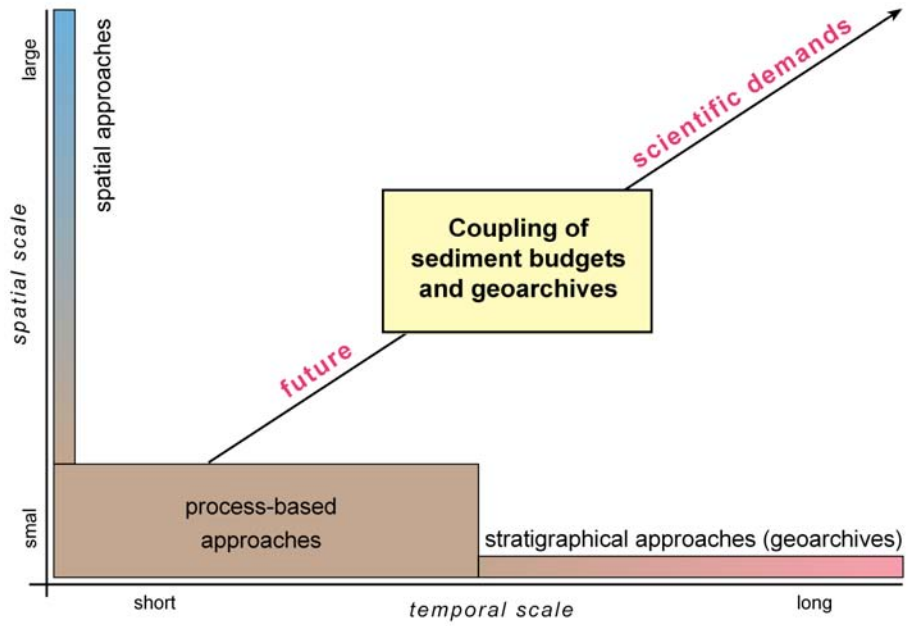

Figure 1.2: Todays domains of spatial, stratigraphical and process-based approaches and future demands to couple large spatial scale with long temporal scales using sediment budgets, modified after Dikau (2006) based on Kirkby (1999a).

CIFS) is of major importance (Wasson, 1996; Lang *et al.*, 2003; Dikau *et al.*, 2005). The LUCIFS activity, which is part of the IGBP-PAGES Focus 5, focuses on the water and particulate fluxes through fluvial systems. However, sustainability of river systems as part of the global ecosystem requires a holistic, conservationist long term perspective, which is best achieved by studying biogeochemical cycles of fluvial systems (Slaymaker & Spencer, 1998). As simple source (hillslope) to sink (oceans, lakes) relations are complicated by deposition of sediment, nutrients and contaminants at intervening locations, a critical component in biogeochemical cycles is the magnitude and residence time of deposition. Therefore, considering biogeochemical cycles, the most important contribution of geomorphologists is the modelling of holistic sediment budgets with a strong focus on time dependent sediment storage at different spatial scales. However, the understanding of sediment storage is limited due to sampling problems and the increasing complexity of geomorphological systems at long temporal scales ($>$ 50 years) and in large catchments ($>$ 1000 km^2).

It is stated that holistic sediment budget models coupled with the strati-

graphical record preserved in geoarchives provide an important approach to fill the gap of studies at large spatial and long temporal scales (Fig. 1.2). Additionally, long term perspectives are of major importance to solve the problems of river restoration projects, which are generally based on inadequate data on natural systems suggesting the need to investigate the "natural" status of fluvial system by palaeohydrological and palaeoecological approaches (Brown, 2002).

In the case of the RheinLUCIFS project, which focuses on the Rhine catchment with a 7500 year long history of human impact, sedimentary geoarchives are used as proxies of sediment flux within fluvial systems (Houben *et al.*, 2006; Lang *et al.*, 2003). Therefore, the RheinLUCIFS objectives are the reconstruction of i) scale-dependent dynamic sediment budget models and ii) the external controls (e.g. climate, population, land use and vegetation) (Fig. 4.2). Based on these independent chronologies of external controls and fluvial response, a better understanding of the scale dependent nonlinear response of fluvial systems will be achieved.

The thesis "**Modelling the Holocene Sediment Budgets of the Rhine System**" is part of the RheinLUCIFS project bundle, which was founded by the German Research Foundation (DFG). Despite the substantial numbers of detail geomorphological studies at small scales, attempts to estimate sediment fluxes (and storage) at large spatial scales are rare (Walling *et al.*, 1998). Therefore, the thesis focuses on the modelling of the Holocene alluvial sediment and associated carbon storage in large catchments.

Due to the large spatial scale of the Rhine catchment it was not possible to gather new data. However, it is stated that scale-related sediment budget models can be developed based on the numerous available data in the Rhine catchment. In fact, a main objective of this thesis is to draw conclusions and integrate data from the multitude of local geomorphological studies and to use suitably simplified budget models at the Rhine catchment scale. In terms of a top down approach that is applied in the RheinLUCIFS activity (Houben *et al.*, 2006), the results obtained at large spatial and long temporal scales fix the boundary conditions for more detailed studies in space and time. The thesis therefore follows the statement of Kirkby (1999b, p. 514):

> *The present trend in fluvial geomorphology is towards increasingly detailed understanding of smaller and smaller features more and more about less and less. The variety of fluvial forms ... illustrates the very limited way in which detailed fluvial research has been able to contribute to a broad understanding of rivers and channelways. It is time to draw conclusions from all that has been learned in the past 50 years, and apply them, in a suitably sim-*

plified way and at relevant scales, to entire fluvial systems, and to studying how such systems have evolved over time.

Therefore the main objectives of the thesis are:

- Developing new approaches to model large scale and long term sediment budgets based on published data and evaluating the implications for large scale modelling.
- Modelling of a time averaged Holocene sediment budget of the non alpine Rhine catchment below Lake Constance (size of the Rhine catchment below Lake Constance = 125 000 km^2).
- Modelling of a long term fluvial carbon budget based on the Holocene sediment budget to evaluate the impact of sediment storage on floodplains on the global carbon cycle.
- Compiling a database on published ^{14}C ages from fluvial and colluvial systems i) to reconstruct phases of increased activity and stability of geomorphological systems in Germany during the last 12 000 years and ii) to calculate time dependent rates of floodplain deposition.

Chapter 2

Scientific framework

2.1 Fluvial Systems

Rivers are the main constituents of fluvial systems. They provide the routeways that carry excess precipitation and sediments from the continents to the oceans. However, rivers are not closed systems that can be understood by looking only at the river channel itself. In fact, the term "fluvial system" is used to describe sediment flux in a broader, more holistic context that takes into account the multitude of processes and landforms that control river behaviour and transport.

Concerning the sediment flux, fluvial systems consist of 3 zones (Fig. 2.1) that are i) the production zone (drainage basin), ii) the transportation zone and iii) the zone of deposition (Schumm, 1977). Based on these zones the control variables that regulate the sediment flux within the river can be divided into upstream controls (history, tectonics, lithology, climate and humans) of the production zone, the local controls (e.g. channel bed substrate, valley morphology, channel bank vegetation) of the transportation zone and the downstream controls (e.g. baselevel) of the depositional zone (Fig. 2.10). Changes in any of these control variables will result in a characteristic response of the fluvial system, which depends on the one hand on the type of change and on the other hand on the configurational state of the system itself (see. Chapter 2.3).

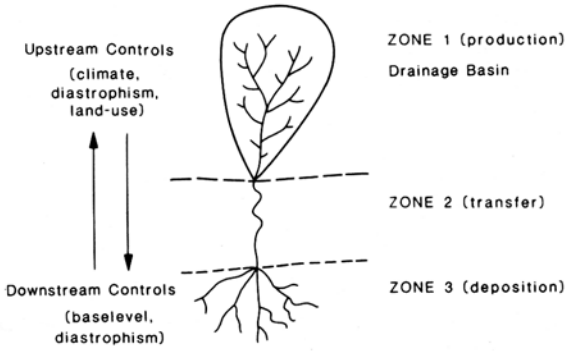

Figure 2.1: Zones of erosion, transportation and deposition within the fluvial system, taken from Schumm (1977).

The simplified representation of fluvial systems based on Schumm (1977) does not take into account the spatial variation of sediment erosion, transportation and deposition. Sediment deposition, for example, is not only limited to the deposition zone at the river delta but occurs along the entire course of the river. To account for the spatial heterogeneity of sediment erosion, transport and deposition the fluvial system is best described in terms of

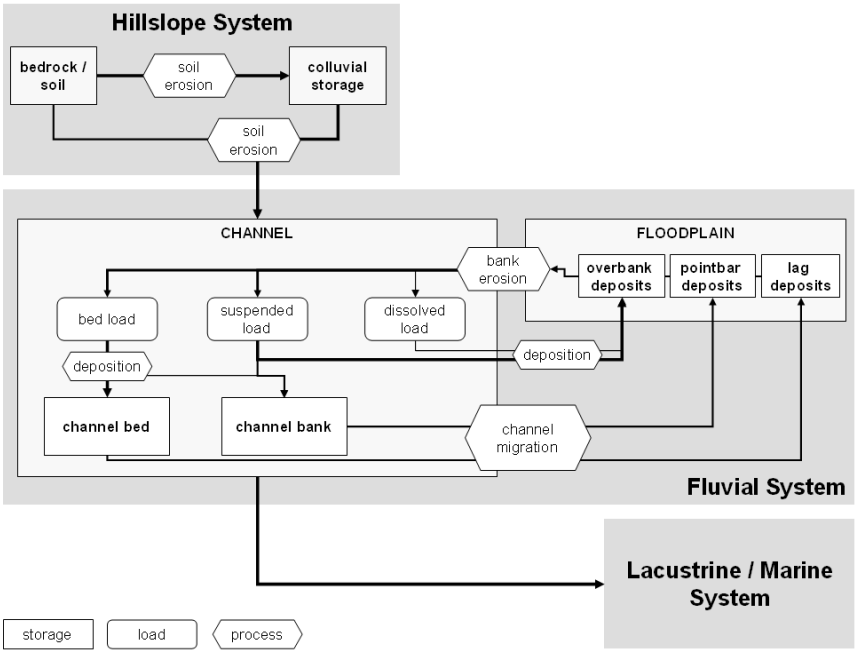

Figure 2.2: Simplified sediment budget of fluvial systems.

a fluvial sediment budget model (Fig. 2.2). The largest amounts of sediment are delivered to the fluvial system from the hillslopes and are yielded to lacustrine and marine systems. In terms of Chorley & Kennedy (1971), fluvial systems are therefore open dissipative systems that build a sediment cascade with the hillslope- and lacustrine-/marine system. The fluvial system itself consists of the channel, with its channel bed and banks, and the floodplain. Sediment is transported and exchanged between these components via different processes that act at different temporal and spatial scales. In the following, the form and process components will be explained in more detail to characterise the fluvial system. However, it is beyond the scope of this thesis to describe the fluvial system in full detail. The description rather focuses on important facts about the sediment flux through the fluvial system.

2.1.1 The Hillslope System

Sediment from the hillslopes is provided by bedrock weathering and subsequent soil erosion. Soil erosion at the hillslope is strongly induced by agricultural activities, whereas climatic fluctuations only seem to be of secondary importance (Bork *et al.*, 1998; Lang, 2002; van Rompaey *et al.*, 2002). In

Central Europe the beginning of soil erosion correlates with the first agricultural activities of the Neolithic Revolution 7500 years BP (e.g. Evans, 1990; Favis-Mortlock *et al.*, 1997; Lang, 2002). The spatial and temporal variation of soil erosion rates varies between 0 and 458 t $ha^{-1}year^{-1}$ (with a median of 2.75 t $ha^{-1}year^{-1}$) is rather large as shown in a review of recent erosion rates in Germany (Auerswald & Dikau, 2006). This variation mainly results from the impacts of single rain storms that may have a great impact on short term measurement. In contrast, long-term mean Holocene erosion rates vary "only" between 1 and 10 t $ha^{-1}year^{-1}$ as shown in chapter 6.1.

The most important soil erosion processes are sheet (interrill), rill and gully erosion. The relative importance of sheet and gully erosion is predominantly a question of scale (Poesen *et al.*, 2003), with dominant sheet and rill erosion at small scales (rill domain) and gully erosion prevailing at larger scale (gully domain). Other factors controlling the soil erosion rate and the relative importance of the two process domains are i) soil type, ii) land use, iii) climate and weather and iv) topography. Data collected from different parts of the world suggest that gully erosion represent from a minimum of 10 % up to 94 % of the total sediment yield (Poesen *et al.*, 2003).

The eroded sediment may not be immediately yielded from the hillslopes to the channel but is stored as colluvial deposit on the slopes or at their foot (Lang & Honscheidt, 1999; Lang *et al.*, 2003; Rommens *et al.*, 2005). Colluvial storage may last several thousand years (depending on the land use induced soil erosion) and therefore influences the coupling between hillslope and channels on a long temporal scale. The degree of hillslope-channel coupling is typically expressed in terms of the sediment delivery ratio (SDR), which is the ratio between the mass or volume of sediment yielded from the hillslope to the channel and the sediment that was eroded[1]

$$SDR = \frac{\text{sediment yield}}{\text{sediment erosion}}. \tag{2.1}$$

Results from small hillslope catchments suggest that more than 60 % of sediment eroded is redeposited on the slope and did not reach the channel system (e.g. Houben *et al.*, 2006; Preston, 2001; Rommens *et al.*, 2005). At the event scale, even 97 % may be deposited at the hillslope (Slattery *et al.*, 2002). These findings, which suggest a limited hillslope-channel coupling, have strong implications for the history of channel systems. If sediment

[1]According to Asselman *et al.* (2003), the hillslope SDR ($HSDR$) as described above must be differentiated from the channel SDR ($CSDR$), which is the percentage of sediment that reached the outlet of a catchment and that entered the channel (for more details see chapter 4.2).

input from the hillslopes is low, rivers are insensitive to external factors that change sediment fluxes on hillslopes.

Important factors that control the *SDR* are the spatial and temporal scales. Generally, *SDR*s decrease with increasing catchment size, due to the increasing storage potential and the decreasing erosion of larger catchments. While short term *SDR*s may be close to zero, long-term *SDR*s must ultimately approximate unity, otherwise hillslopes would be progressively fill with sediments (Slattery *et al.*, 2002). Apart from the spatial and temporal scales, variations in *SDR*s can also be attributed to land use pattern, the type of soil erosion and the configurational state of the system. The varying degree of hillslope-channel coupling for catchments in Central Europe during the last 7500 years is explained by variations in land use patterns by Lang *et al.* (2003)(see also Chapter 3.6).

Different types of soil erosion result in different *SDRs*. Sediment eroded by sheet or rill erosion is transported only limited distances resulting in low *SDR*s (Houben *et al.*, 2006). In contrast, gullies are effective links between the upland hillslope and the permanent channel. Therefore, they increase the hillslope-channel connectivity and deliver a large fraction of eroded material to the channels (Poesen *et al.*, 2003). The systems configuration (e.g. hydraulic conductivity of soils, (micro-) topography, cultivation direction and transient boundaries), influences the flow paths and hence controls the travel distance and process types on the hillslope.

Due to the short transportation distance at the hillslope scale, there is a direct link between sediment erosion and colluvial deposition. In combination with the short *reaction time*, colluvial deposits are effective geoarchives to reconstruct land use and climate impacts on the hillslope system. However, due to the nonlinear relation between the external impact and the resulting erosion (Boardman & Favis-Mortlock, 1999), the magnitude of the external impact can not directly be inferred from the amount of colluvial storage.

2.1.2 Sediment transport in river channels

Once the sediment enters the river channel it is transported as bed load, suspended load and/or dissolved load. Due to the effective transport through river catchments, suspended and dissolved loads are of major importance, regarding the denudation of catchments. In contrast, bed load transport requires high transport energy because of its larger grain size, suggesting a limited impact on catchment denudation. However, bed load is an important factor controlling the adjustment of channel forms (Knighton, 1998).

The amount of suspended and dissolved load are strongly dependent on the weathering and erosion rate on the hillslopes, while the amount of bed

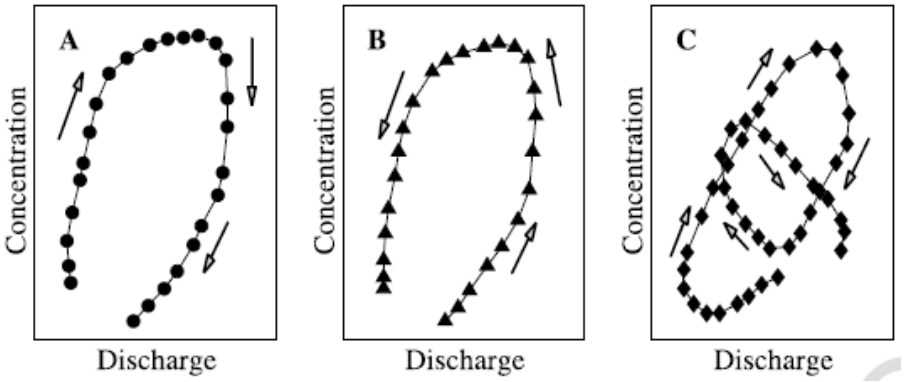

Figure 2.3: Hysteresis in sediment concentration curves. A) Clock-wise hysteresis, B) Counterclock-wise hysteresis and C) complexe type (Morehead *et al.*, 2003)

load is controlled mainly by the erosion of the channel and its stream power that influences the transport capacity of the river. In humid regions with strong human impact and increased soil erosion rates suspended sediment can account for more than 95 % of the solid sediments transported by the river. The relative proportion of bed load is greatest (approximately 25-35 %) in arid regions with extreme/sporadic precipitation and flood events and in mountain regions with high stream power and a majority of clastic sediments. Due to the major importance of the suspended sediment its transport within the channel will be discusses in more detail, while neglecting the dissolved and bed load[2].

In general, the suspended sediment load (in the following termed: sediment yield SY) is measured by the suspended sediment concentration C (typically given in mg l^{-1}) and the discharge Q [m^3 s^{-1}]:

$$SY = CQ \qquad [\text{t a}^{-1}]. \tag{2.2}$$

While discharge Q and therefore SY generally increases with catchment size (Milliman & Syvistki, 1992; Church *et al.*, 1999), the scaling behaviour of specific sediment yield SSY, which is defined by the sediment yield per catchment area, is more complex. This follows from its strong dependence on the suspended sediment concentration and therefore on the spatially variable sediment supply to the river. At a station there is an increase in sediment concentration with discharge, which is described commonly by a rating curve

[2]For more information on the factors controlling dissolved and bed load see for instance Leopold *et al.* (1964); Chorley *et al.* (1984); Knighton (1998); Bridge (2003)

in the form of a power function (Asselman, 2000; Morehead *et al.*, 2003):

$$C = aQ^b \qquad [\text{mg l}^{-1}] \tag{2.3}$$

where a is the rating coefficient and b the unitless rating exponent. However, the accuracy of the sediment rating curve is often very low and there is a large scatter, due to hysteresis effects (Fig. 2.3), changing river morphology in response to extreme events and changing land use and climate (Asselman, 2000; Morehead *et al.*, 2003). Hysteresis effects commonly result from changing conditions in sediment availability. At the event scale, for example, clockwise hysteresis results from the depletion of sediment with higher sediment concentrations at the rising limb of the flood than during the falling limb (Fig. 2.3a).

Sediment depletion occurs as well at the seasonal scale. Maximum sediment concentrations are commonly observed during the first flood of the runoff season, when fine sediments that are temporally deposited on the channel bed during the low flow season are available. Later in the hydrological year, sediments from more distant source-areas are transported during a flood, leading to a time lag between maximum discharge and maximum sediment concentration and therefore to counter-clockwise hysteresis of single floods (Asselman, 2000, Fig.2.3b). Thus, the timing of sediment supply from tributaries and hillslopes is a of major control of suspended sediment transport within the channel.

Due to the large variation of the sediment concentration at any given discharge, the concept of dominant discharge (Wolman & Miller, 1960) that tries to find a most effective discharge with maximum cumulative sediment transport needs to be critically discussed. Wolman & Miller (1960) stated that large floods may eventually transport large amount of sediments but recur too infrequently to have greater cumulative effect than smaller floods, which transport less sediment but occur more frequent. However, the availability of sediment that changes rapidly during single floods and during the hydrological years may control sediment transport much more than discharge and therefore limit the link between dominant discharge and maximum sediment transport.

At the catchment scale the link between discharge and sediment concentration (or specific sediment yield) is even more complex. For example, Milliman & Syvistki (1992) showed that the correlation between catchment size and SSY, is stronger than the correlation between discharge and SSY. Whether the suspended sediment concentration C or the SSY increases with catchment size or not depends on the relative increase of the sediment yield SY and discharge Q with catchment size. The general trend of decreasing

sediment concentrations and specific sediment yields (SSY), which follows from a smaller increase of SY compared to Q, is primarily explained by the increasing storage capacity of larger catchments (Milliman & Syvistki, 1992; Walling, 1983; Walling & Webb, 1996). To a large extent the increasing storage capacity may result from the construction of reservoirs that hold back almost all suspended sediments and alter the sediment flux of fluvial systems (Vörösmarty *et al.*, 2003; Walling & Fang, 2003). As shown by Dedkov (2004) the general trend of decreasing SSY is, however, only characteristic of intensively cultivated basins of the temperate belts, while catchments with limited cultivation within the Eurasian belt show increasing SSYs with catchment size. In addition to drainage area and human impact, relief (e.g. maximum elevation, mean catchment slope), tectonics, precipitation (rather variability than mean value), vegetation, temperature and time are important factors controlling the sediment flux in fluvial systems (Milliman & Syvistki, 1992; Hay, 1998; Harrison, 2000; Kirchner *et al.*, 2001; von Blanckenburg, 2005).

To summarize the above discussion, suspended load within the river channel is *supply-limited* and not *capacity-limited*, suspended sediment concentration is generally controlled by the sediment supply to the river and therefore by hillslope erosion rather than the transport capacity. The findings of Dedkov (2004) once more suggest the importance of the human impact and therefore human induced sediment supply to rivers. Measurements of the SY have formed the bases for most of the estimates of land degradation rates. However, the link between SY and land degradation is limited by sediment storage within the catchment, resulting in decreasing specific sediment yields and sediment delivery ratio SDR with catchment size (Walling, 1983).

2.1.3 Floodplains

A floodplain is that part of the landsurface in direct contact with the river that is or has been inundated by floods. Floodplains support particularly rich ecosystems and thus are important areas for human recreation, as habitats and corridor for wildlife. The high biodiversity of floodplain results from the dynamic fluvial processes that control the topography and grain size of the deposits and thus the hydrology, nutrient levels and finally the vegetation. However, due to their proximity to the river, floodplains are areas of major human impact, which has lead to increased flood-related risks. From a geomorphological point of view, floodplains are major sinks of suspended sediment (Walling *et al.*, 1996; Brown, 1996; Walling *et al.*, 1998), nutrients (Burt, 1996; Owens & Walling, 2003; van der Lee *et al.*, 2004), heavy metals (Taylor, 1996; Macklin *et al.*, 1997; Martin, 2000; Middelkoop *et al.*, 2002) and carbon (Walling *et al.*, 2006). In contrast to the channels in

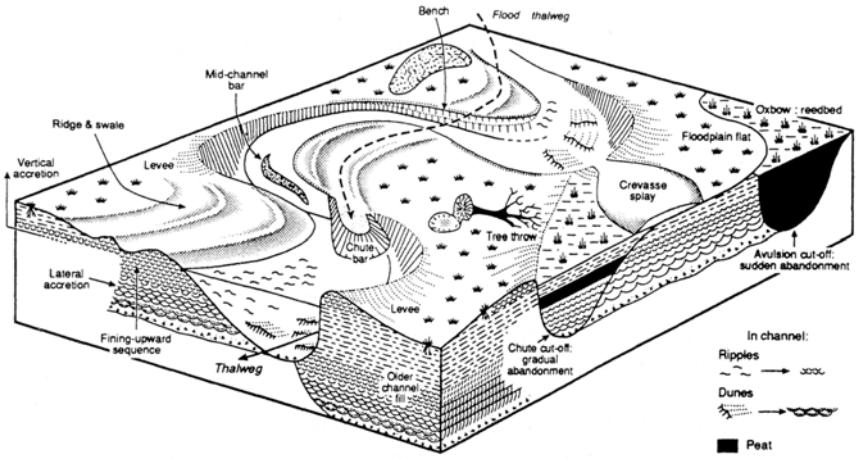

Figure 2.4: Floodplain landorms associated with meandering rivers, taken from Brown (1996) after Allen (1965).

which suspended sediment is stored only temporal (Asselman, 1999; Walling *et al.*, 1998) floodplain storage may last for several thousand years. Thus, floodplains have well-preserved records of the biogeochemical environment and are vital geoarchives to reconstruct palaeoenvironments. In terms of the connectivity of geomorphological landforms, floodplains are important links between the hillslope and the channel (Burt, 1996; Brierley & Fryirs, 2005). Generally, the importance and extend increases with increasing catchment size and declining hillslopes (Fig. 2.17).

Floodplains are formed by a combination of within-channel and overbank deposits (Fig. 2.4). The relative contributions of within-channel and overbank deposits largely depend on the sediment supplied to the channel, its grain size, the energy of the river to transport sediment (e.g. stream power). Based on these factors channels and their corresponding floodplains can be generally classified into three types of channel pattern: straight, meandering and braided (Leopold & Wolman, 1957; van den Berg, 1995; Lewin & Brewer, 2001, Fig. 2.5a-c). In addition to these classic single-channel patterns, anastomosing channel systems with multiple channels have been recognized as a fourth basic pattern (Nanson & Knighton, 1996; Makaske, 2001, Fig. 2.5d). Floodplains of braided rivers with high stream power and large gravely sediment supply are mainly created from within-channel deposits. In contrast, floodplains of meandering and anastomosing rivers with lower stream power and more abundant fines show a broad range of the proportions of within-channel deposits and overbank fines. The proportion is controlled by the

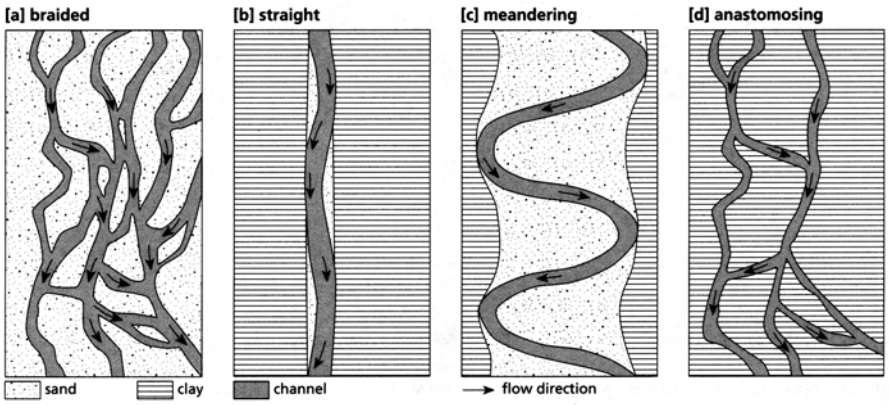

Figure 2.5: Channel patterns, taken from Berendsen & Stouthamer (2001).

degree of channel migration (lateral accretion) and overbank deposition (vertical accretion) of the meandering river (Wolman & Leopold, 1957; Nanson & Croke, 1992; Brown, 1996).

Channel migration is the combined effect of bank erosion at the concave banks of river meanders and the lateral point bar accretion at their convex bank. The migration rate is strongly controlled by bank erosion and therefore depends on the bank stability and the shear stresses exerted by the flowing water. Rivers with competent, clay rich, vegetated banks show smallest bank erosion rates. In contrast non-cohesive, sandy banks with lacking vegetation are prone to bank erosion. Additionally, soil moisture conditions and the degree of preparation of the bank material (e.g. due to weathering) are important factors of bank stability. The shear stress of the water is given by its velocity gradient at the banks and thus depends on the discharge and the ratio of curvature radius r_c to channel width W_c, with maximum erosion were $2 < r_c/W_c < 3$ (Knighton, 1998). As shown in a review of the measurement of river bank erosion and lateral channel change (Lawler, 1993), typical bank erosion rates range from 0 to 790 m/yr with more frequent values between 1 and 10 m/yr.

Visual effect of the channel migration is the scroll pattern of point bar deposits at the concave side of meanders. These forms mark the former position of river meanders. Generally, point bar deposits are characterised by sands and gravels that show an inclined stratigraphical layering parallel to the slope of the concave bank. However, Wolman & Leopold (1957, p. 92) point out that "*the alternation of high and low flow and the concomitant shifts in the velocity and streamline pattern at any given place give rise to*

considerable heterogeneity in the point bar deposits". Therefore they emphasis the difficulty involved in distinguishing point bar and overbank deposits from grain size analysis alone.

Wolman & Leopold (1957) concluded that lateral accretion is the dominant process and therefore disregarded flood deposition in their classical model of floodplain formation. However, it has been shown that it is of major importance along certain low-gradient, single-thread and anastomosing channels (Nanson & Croke, 1992; Brown, 1996; Walling *et al.*, 1996; Knighton, 1998). These channel types are characterised by abundant suspended load and a high frequency over bankful discharge and therefore promote floodplain deposition by vertical accretion.

Vertical accretion results from the overbank deposition of sediment during floods. Sediment is transported from the channel to the floodplain i) by water flow perpendicular to the channel, e.g. in cut-off channels that are reactivated during the floods and/or ii) by turbulent diffusion[3]. In general, the rate of overbank deposition depends on the frequency of inundating flows and their sediment load. Due to changing sediment loads with time, floods of similar size do not necessarily deposit a similar amount of overbank sediments (Benedetti, 2003). At the local scale, major factors that control overbank deposition are: i) flow velocity (mainly controlled by floodplain topography and distance from channel), ii) duration of inundation (mainly controlled by floodplain topography) and iii) roughness of the floodplain surface (mainly controlled by floodplain vegetation). In the case of turbulent diffusion there is a strong decreasing tendency of the amount and grain size of sediments deposited on the floodplain with channel distance (Pizzuto, 1987; Asselman & Middelkoop, 1995; Walling *et al.*, 1998). However, in most situations sediment transfer is the effect of a combination of turbulent diffusion and convection. In this case, floodplain topography (Asselman & Middelkoop, 1995) and the distribution and nature of vegetation may be of major importance.

A very broad spread of deposition rates is reported in various papers. During a single flood, sediment deposition of 0.82 mm and 0.47 mm was estimated by Asselman & Middelkoop (1995) for small study site at the Waal and the Meuse in the Netherlands. At the Mississippi Gomez *et al.* (1997) reported values between 2 and 200 mm of a flood event that happened in 1993. Long term deposition rates are measured based on ^{137}Cs-concentrations. These

[3]Turbulent diffusion is the transport of sediment from areas with high sediment concentrations to areas with low sediment concentrations (Pizzuto, 1987; Nicholas & Walling, 1997). In the case of flooded channel systems, turbulent diffusion results in sediment transport from the channel (high sediment concentration) to the floodplain (low sediment concentration)

measurements integrate over the last 40 years, since maximum ^{137}Cs-fallout. At the River Ouse (Yorkshire, UK), for example, Walling *et al.* (1998) estimated overbank sedimentation rates ranging from 0.08 to 5.2 mm year^{-1} (mean $\approx$ 1.6 mm year^{-1}) that corresponded to 39% of the suspended sediment yield of the River Ouse. ^{137}Cs-measurements on the Upper Mississippi River resulted in larger values ranging from 4.4 up to 14.4 mm year^{-1} with a mean of 12.5 mm year^{-1} (Benedetti, 2003). The high values are the effect of intense agricultural land disturbance, as compared the mean values of 1.4 mm year^{-1} estimated based on ^{14}C-measurements at the same locations. For more values of vertical accretion rates see Rumsby (2000), who gives a short review over a broad range of spatial temporal scales and applied methods.

Due to the successive raising of floodplains resulting from the accumulation of overbank fines, the magnitude of successive floods leading to overbank deposition must continuously increase to inundate the floodplain. Therefore, there is a limit of overbank deposition that results in equilibrium of floodplain geometry and flow regime. The interacting balance of the two fundamental processes (lateral and vertical accretion) causes a fining-upward sequence of gravely channel lag deposits, sandy point bar deposits and silty overbank deposits on top.

However, the equilibrium of floodplain geometry and flow regime is disturbed by high energy floods that complicate the general picture of floodplains. Crevasse splays, which form at levee breaks, chute scour, chute cutoffs and chute fills (palaeochannel fills) are created by geomorphic effective floods and are therefore important styles of deposition in high energy floodplains (Nanson & Croke, 1992, Fig. 2.4). In cases of confined channels with neglecting channel migration and catastrophic floods, floodplains develop in disequilibrium with longer episodes of vertical accretion and single flood events with catastrophic stripping (Nanson, 1986; Kemp, 2004). In active geomorphic regions with steep slopes rockfalls, landslides, debris cones and mudflow deposits may exist in floodplain environments and obscure their classical geometry as shown in Fig. 2.4 (Brown, 1996).

2.1.4 Importance of carbon flux in fluvial systems

The amount of carbon dioxide (CO_2) in the atmosphere has increased by more than 30 % since pre-industrial times and is still increasing at an unprecedented rate on average 0.4 % per year, due to anthropogenic transformation of fossil fuels and land use change (compare Fig. 1.1). However, the growth rate of CO_2 in the atmosphere is presently less than half of what would be expected from anthropogenic CO_2 release into the atmosphere. The missing carbon in the atmosphere results from CO_2 absorption of the

oceans and the terrestrial biospheres (plants and soils), which are major sinks for anthropogenic carbon (Sarmiento & Gruber, 2002). Especially soils that hold about 1500 Gt organic carbon (twice as much as stored within the atmosphere as CO_2) are an important link in the global carbon cycle (Knorr *et al.*, 2005; Lal & Kimble, 1999; Powlson, 2005). Therefore, minor changes in organic carbon content in soils can significantly change the CO_2 concentration in the atmosphere and accelerate climate change. There has been an increasing recognition of the role that soil erosion plays in cycling carbon through landscapes (Lal, 2004, 2005; Quinton *et al.*, 2006). Onsite, erosion acts as mechanism for the removal of carbon from soils exposing carbonate rich subsoil. Offsite, soil erosion acts as a transport agent, adding carbon through sediment accumulation to colluvial storage and to the fluvial system.

Beside the soil erosion processes on the hillslope, the transport of water and sediment in fluvial systems is an important link in the global carbon cycle and a major input of organic carbon to the oceans (Ludwig *et al.*, 1996; Meybeck, 1993; Schlünz & Schneider, 2000). At short-terms, rivers are sources for atmospheric CO_2 due to the high riverine CO_2 concentrations, especially in humid tropics, which can be 5-30 times supersaturated with respect to atmospheric equilibrium (Mayorga *et al.*, 2005). High CO_2 concentrations in rivers result from the high CO_2 concentrations of the groundwater input and the heterotrophic CO_2 production within the channel. Important factors controlling the riverine CO_2 concentration and therefore the amount of CO_2 exported to the atmosphere are authochtonous primary production within the channel and allochthonous organic carbon import to river system from terrestrial ecosystem (Cole & Caraco, 2001). At long-terms, fluvial systems acts as a major sink for atmospheric CO_2 due to the long-term deposition of organic carbon in floodplains and wetlands (Macaire *et al.*, 2006; Walling *et al.*, 2006, compare also Chapter 4.3.2).

2.2 Holocene environmental change

The last 2.5 million years (the Quaternary period) are characterised by extreme climate variability at different time scales (Fig. 2.6). At long time scales, gradual trends of warming and cooling were driven by tectonic processes, which resulted in the changing distribution of the continental masses and the building of large mountains. At shorter time scales, fluctuations of the earths orbital parameters (with typical periods of 100, 41, 23 and 19 kyr) lead to periodic changes and the development of glacial and interglacial conditions (Wilson *et al.*, 1999). The Holocene is the youngest part of the Earth's history and the latest series of warmer intervals that interrupted colder climates during the Quaternary. Although the beginning of the Holocene is marked by a strong temperature increase at the end of the late glacial, approximately 11 700 years ago (Adams *et al.*, 1999; Litt *et al.*, 2001; Rasmussen *et al.*, 2006), it would be quite wrong to assume that the Holocene is characterised by a constant warm climate with stable geomorphological systems (e.g. landforms) and ecosystems. Furthermore and in contrast to the former interglacials of the Pleistocene epoch, the Holocene is characterised by the emergence and evolution of the human race (Roberts, 1998).

Geoscientists generally consider the human impact as an independent factor that controls the environmental systems. However, there is growing evidence that there are complex feedbacks between natural systems on the one hand and social systems on the other hand. With respect to these complex feedbacks, there is a growing debate on the impact of climate change on prehistoric and historic cultures. Even though the complex feedbacks between the natural and social systems must be considered to understand long-term development of the Earths system, these will not be discussed in more detailed here. Good introductions to this topic are given by Redman (1999); deMenocal (2001) and Diamond (2005). However, in the following chapter a short introduction of the changes of the Holocene climate and of the human activities will be given.

2.2.1 Climate change

Holocene climate changes in Europe are characterised by long-term trends, centennial to millennial fluctuations and multi-annual and multi-decadal events (Adams *et al.*, 1999; Huntley *et al.*, 2002; Negendank, 2004, Fig.2.7). The first half of the Holocene has witnessed a general increase of the mean annual temperature that peaked around 5 kyr BP at a value approximately 2.5°C higher than today (Holocene thermal maximum). The warmer tem-

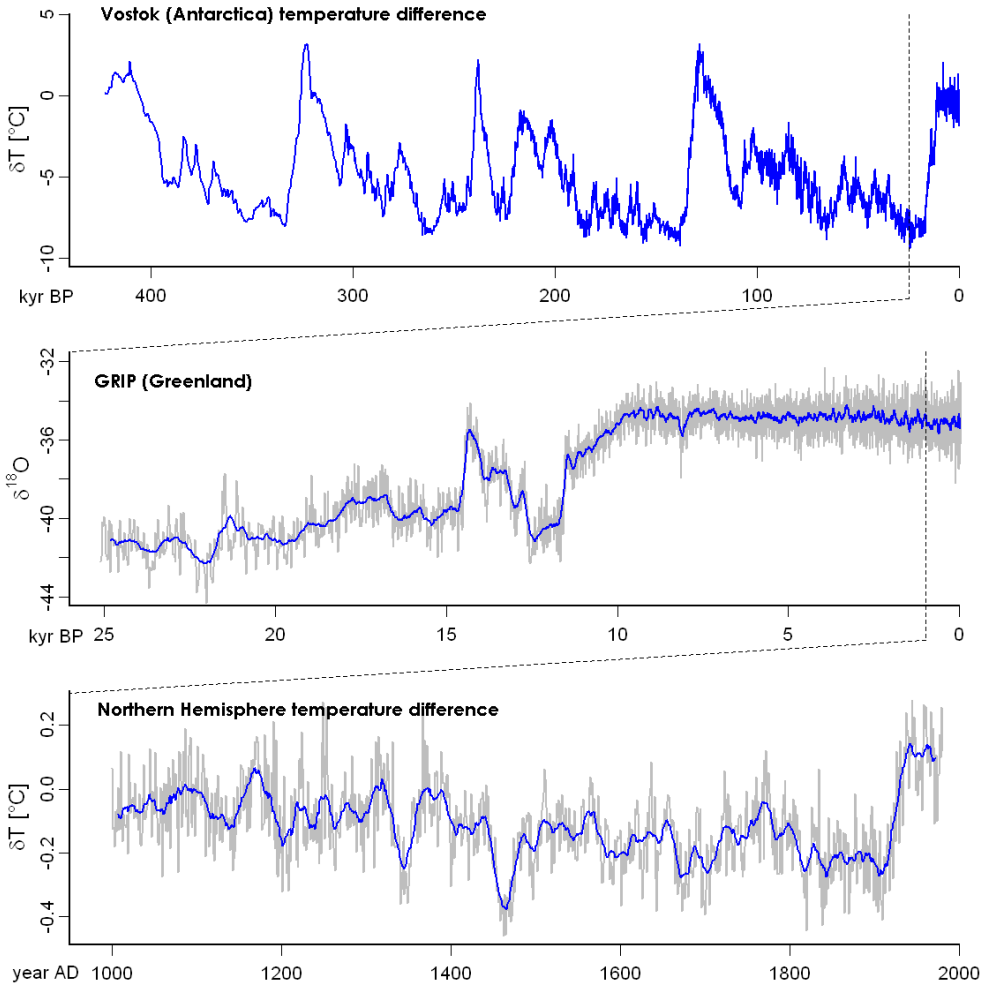

Figure 2.6: Quaternary temperature variability at different time scales modified based on Oldfield & Alverson (2003). Temperature differences for the last 400 ka BP reconstructed based on δD of the Vostok Ice Core (Petit *et al.*, 1999). Millennial temperature variability associated with δ^{18}O variations in the GRIP Ice core (Dansgaard *et al.*, 1993). The blue line represents the $\approx$ 100 year running mean. Temperature reconstruction of the last 1000-years taken from Mann *et al.* (1999). Gray line: values every year, blue line: 30-years running mean.

peratures were probably caused by increased solar radiation of the Northern hemisphere, due to the changing precession of the Earth's orbit. The increased solar radiation in turn resulted in a northward shift of atmospheric circulation, with a stronger influence of the Subtropical high pressure belt in Central Europe (Roberts, 1998). Since 4.1 kyr BP the temperature decreased again and reached its minimum 2.2 kyr BP. The last 2000 years are characterised by shorter fluctuations with the Roman and Medieval thermal optimums and the Little Ice Age (LIA) that culminated at around 1700 AD with a mean annual air temperature approximately $1 - 1.5°C$ lower than todays modern optimum (Negendank, 2004; Matthews & Briffa, 2005, Fig.2.7)[4]. These millennial-scale cycles reflect modulations of the baseline trends. Based on ice rafted debris (IRD) records that are used as proxies of the North Atlantic sea surface temperature, Bond *et al.* (1997) showed that these cycles are typical features during the last 12 000 years. Eight IRD cycles, which peak at about 1.4, 2.8, 4.2, 5.9, 8.1, 9.4, 10.3 and 11.1 kyr BP and a return period of approximately 1500 years, can be linked to the solar driven, atmospheric ^{10}Be and ^{14}C record (Bond *et al.*, 2001). Thus, their findings suggest a persistent solar influence on the North Atlantic climate during the Holocene. In contrast to the long-term trends that are caused by variations of solar radiation due to changing orbital parameters of the Earth, the short-term fluctuations, as recognized by the atmospheric ^{10}Be and ^{14}C records, result from the irradiance changes of the sun itself. However, Bond *et al.* (2001) argue that periodic solar irradiance decreases of only approximately 0.25 % may have been too small to cause significant temperature decreases. Therefore, they suggest that the irradiance decreases were amplified by complex feedbacks in the thermohaline circulations driven by the North Atlantic sea surface temperature and therefore produced global climate responses.

In contrast to the other cycles, the drift-ice cycles that peak at 11.1 and 8.1 kyr BP are clearly detected in the Greenland Ice Cores (Fig. 2.6), suggesting stronger impacts than solar irradiance decreases alone. While the 11.1 kyr BP cycle may be correlated to the abrupt transition at the end of the Younger Dryas (last Heinrich event), the 8.1 kyr BP cycle is often attributed to meltwater outflow into the North Atlantic Ocean and a slowdown of North Atlantic Deep Water formation (Adams *et al.*, 1999; Alley & Agustsdottir, 2005; Rohling & Palike, 2005).

At short time scales extreme cold events have occurred during the Holocene, which are probably caused by volcanic eruptions and/or cosmic dust input.

[4]For a review of the climate in the Rhine catchment during the last 1000 years so also Glaser *et al.* (2005)

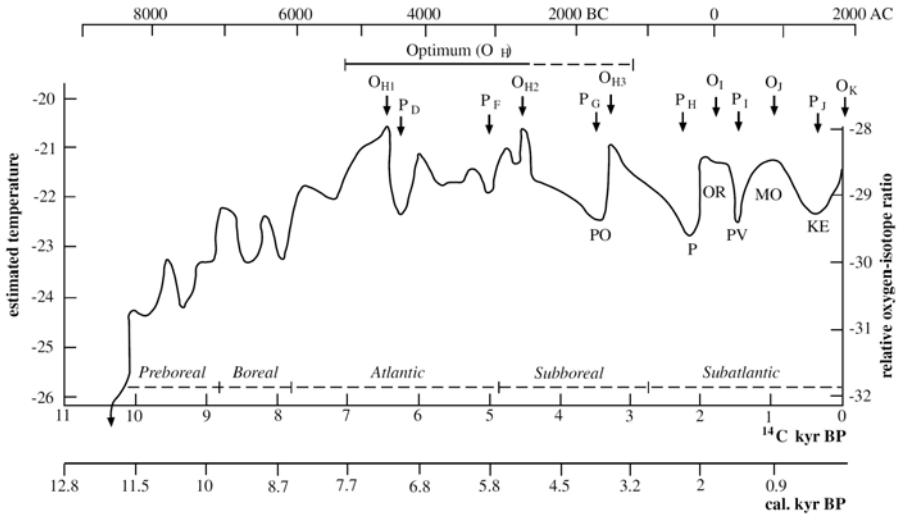

Figure 2.7: Holocene temperature variability taken from Negendank (2004). O = temperature optimum, P = temperature minimum, PO = Piora Oscillation, OR = Roman Optimum, PV = pessimum of the Migration time, MO = Medieval optimum, KE = Little Ice Age.

For example, in approximately 1410 years BP (AD 540) global tree ring chronologies record the joint second worst growth year in the last 1500, which may correspond to the increased hazard arising from the fragments of dead comets that intersected the Earths orbit (Huntley *et al.*, 2002).

2.2.2 Human Impact

While natural Earth system drivers, such as lithology, relief, climate and vegetation had a major impact on Earth's environment during the precedent Pleistocene, it is now believed that anthropogenic forcing is the dominant agent of environmental change during the Later Holocene. The impact of human activities has increasingly changed the Earth's environment since the beginning of the Neolithic Revolution, the transition from hunting and gathering to agricultural activities.

Based on the cultural grade of human activity, archaeologists generally sub-divide the time since the Neolithic Revolution in Europe into eight periods: Neolithic, Bronze Age, (Pre-Roman) Iron Age, Roman Iron Age, Roman, Early-Medieval, High/Late Medieval and Modern Period. However, it must be stressed that the cultural periods are not fixed in space but are diachronous between different regions within Central Europe, resulting from

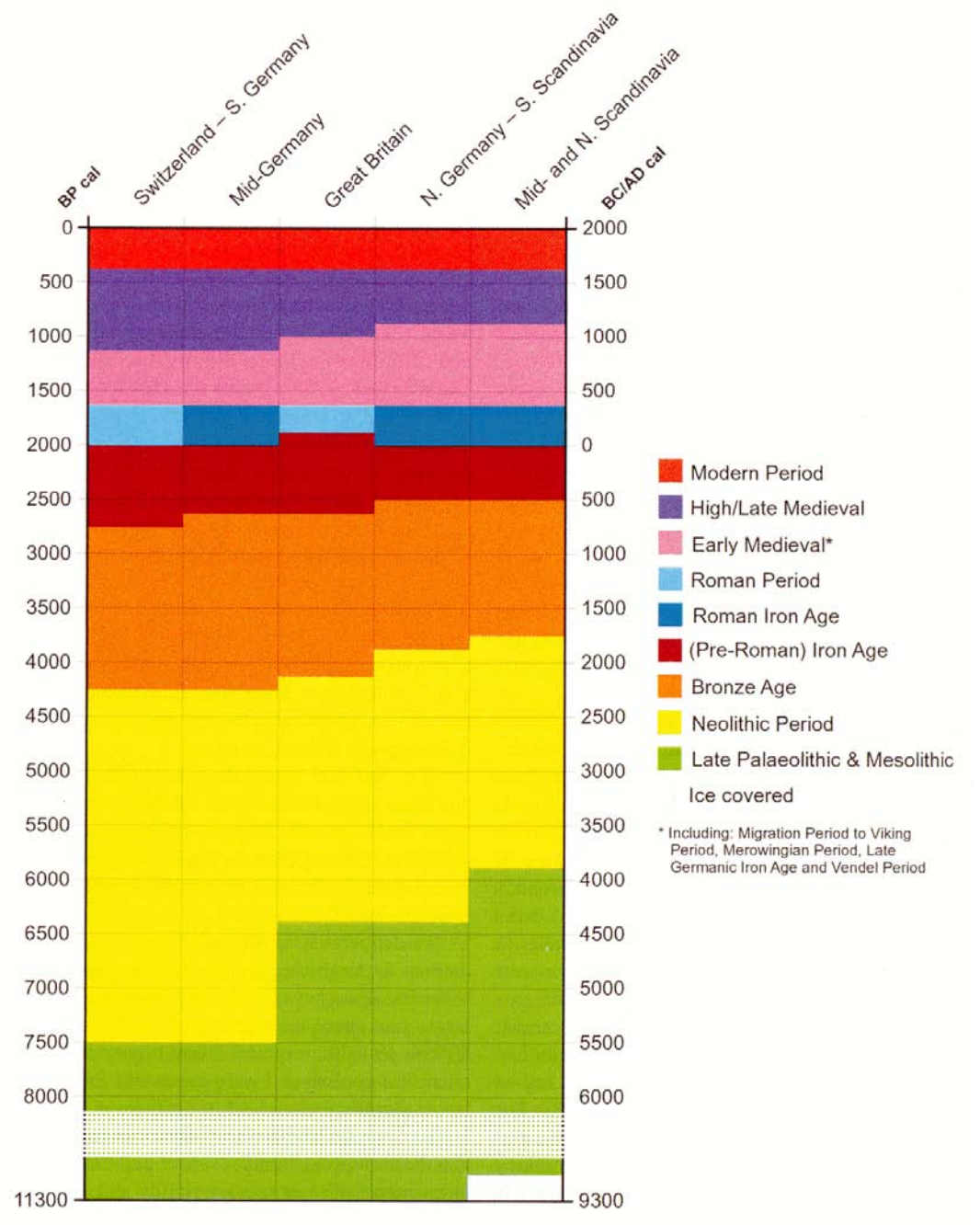

Figure 2.8: Chronology of cultural periods in various regions of Europe (Huntley *et al.*, 2002).

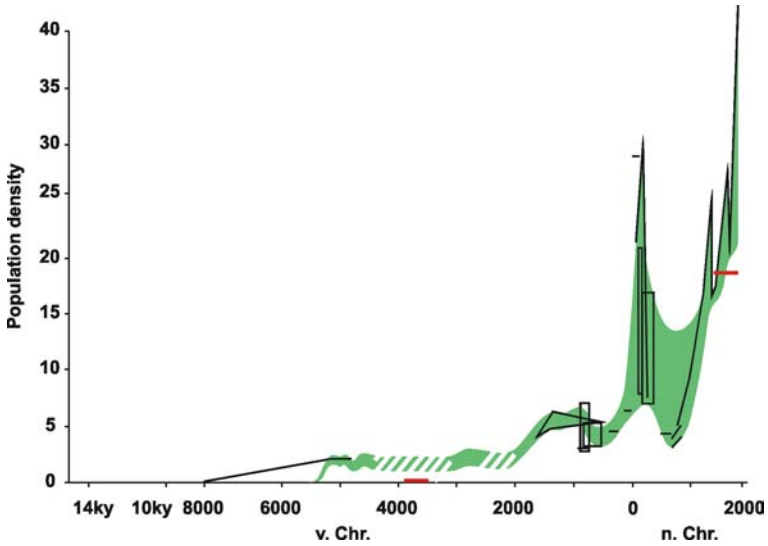

Figure 2.9: Population growth during the last 14 000 years in Central Europe, taken from Zimmermann (1996).

the differences in human history (Fig. 2.8). The Neolithic period, for example, started in Switzerland and South Germany already 7500 years BP, while first Neolithic settlements in Mid- and North-Scandinavia started not before 6000 years BP. Furthermore, the Roman Period is limited to Switzerland, Southern Germany and Great Britain.

These periods are characterized by increased population densities in Central Europe as described by Zimmermann (1996)(Fig. 2.9). A first major population increase occurred around 2000 BC during the Bronze Age that was followed after a small population decrease by the Roman period with more than 30 inhabitants per km^2. Due to the collapse of the Roman Empire after 400 AD, there was a dramatic population decrease during the migration period in the Early-Medieval. Since the High Medieval the population in Central Europe generally increased with shorter drawbacks that were caused by famine and epidemic diseases (Zimmermann, 1996; Bork *et al.*, 1998).

Early environmental change at the beginning of the Neolithic Revolution was limited to local and regional land use and land cover changes (Oldfield & Dearing, 2003; Zimmermann, 2003). The advent of agricultural production and the corresponding domestication of plants and animals made it necessary to deforest the pristine forests that covered the Central European landscape. Farming activities were focused on loess covered areas, which are characterised by a high agricultural productivity.

During the following Bronze, Iron and Roman period mining activities

and metalworking had a major impact on the development of the early civilizations and therefore on the colonised landscapes (Roberts, 1998). The development of the plough made it possible to extend agricultural land use into upland areas that were until then not favourable for agriculture and settlement (e.g. the Black Forest, Rhenish Slate Massive). In most loess covered areas (e.g. the Upper Rhine Graben around Freiburg, the Kraichgau and the Lower Rhine) that were already populated the complete forests were cut and transformed to agricultural land.

Furthermore, urbanisation and water management put additional pressure on the Earth's environment. For example, Herget (2000) described the building of towpaths along the River Lippe already during the Roman period 2000 years ago, which may have changed the natural channel planform from an anastomosing to a meandering river. Regarding the River Rhine, first embankments in the Rhine delta, were build in 1150 AD (Ten Brinke, 2005). Since the early 19th century the River Rhine and its tributaries have been strongly regulated (Herget *et al.*, 2005). Channelization, the large-scale construction of embankments and dams resulted in a decreasing sediment exchange of the river channels and their neighbouring floodplains.

Since the beginning of the Industrial Revolution (mid 18^{th} century) the combustion of fossil fuels for industrial or domestic usage, biomass burning, and land use change (mainly deforestation) produced greenhouse gases and aerosols which affect the global composition of the atmosphere. The amount of carbon dioxide (CO_2) in the atmosphere has increased by more than 30 % since pre-industrial times and is still increasing at an unprecedented rate on average 0.4 % per year Houghton *et al.* (2001), resulting in a warmer atmosphere and stronger climatic extremes. The increase of the global average surface temperature over the 20^{th} century by about 0.6° C is likely to have been the largest during the last 1 000 years (Fig. 2.6) and even since the beginning of the Holocene, suggesting that human activities can no longer be neglected to influence the environment at a global scale. However, in contrast to the prevailing opinion, Ruddiman (2003) proposed that the global human impact started much earlier, when humans reversed a natural decrease of CO_2 (after 8000 years ago) and methane (after 5000 years ago) by starting to clear forests and by irrigating rice, respectively.

While the history of past cultures is well known, mainly based on archaeological evidences, the major question of the timing and extent woodland transformation to arable land and pasture needs to be answered (Bork & Lang, 2003; Herget *et al.*, 2005). Only if we know the impact of human activity on land use changes are we able to understand the human impact on fluvial systems. However, first results that may help to answer this question are presented by Zimmermann *et al.* (2004).

2.3 Fluvial response to environmental change

Although there is considerable order in fluvial systems[5], river characteristics can vary greatly in time and space (Schumm, 2005). For example, a meandering reach can be connected to a braiding reach separated by only a few kilometres. Furthermore, a meander that is currently part of the active channel may be deactivated during a single flood. The large variability of rivers results from i) the numerous controls acting on river morphology and behaviour that change in time and space at different scales (Fig. 2.10), ii) from the discontinuous character of river networks at junctions of two river segments and iii) different timescales of adjustment of form components of fluvial systems (Fig. 2.11). Regarding the external controls, lithology, soils and baselevel (especially sea level) vary on long terms (e.g. 10^3 to 10^6 years), while climate, hydrology and land use can even change on very short temporal time scales (approx. 10^0 to 10^2 years). The timescale of adjustment of the form components to these external changes strongly correlates with their characteristic length scale (Fig. 2.11). For example, the bed configuration (e.g. ripples and dunes) with characteristic lengths of 10^0 m may change within seconds. In contrast, the longitudinal profile form of the river with a characteristic length scale of 10^3 to 10^4 m adjusts on times scales of 10^4 years. Based on Knighton (1998) the adjustment of the channel geometry to external controls can be considered in terms of four degrees of freedom that are: i) configuration of the channel bed (e.g. grain size, form like ripples and dunes), ii) the cross section of the channel (e.g. its size and form), iii) channel pattern (compare Chapter 2.1) and iv) the channel slope (longitudinal profile).

Changes of fluvial systems are of major importance to the human dimension, due to the direct linkages between human activities and fluvial processes. These changes are driven by the external controls and the effects of the internal configurational state. Therefore their impacts on fluvial systems will be discussed in the following sections.

2.3.1 Climate impacts on fluvial systems

The importance of low frequency, large magnitude climate changes on river development during the Pleistocene is now well established. Pleistocene river aggradational episodes coincide with glacial and stadial events, while phases of river incision occur during interglacial or interstadial (e.g. Rohdenburg,

[5]For example, the Horton law describing the structure of channel networks or the downstream increasing channel width with discharge show strong regularities.

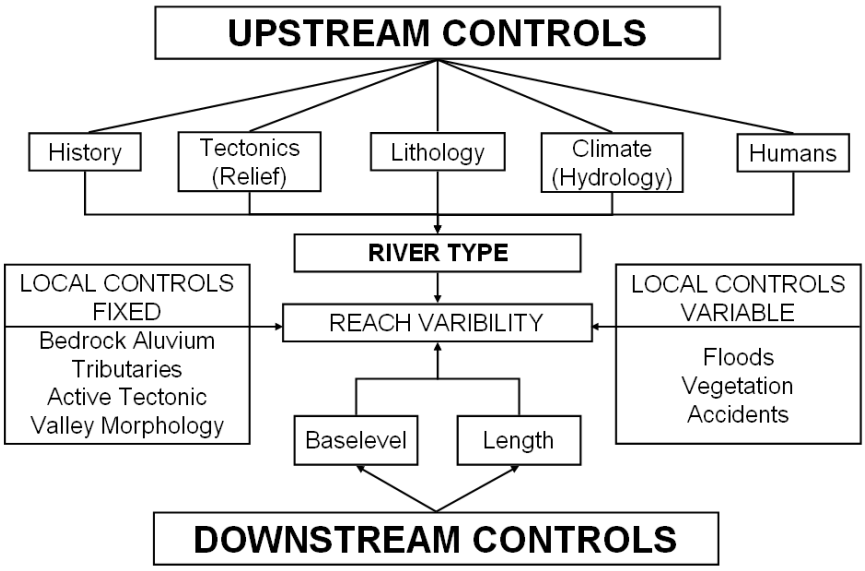

Figure 2.10: Upstream, local and downstream controls of fluvial response, taken from Schumm (2005).

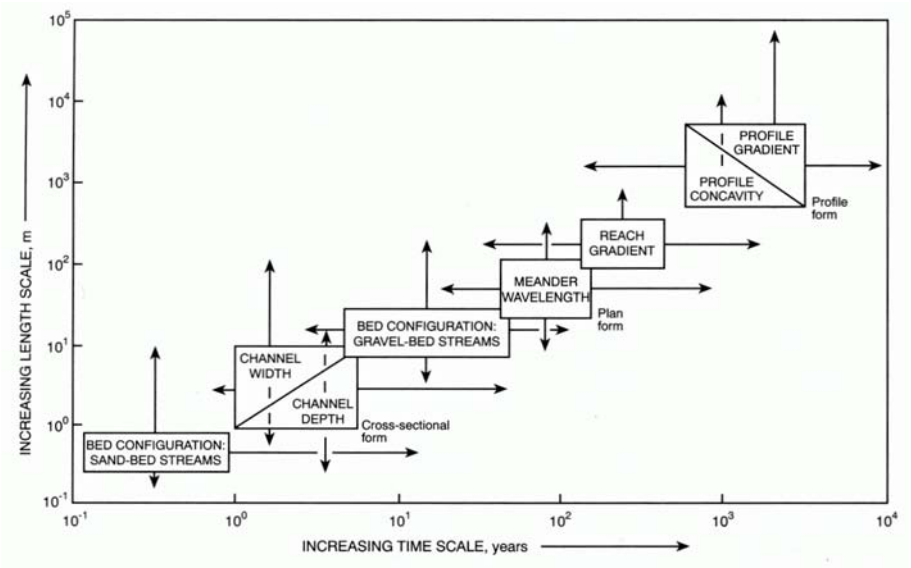

Figure 2.11: Spatial and temporal scales of forms and components of fluvial systems, taken from (Knighton, 1998).

1970; Mol, 1997; Vandenberghe & Maddy, 2001; Macklin *et al.*, 2002). Despite their greater aridity glacial and stadial events are characterised by enhanced geomorphological activity and effective hillslope channel coupling due to increased frost shattering, the high efficiency of glacial, aeolian and solifluction processes. Considering the fluvial transport, the shift towards more arid conditions and the high surface runoff due to permanently frozen grounds, increased the frequency of large floods. Based on Molnar (2001) such a shift, despite a decrease in precipitation and discharge, could have doubled incision rates and increased fluvial transport capacity.

A large number of studies focus on the Late Glacial and the Late Glacial-Holocene transition, which is characterised by strong climate changes and considerable fluvial responses; global warming, moister conditions, denser vegetation cover and reduced sediment supply caused a shift of braiding to meandering associated with channel incision (e.g Tebbens *et al.*, 1999; Andres *et al.*, 2001; Starkel, 2002b; Bogaart *et al.*, 2003; Litt *et al.*, 2003; Leigh, 2006).

The significance of more frequent changes during Holocene, however, is still under dispute. Evidences of climate impacts have been shown by different authors. For example, Aalto *et al.* (2003) identified a correlation between the El Nino/Southern Oscillation cycle and the formation of the Bolivian floodplains. The Southern Oscillation modulates downstream delivery of sediments as well as associated carbon, nutrients and pollutants to the Amazon main stem.

Starkel (2002a) qualitatively describes the response of Poland Rivers to changing frequencies of floods. Phases of increased floods are characterised by straightening and widening of channels followed by a tendency to braiding and avulsions. In contrast, narrow and deeper meanders are developed in times with less frequent floods. Whether the rivers incise or aggradate depend on the sediment supply that is mainly determined by vegetation cover and land use.

Large scale simultaneous river incision on the climate-sensitive, prairie-grassland of the Great Plains occurred around 1000 years BP (Daniels & Knox, 2005). Based on a proxy records of palaeohydrologic conditions in and around the Great Plains, Daniels & Knox (2005) suggest that widespread droughts that coincide with the Mediaeval Warm Period caused this incision phase.

The climate impact on the valley bottoms in Germany is described by Schirmer (1995) and Schirmer *et al.* (2005) (compare also Chapter 3.5). The widespread occurrence of seven Holocene fluvial accumulation phases of the major Rhine tributaries suggests a dominating climatic impact that is only amplified by agricultural activities since the Neolithic (Fig. 2.12).

Recently, the International Council for Science (ICSU) project "Past Hy-

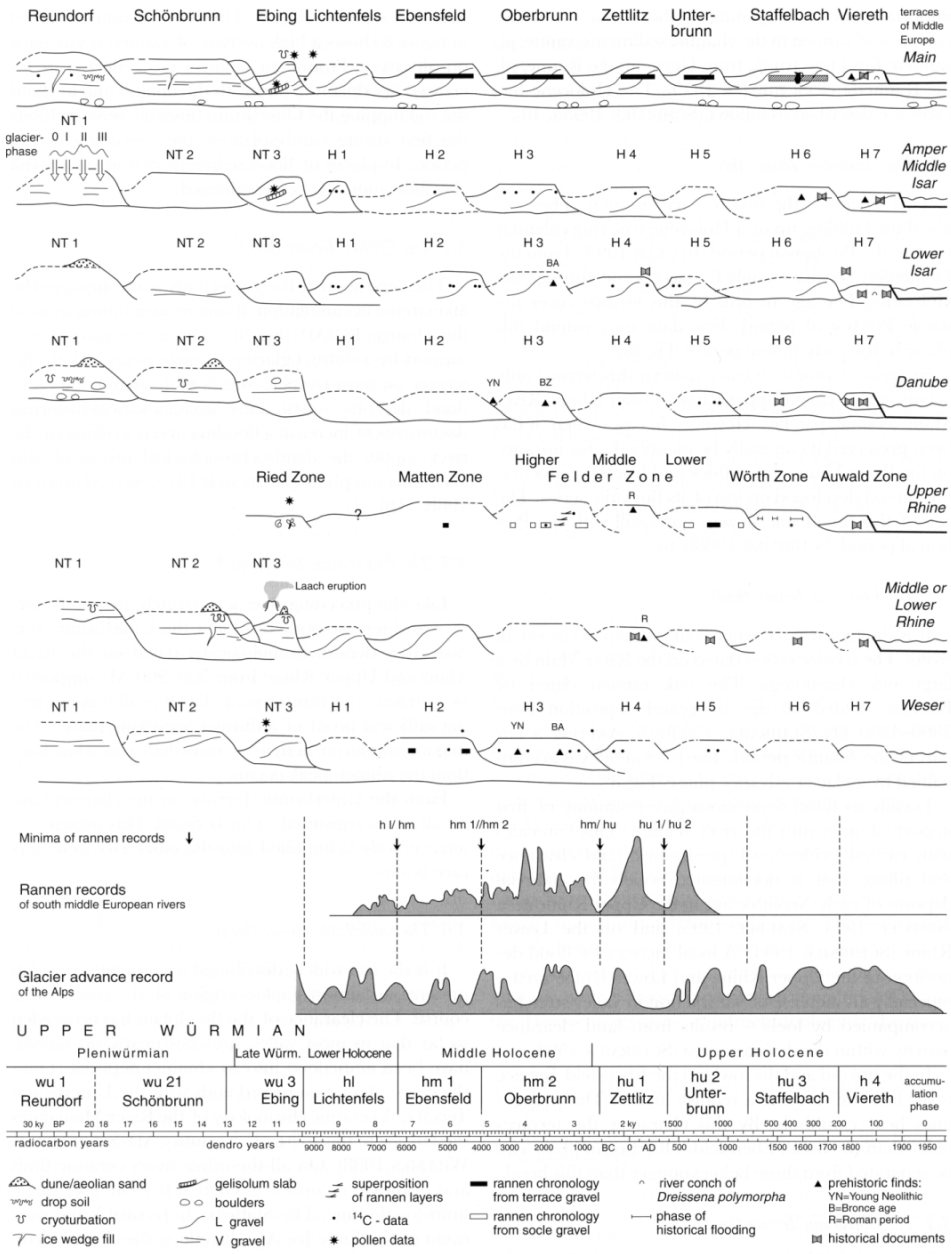

Figure 2.12: Phases of increased deposition during the Holocene as described by (Schirmer, 1995). NT1-NT3 = lower terrace levels deposited during the Late Glacial. H1-H7 = Holocene terrace levels. For more details see (Schirmer, 1995).

drological Events Related to Understanding Global Change" provided the framework to analyse and compare Holocene river sequences in Europe in a systematic manner (Gregory *et al.*, 2006; Macklin *et al.*, 2006). Cumulative probability distribution functions (CPDF) of ^{14}C ages obtained on Holocene fluvial units were compiled and analysed for different countries (UK, Poland and Spain) and compared to identify possible large-scale hydro climatic teleconnections. The techniques developed by Macklin & Lewin (2003); Lewin *et al.* (2005) and Johnstone *et al.* (2006) using ^{14}C ages from Great Britain were applied by Starkel *et al.* (2006) for Poland and Thorndycraft & Benito (2006b,a) for Spain. A comparison of the results from Great Britain, Spain and Poland is given by Macklin *et al.* (2006). 15 Holocene periods of major flooding are identified by peaks in the CPDFs that occur in two or more areas simultaneously. These periods are interpreted as hydroclimatic teleconnections across Europe and therefore suggest a synchronous climate impact on fluvial systems during the Holocene. However, due to shortcomings in the applied methods, these results must be interpreted with care (for more details see Chapter 4.4.1, 5.4.1 and 6.3.1).

At shorter time scales, the impact of the Little Ice Age (LIA) on fluvial systems in Central Europe is reviewed by Rumsby & Macklin (1996). The authors suggest that at the beginning and the end of the LIA (1250-1550 AD and 1750-1900 AD) North, West and Central Europe experienced enhanced fluvial activity. However, fluvial activity decreased during the most severe phase of the last neoglacial. In New South Wales channels responded to alternating from flood-dominated to drought-dominated regimes during the last 100 years (Erskine & Warner, 1999). During catastrophic floods, bank erosion (causing channel widening) generates almost the complete sediment yield. In contrast, in-channel sediment storage occurs during drought-dominated regimes. Due to the frequent changes of the flood regime and the delayed and buffered response, Erskine & Warner (1999) suggest that channels in New South Wales are in a state of "cyclical disequilibrium", as they are not able to adjust to a new equilibrium before a new change of the flood regime occurs.

2.3.2 Human impact on fluvial systems

Humans have had a plethora of impacts on fluvial systems, either directly or indirectly (Gregory, 2006). Direct impacts concern the modification of the river channels in terms of river management, e.g. channelization, the construction of dams and embankments, diversion and culverting. Indirect impacts include upstream land use changes such as deforestation, intensive agriculture, mining, incidence of fire, and urbanisation. Downs & Gregory

Table 2.1: Six chronological phases of river use and the management methods used for each, taken from Downs & Gregory (2004).

Chronological phase	**Characteristic developments**	**Management methods employed**
1. Hydraulic civilizations	River flow regulation Irrigation Land reclamation	Dam construction River diversions Ditch building Land drainage
2. Pre-industrial revolution	Flow regulation Drainage schemes Fish weirs Water mills Navigation Timber transport	Land drainage In-channel structures River diversions Canal construction Dredging Local channelization
3. Industrial revolution	Industrial mills Cooling water Power generation Irrigation Water supply	Dam construction Canal building River diversions Channelization
4. Late 19^{th} to mid 20^{th} century	River flow regulation Conjunctive and multiple use river projects Flood defence	Large dam construction Channelization River diversions Structural revetment River basin planning
5. Second part of 20^{th} century	River flow regulation Integrated use river projects Flood control Conservation management Re-management of rivers	Large dam construction River basin planning Channelization Structural and bioengineered revetments River diversions Mitigation, enhancement and restoration techniques
6. Late 20^{th} and early 21^{th} century	Conservation management Re-management of rivers Sustainable use river projects	Integrated river basin planning Re-regulation of flow Mitigation, enhancement and restoration techniques Hybrid and bioengineered revetments

(2004) summarize the history of human impact on river channels over the last 5000 years using six chronological phases (Tab. 2.1).

The effects of the direct impacts on the river channels on the sediment flux are of opposed character. Some impacts cause sediment loads to increase, whilst others cause decreased sediment fluxes (Gregory, 2006, Tab.3 there). Concerning the recent global sediment flux by rivers to the ocean, reservoir construction is probably the most important influence that may buffer increased sediment fluxes caused by increased soil erosion (Walling & Fang, 2003). Based on a global study of 633 of the world's largest reservoirs, Vörösmarty *et al.* (2003) estimated that more than 50% of the basin-scale sediment flux in regulated basins is potentially trapped in artificial impoundments. Therefore, the global sediment flux to the oceans is reduced by 25-30%, causing significant impacts on the world's coastal zones. While sedimentation occurs upstream of the reservoirs, downstream regions suffer from severe channel incision and the subsequently lowering of the groundwater table.

In contrast, channelization and the building of embankments, for example, may enhance the sediment throughput. Downstream effects of channelization, which are bank erosion and increased sediment flux, arise from increased flow velocities and stream power. Furthermore, channelization and the construction of embankments reduce the channel-floodplain connectivity and therefore the river's ability to store sediments along its floodplains (Kesel, 2003; Verstraeten *et al.*, 2003; Wohl, 2005).

Indirect human impacts on fluvial systems concern the change in sediment supply from the hillslopes due to changing land use and their effects on the river channels and floodplains. The enhanced conversion of natural vegetation to agricultural land during the last 200 years generally increased soil erosion rates by an order of magnitudes or more (Morgan, 1986). Increased soil erosion, in turn, is recognized by increased sediment yields and floodplain deposition of the rivers (Walling & Webb, 1996; Panin, 2004). Over the last 100 years, the human impact has been evidenced by direct measurements of the suspended sediment yield (Walling, 1999; Walling & Fang, 2003). However, increased sediment yields caused by land use changes were only measured at a limited number of sites, due to the buffering effect of fluvial systems (e.g. by the construction of reservoirs). At longer time scales, accelerated sedimentation rates on floodplains are correlated with the increasing human pressure (Fig. 2.13). In the Upper Mississippi Valley (Driftless Area, USA), the shift from natural land cover to landscapes dominated by agricultural land use of the last 200 years increased rates of floodplain deposition by an order of magnitude (Knox, 2006, Fig. 2.13a). This shift caused the most dramatic change of the fluvial activity of the Mississippi and its tributaries

during the last 10 thousand years.

In the case of the Old World, the human impact can be traced back much earlier. The Yellow River (China), for example, shows a two stage accelerated sedimentation due to human activities (Xu, 1998, Fig. 2.13b). The transformation of the natural vegetation at the start of the Sui Dynastie (at approx AD 581) lead to stage I of the human induced acceleration of the sedimentation rates, which is superimposed on the climatic driven acceleration that started around 5000 yrs. BP. Stage II resulted from the construction of artificial levees that started approximately 475 BC. Levee construction caused a complex response of the lower Yellow River, which is described by Xu (1998) in three phases. First, due to increased transport capacity larger amounts of sediment was transported to the delta causing a much higher rate of the delta accumulation. Second, the delta aggradation caused a significant decrease of the channel slope, which in turn reduced the river's transport capacity causing increased sedimentation, which was limited to the floodplain enclosed by the artificial levees. Third, the increased sedimentation raised the river channel relative to the floodplain, causing a higher frequency of avulsions since 1855 AD.

2.3.3 The internal configurational state

The response of the fluvial system to changing controls is not only or necessarily a function of the magnitude of the extrinsic factor but upon the **sensitivity** (Brunsden & Thornes, 1979) and therefore upon the **configurational state of the fluvial system**[6] (Lane & Richards, 1997; Brown & Quine, 1999). In the case of the Upper Mississippi, for example, Holocene palaeoflood chronologies suggest that even modest changes of the climate equivalent resulted in highly sensitive response of the fluvial system (Knox, 2000). In contrast, fluvial systems are able to buffer the effects of external changes as shown by Trimble (1999) in the Coon Creek (Wisconsin). Decreasing erosion rates on the slopes, due to improvements in agricultural land management, did not change the sediment yield at the channel outlet because the sediment storage within the main valley decreased at the same rate. Consequently, regarding the magnitude of the response in relation to the hydrological impact, fluvial systems can be grouped into hyper- and under-sensitive systems as shown in Fig. 2.14. Whether fluvial systems respond hyper- or under-sensitive is mainly controlled by their configurational state, which in turn is given amongst others by the abundance of sediments,

[6] In the following the terms "systems configuration" and "configurational state of the system" will be used synonymical.

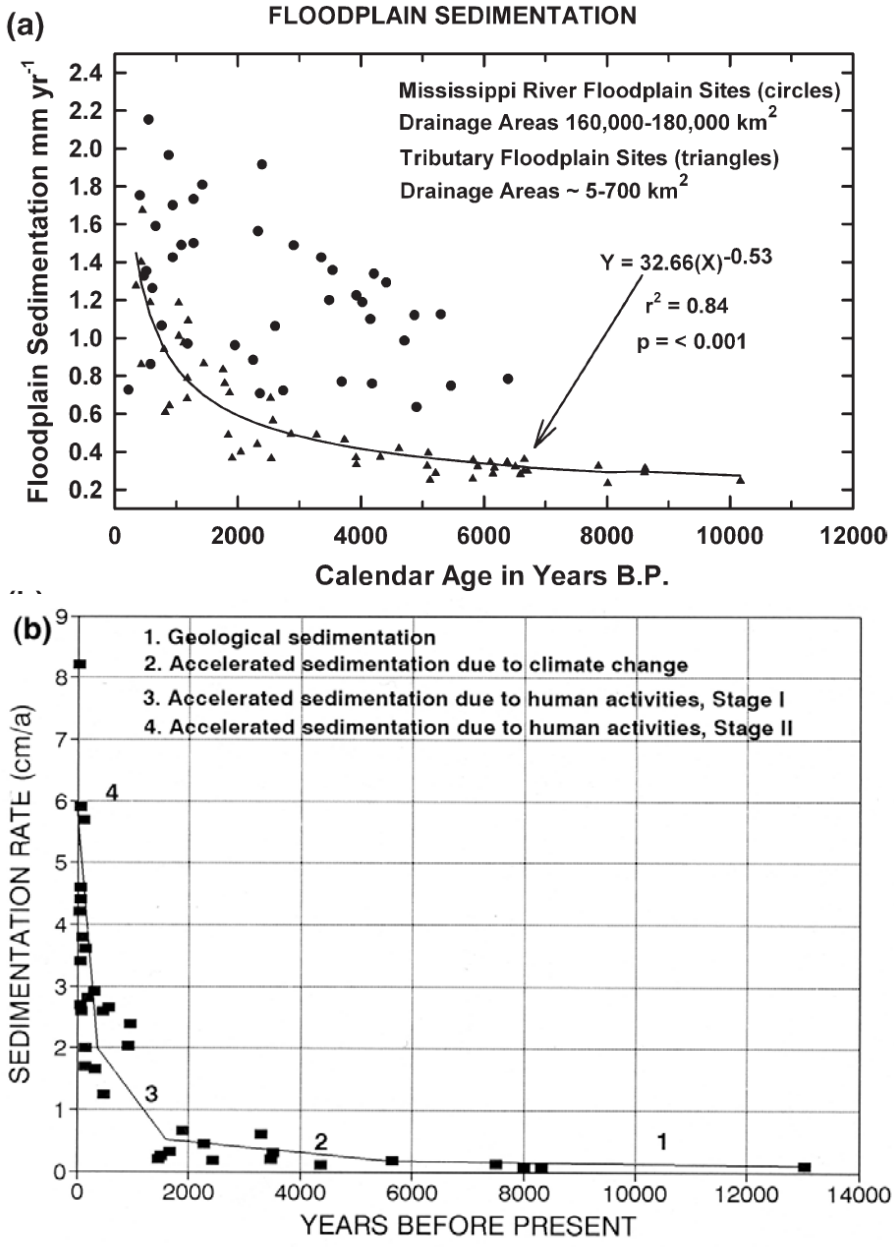

Figure 2.13: Sedimentation rates of the floodplains of a) the Mississippi River (USA) and b) the lower Yellow River (China) after Knox (2006) and Xu (1998), respectively.

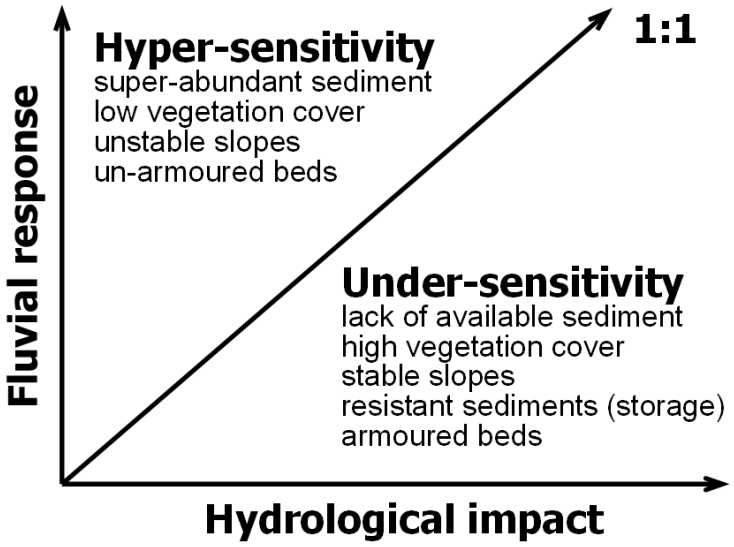

Figure 2.14: Simplified representation of unbalanced response of fluvial systems and some internal controlling factors, modified after Brown & Quine (1999).

the degree of vegetation cover, the stability of the slopes, and the degree of armouring of the channel bed. However, since every factor that controls the configurational state may change, the sensitivity of fluvial systems is not constant but changes in space and time.

Furthermore, the **spatial scale** is an important term that determines the sensitivity of fluvial systems. As shown in Fig. 2.17, more effective storage, longer residence times of sediments, decreasing sediment delivery and slower reaction time of large basins suggest a weaker level of spatio-temporal coupling of large basins (Brierley & Fryirs, 2005). Small systems generally show episodic changes with short reaction times that obscure long term directional response, while larger systems allow aggregated responses to external forcing as demonstrated by Brown & Quine (1999). Based on a global review of lacustrine sedimentation rates, Dearing & Jones (2003) calculated the relative magnitude of the human impact by dividing the sedimentation rate within a lake after and before the human impact. The data suggest that the relative magnitude change diminishes with drainage basin area (Fig. 2.15).

In the case of the modified sediment flux in the Upper Murrumbidgee catchment (South Australia), Olley & Wasson (2003) discuss the different response of the headwaters and the main channel since the European settlement (1820 AD), which caused severe gully formation. The headwaters

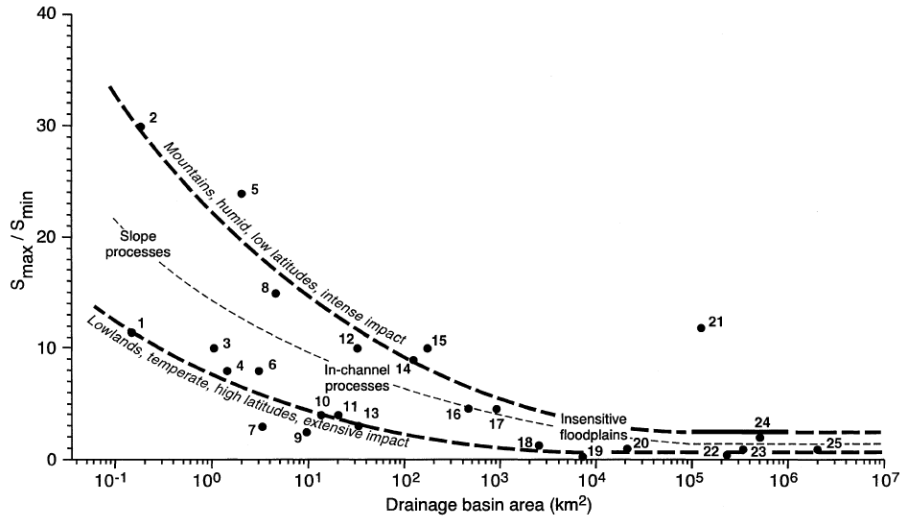

Figure 2.15: Influence of drainage basin area on the relative magnitude (S_{max}/S_{min}) of change in response to human impact, taken from Dearing & Jones (2003). S_{max} = sedimentation rate after human impact. S_{min} = sedimentation rate before human impact.

showed a rapid 250 fold increase of sediment yield and a almost complete decline until 1950 after the stabilisation of the gullies. The main channel's sediment yield increased more slowly by a factor of 200. In contrast to the headwaters, the decline of the sediment yield is still in progress and is by now 100 times the pre-European rate.

On the Russian Plain, Sidorchuk & Golosov (2003) observed a similar time lag between soil erosion and floodplain sedimentation. While soil erosion stabilised after 1980, the floodplain sedimentation in smaller rivers still increase.

In Central Europe, Lang *et al.* (2003); Houben (2006) and Rommens *et al.* (2006) recognized long time lags between the onset of the floodplain deposition and the increased soil erosion on the slope. Due to the limited slope-channel coupling before the Iron Age, sediment erosion, transport and deposition was restricted to the slopes. Floodplain sedimentation did not start before the Iron Age, when agricultural activities intensified and soil erosion dramatically increased (Lang *et al.*, 2003, there Fig. 8).

At even longer time scales, fluvial systems may still adapt to the impacts of the Late Pleistocene. In contrast to the general model of declining specific sediment yields with catchment size, data from British Columbian rivers reveal a pattern of increasing specific sediment yield at all spatial scales up

to 3×10^4 km^2. Church & Slaymaker (1989) suggest that this results from the dominance of secondary remobilization of Quaternary sediments along river valleys over primary denudation of the land surface. Therefore, rivers are still responding to the last glaciation, giving a landscape relaxation time greater than 10 kyr.

In a broader context, the Pleistocene history (e.g. valley formation and sediment supply) set the boundary conditions within which river systems have operated during the Holocene and therefore influenced the river channel pattern, the sedimentological style and the Holocene river evolution (Macklin, 1999; Brown & Quine, 1999; Slaymaker, 2006). For example, the different influence of the Late Pleistocene **inheritance** of upland and lowland rivers of Great Britain resulted in different sensitivity to Holocene climate and land use change as proposed by Macklin (1999). Formerly glaciated upland rivers are characterised by coarse gravel-bed rivers and are thus competence-limited resulting in a strong climatic signal in the Holocene sedimentary record. In contrast, lowland rivers, which were not directly affected by Late Pleistocene glaciation, are characterised by much lower stream power and finer sediment loads. The latter rivers are therefore supply-limited suggesting a stronger influence of the human impacts on their Holocene sedimentary record (Macklin, 1999).

The dependence of specific sediment yield SSY on the spatial scales (e.g. catchment area A_d) for a region as large as Canada was analysed by Church *et al.* (1999) and Schiefer *et al.* (2001). They suggest that the scaling exponent b given by:

$$SSY = a \times A_d^b \tag{2.4}$$

strongly depends on the Quaternary glacial legacy in Canada. Values greater than zero (increasing SSY with catchment size) indicate recruitment of sediment along the channel and channel degradation, caused by the abundance of Pleistocene glacial sediments and the adaption to the Holocene environmental conditions.

To summarise, the spatial scale is an important control of the fluvial response (Fig. 2.16). To due larger travel time distance and the increasing storage with catchment size, the response of large catchments to external impacts are smoothed and delayed, in contrast to small catchments, which show a strong and immediate response to external impacts.

Considering the configurational state, Richards (2002) emphasises the effects of the **drainage basin structure**, which cause a smoothed and delayed response of the fluvial system. The topology of drainage networks, for example, does have a strong impact on sediment storage and release. Elongated drainage networks with small network widths will stronger buffer discharge

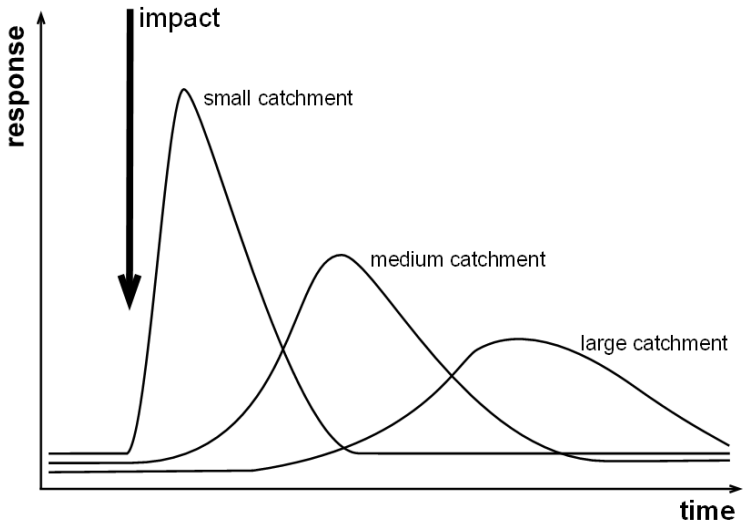

Figure 2.16: Conceptual model of external impact and scaled dependent response of fluvial system.

and therefore sediment yield than compact drainage networks with a larger network width.

Beside the disproportionate response that results from the varying sensitivity of fluvial systems, the adaption to a new equilibrium is not always straight forward. As described by Schumm (1979) the lowering of the base level caused a **complex response** of fluvial system with several cut and fill-phases that result in the formation of a complex staircase of fluvial terraces. Therefore, system response may by "highly" nonlinear with a complex change (with several ups and downs) to a single impact. In the case of the complex response, nonlinearity follows from the sediment storage that obscure the correlation between causes and effects (Phillips, 2003).

Nonlinear system behaviour corresponding to storage is also shown at shorter temporal scales, for example, in clockwise hysteresis of discharge - sediment concentration plots of single floods as described earlier (Chapter 2.1): On the rising limb of the flood, sediment concentrations are higher, due to the availability of sediments, than at the falling limb where sediment concentrations are lower, due to the sediment clearance of the channels after the flood peak.

In addition to the effects of sediment storage, **thresholds** are an important source of nonlinearity in fluvial systems (Schumm, 1979; Phillips, 2003). Thresholds generally are an expression of a system's resistance to external forces. For example, bed load is not transported unless the shear stress ex-

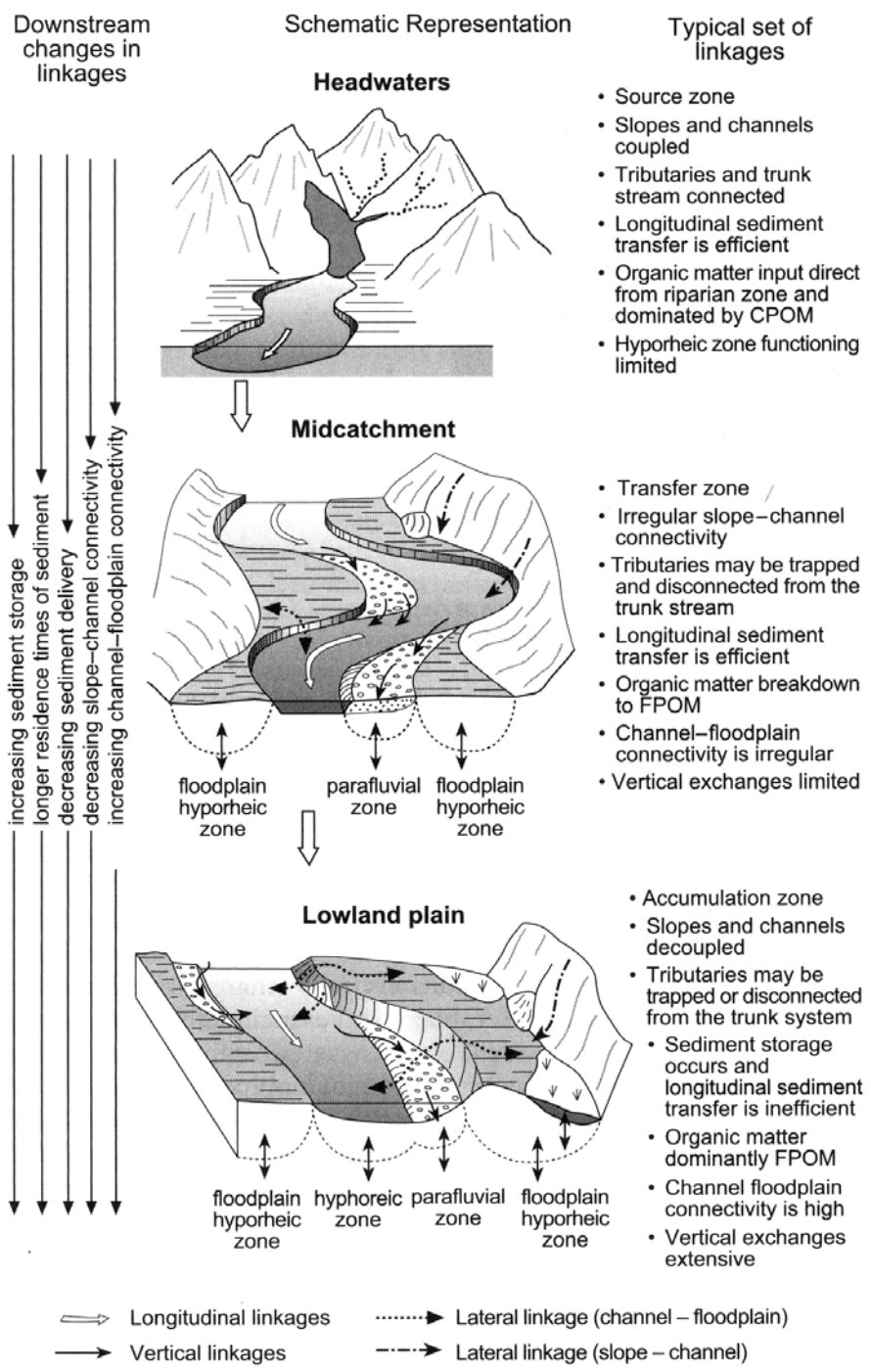

Figure 2.17: Spatial scaling of landscape connectivity in fluvial systems, taken from Brierley & Fryirs (2005).

erted by the running water exceeds a critical shear stress threshold, which is determined by armouring and the grain size of the channel bed. Considering channel migration, thresholds control the occurrence of bank failures. Slips and slab failures as the major bank erosion processes take place if the shear stresses (mainly controlled by the bank slope and the soil moisture content) exceed the threshold of bank stability (given by the cohesion of the bank material and type and degree of the vegetation) (Knighton, 1998; Fonstad & Marcus, 2003).

If system response is controlled by thresholds the correlation between magnitude of the impact and the magnitude of response is obscured. When the system is stable (far away from a threshold) large impacts may have a limited or no impact on the system. In contrast, when a system is near a threshold, small perturbations may cause dramatic responses. In the later case, the dynamical instabilities result in chaotic behaviour of the system's response (Phillips, 2003).

In general fluvial systems change their morphology and behaviour in response to environmental change. However, **autogenic adjustments** occur without any change of the external controls (Brown & Quine, 1999) but are part of the dynamic equilibrium of the system that may follow from the interaction of the system components at small scales. For example, flat or irregular channel beds are transformed into regular ripples and dunes by the collective behaviour of sand grains caused by the action of running water. At larger scales, straight channels form regular meanders that are initiated by the unstable growth of small flow perturbations (Knighton, 1998; Hooke, 2003). The meanders will grow, narrow their necks and finally be cut off from the current river leading to the formation of oxbow lakes, without changes of the external conditions.

As a result of the collective nonlinear interaction of system components at small scales, *fluvial systems are able to (self-) organize order that emerges at larger scale* (Phillips, 2006). The concept of **self organised critically** (Bak, 1988, 1996), which explains the complexity of natural systems using a holistic approach was recently applied to bank erosion processes and meander development in fluvial systems (Stolum, 1996; Fonstad & Marcus, 2003; Hooke, 2003). Hooke (2003), for example, observed an increasing sinuosity of the River Bollin (UK) to a maximum value of approximately 3 during the last 100 years. Since 1984 a series of meander cut-offs rapidly reduced the sinuosity. Here, findings suggest that rivers develop to a supercritical sinuosity at which a larger numbers of cut-offs occur, which are not simply due to increased occurrence of floods, but are caused by self-organization of the fluvial system.

In self organized systems each larger scale level includes the cumulative

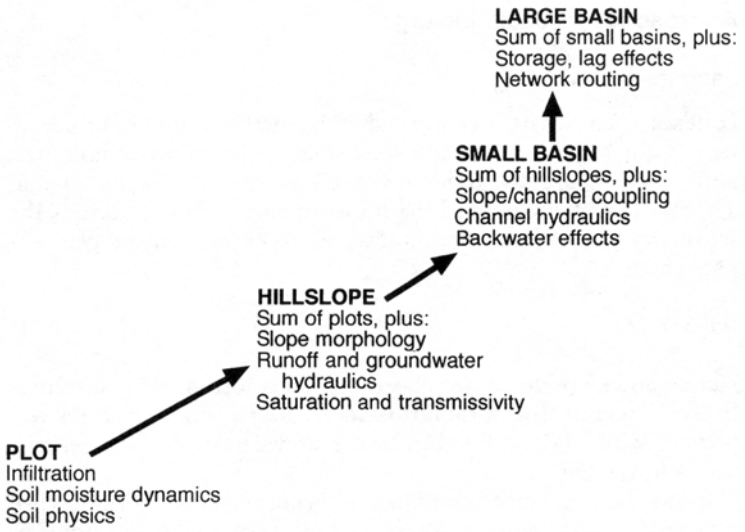

Figure 2.18: Scale linkages in the hierarchy of catchments concerning their hydrology, taken from Phillips (1999). The processes at a certain level can not be explained by the sum of each process acting at lower levels. Each transition from a level to the next higher level is linked to new considerations (e.g. processes and forms) that increase the systems complexity at each higher level.

effect of lower levels and new considerations as well that emerge at different 'levels' (Phillips, 1999; Harrison, 2001). Concerning catchment hydrology, for example, the discharge in small basins does not only depend on the sum of the discharge of the hillslopes, but also on the hillslope channel coupling, the channel hydraulics and backwater effects (Phillips, 1999, Fig. 2.18). The new considerations at the higher level result from the properties of fluvial systems at lower levels and from the scale dependence of hydrological and geomorphological processes. On the other hand processes that act at smaller scales are influenced by the condition at the higher level. Therefore, spatial scales are linked in both directions. The hierarchy of systems suggest that the understanding of river behaviour at large scales (e.g. the Rhine catchment) will neither be achieved by focusing on the large scale nor by reductionist approaches, which entirely focus on system components at smaller scales. Rather a holistic, narrative approach is imperative, in which scale linkages are explicitly considered (Harrison, 2001).

2.3.4 Relative importance of land use and climate impact

In general, the external controls of land use and climate do not impact fluvial systems independently. Extreme rainstorms that precipitate on a completely forested landscape, for example, may have hardly any effect on the sediment flux on the slopes or in the river channel. On the other extreme deforestation does not have any impact without any precipitation that causes soil erosion and consequently increases the sediment yield of a river. Whether fluvial systems respond to changes in land use or climate depend on the relationship between external and internal controls. The relative importance of these factors on the valley floor evolution, however, is still uncertain. A number of studies indicate that river systems are highly sensitive to climate fluctuations that have been modified by land use changes (Knox, 2000; Schirmer, 1995; Coulthard & Macklin, 2001; Macklin *et al.*, 2006). Especially in Germany, several authors suggest that the human impact dominates the sediment flux not only on hillslopes but also in channels (Macklin & Lewin, 2003; Kalis *et al.*, 2003; Lang *et al.*, 2003; Zolitschka *et al.*, 2003).

Reinforcing land use, climate change and extreme soil erosion had major social impacts during the 13th century in Central Europe (Bork *et al.*, 1998; Lang *et al.*, 2003). Half of the total hillslope erosion since AD 650 occurred between AD 1310 and 1350. The extreme soil erosion was favoured by intensive agricultural land use, which is characterised by wood land coverage less than 20 %, and an increased number of extreme rainfall events, especially the AD 1342 event (Fig. 2.19). The 1000 year rainfall event was widespread throughout Central Europe and caused the formation of deep gullies, the accumulation of fans and deltas and major flooding with the highest ever recorded river levels at several sites. In consequence to the 1342 event, more than one third of the population died and reforestation took place in response to the decreasing land use pressure.

To predict the relative importance land use and climate impacts on the Rhine system Asselman *et al.* (2003) combined hydrological, soil erosion, channel transport and floodplain deposition models. Based on the scenarios of a warmer, wetter and more extreme climate and a reduction in population in Central Europe during the next 100 years, the model results suggest an increased sediment supply to the rivers in the Alpine Rhine catchment and a decrease in the lowlands. Averaged over the entire basin, the erosion and sediment supply will only grow weakly. In contrast to the reinforcing land use and climate impact that dramatically increased the sediment flux through the fluvial system in the past, the tendency towards increased sediment flux given by a wetter and more extreme climate will be diminished by the decreasing

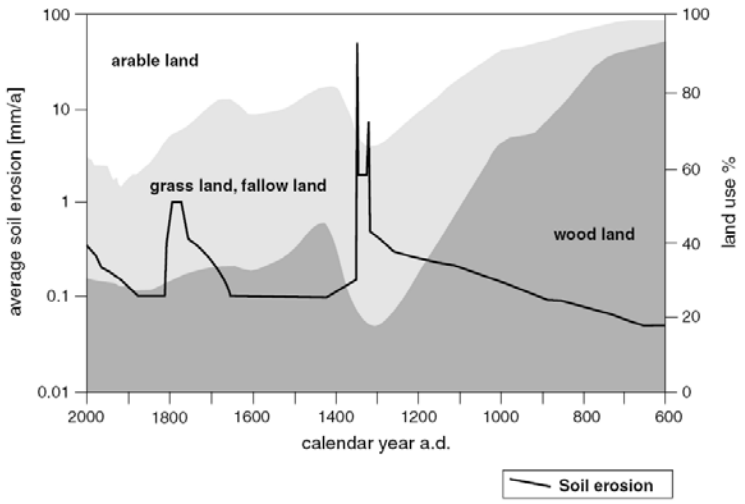

Figure 2.19: Soil erosion and land use in Central Europe during the last 1400 years, taken from Lang *et al.* (2003) based on Bork *et al.* (1998).

land use pressure caused by the decreasing population density as suggested by the land use scenarios applied by Asselman *et al.* (2003).

Even though a growing number of studies focused on the relative importance of land use and climate impacts, there are still strongly divergent views regarding the extent to which humans have influenced fluvial systems in the past. The controversy partly results from the pure dating control of the sedimentological record and the fact that fluvial archive depend on both: the human action and the natural climatic change. Furthermore, the controversy results from the strong dependency on the systems configuration that obscures the correlation between the cause (external impact) and effect (fluvial response), suggesting that there is no general rule between the relationship of land use and climate change but a complex interaction between external (e.g. land use, climate) and internal controls. The effects of the configuration must be clarified before the depositional record can be linked to the causes of change (Lane & Richards, 1997; Richards, 2002).

Chapter 3

Study site: Rhine catchment

3.1 General geographical setting

The River Rhine drains large parts ($\approx$ 185 000 km^2) of Central Europe between the European Alps (highest elevation 4275 m asl) and the North Sea (Fig. 3.1). The Rhine basin is shared by nine countries (Tab. 3.1). The River Rhine runs 1320 km from its source in the Swiss Alps (Lake Toma, 2344 masl) to its outlet near Rotterdam (NL). Regarding the landscapes that are passed by the River Rhine, the river is subdivided into six major sections: the Alpine Rhine, the High Rhine (between Lake Constance and Basel), the Upper Rhine, the Middle Rhine (between Bingen and Bonn), the Lower Rhine and the Rhine Delta (Fig. 3.1).

3.2 Geological and geomorphological setting

The Rhine basin comprises a large number of landforms ranging from the European Alps in the South to lowlands in the North. Above Basel, the major landscapes are the Alps, the Alpine foothills, the Swiss Midland and the Swiss Jura. At Basel, the River Rhine enters the Upper Rhine Graben. With an overall length of 300 km and a mean width of 40 km it forms the major segment of the Cenozoic Rift system of Western Europe. Since its formation, the Upper Rhine Graben is filled with Tertiary and Quaternary sediments, which are up to several kilometers thick[1]. At Bingen, the river enters the Middle Rhine Gorge in the Rhenish Slate Massive. The River Rhine incised an approximately 250 m deep antecedent valley since the tectonic uplift of the Rhenish Slate Massive that started during the Oligocene (Andres, 1989). North of Bonn, the River Rhine passes the Lower Rhine Embayment and the Dutch delta.

Along its path to the North Sea the River Rhine is fed by several major tributaries (Fig. 3.1 and Tab. 3.1 left). The tributaries of the Rhine drain large part of the German Central Uplands (e.g. Rhenish Slate Massive, Odenwald) and Depressions (e.g. the Hessian Depression) and the South German Escarpments. The latter is formed by slightly tilted Mesozoic sedimentary layers of different rock stability and erodibility (Bremer, 1989).

The large scale morphological structure of the Rhine basin, which results mainly from the tectonic activity, is an important factor controlling the form of the longitudinal profile of the Rhine. As shown in Fig. 3.2, three large sedimentary basins (Lake Constance, the Upper Rhine Graben and the Lower Rhine Embayment-Southern North Sea Basin) act as major sediment sinks

[1]For more details on the evolution and neotectonics of the Upper Rhine Graben see for instance the project summary of the EURO-URGENT project (Behrmann *et al.*, 2005)

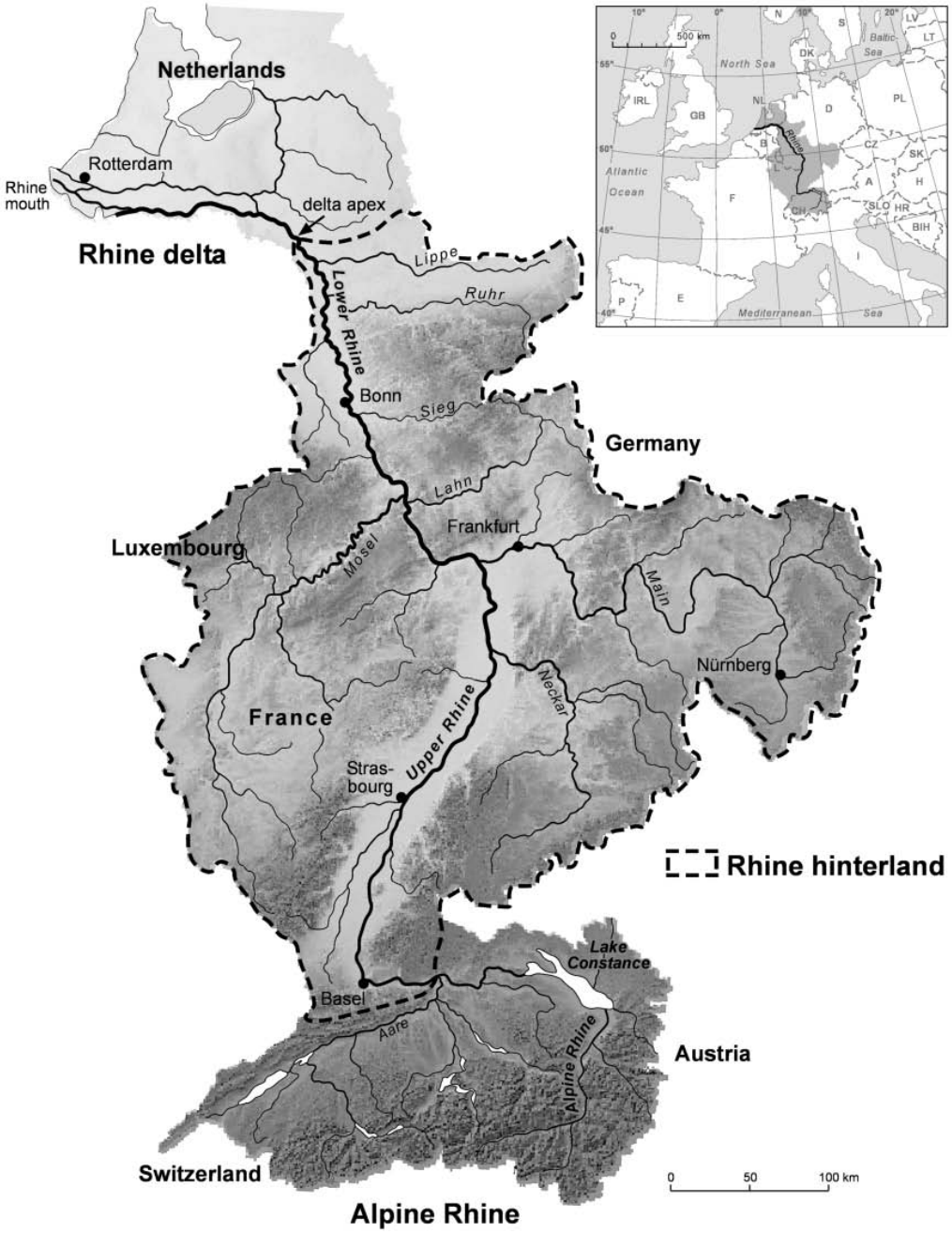

Figure 3.1: The Rhine catchment with main tributaries. River network data are taken from the Bundesanstalt für Gewässerkunde (Koblenz), shaded relief is calculated using the 3arcsec SRTM-DEM).

Table 3.1: Areas of the Rhine catchment shared by different states (left) and major tributaries with corresponding catchment area (right). Numbers are taken from Hofius (1996).

state	**km^2**	**%**
Germany	105 478	55.60
Switzerland	27 963	14.76
The Netherlands	24 500	12.91
France	23 556	12.42
Belgium	3 039	1.60
Luxembourg	2 513	1.32
Austria	2 501	1.32
Liechtenstein	106	0.06
Italy	51	0.03
Sum	189 707	100

tributary	**km^2**	**%**
Aare	17 800	9.38
Ill	4 800	2.53
Neckar	14 000	7.38
Main	27 200	14.34
Nahe	4 100	2.16
Lahn	5 900	3.11
Mosel	28 100	14.81
Ruhr	4 500	2.37
Lippe	4 900	2.58
Rest	111 300	58.67

and therefore as base levels of erosion in the Rhine system. The base levels of erosions are discontinuities in the River Rhine profile, with low channel slope above and increased channel slopes below these base levels.

Concerning the sediment transport in the Rhine catchment the Alps are almost completely decoupled from the non alpine part of the Rhine catchment, due to the near complete sediment sink of the Lake Constance. The European Alps and the upland areas in Germany (e.g. Rhenish Massif, Black Forest) are major sediment sources. The upland areas are mainly covered by periglacial slope deposits and loess, which was developed during the last Late Glacial by aeolian deposition (Thiemeyer *et al.*, 2005). The Loess covered rolling hills comprise large areas of the catchment and became intensively cultivated during the Holocene. The agricultural activity increased soil erosion and consequently the hillslopes became a main source of sediment carried downstream by the River Rhine and its tributaries (Bork *et al.*, 1998; Houben, 2002; Lang *et al.*, 2003; Mäckel *et al.*, 2003).

3.3 Climate, hydrology and modern sediment flux

The temperate climate in the Rhine catchment is dominated by the mid-latitude westerlies and the maritime Atlantic influence of the Gulf Stream. The precipitation pattern in the Rhine catchment is strongly influenced by the topography as shown in Fig. 3.3. Precipitation maximums are located

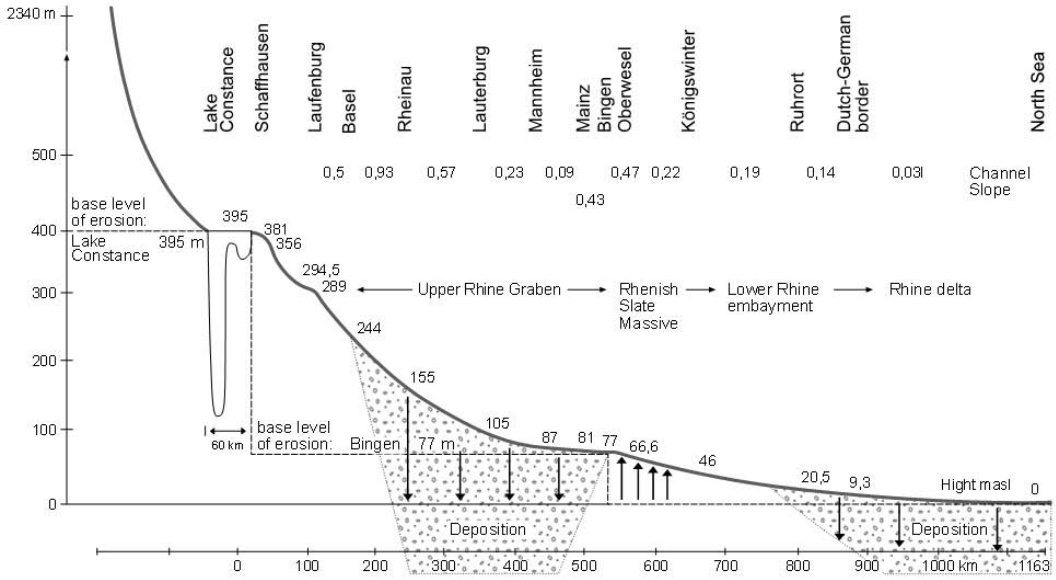

Figure 3.2: Long profile of the River Rhine, taken from Zepp (2004).

in the Swiss Alps with more than 2000 mm year^{-1}. Minima are located in topographic depressions (e.g. Upper Rhine Graben around Freiburg and the Hessian basin) with mean annual precipitation less than 500 mm year^{-1}.

Mean low flow, mean annual discharge and mean flood discharge at Lobith (near the Dutch-German border) are 1000 m^{3}s^{-1}, 2500 m^{3}s^{-1} and 6000 m^{3}s^{-1} respectively (Spreafico, 1996). Due to the strong precipitation differences the Alps contribute approximately 50 % of the run off at Lobith, even though the Alps comprise less than 20 % of the catchment area. During the summer the alpine contribution even exceed 70 % due to snow and glacier melt. The influence of the snow and glacial melt upstream of Lobith is even stronger, as shown in Fig. 3.4. The hydrological regime shifts from a glacio-nival upstream of Mainz, with peak discharges during the summer months (June and July), to a dominantly pluvial regime downstream of Mainz, with peak discharges during the winter months (January to March).

Signs of increased flood risk along the River Rhine accumulated during the last 15 years. For example, severe floods occurred during the nineties and especially in December 1993 and January 1995 (Glaser *et al.*, 2005). The increased flood risk started a lively discussion about the natural or human causes that resulted in different activities of the International Commission for the Protection of the Rhine (IKSR/CIPR/ICBR) and the International Commission for the Hydrology of the Rhine basin (CHR/KHR).

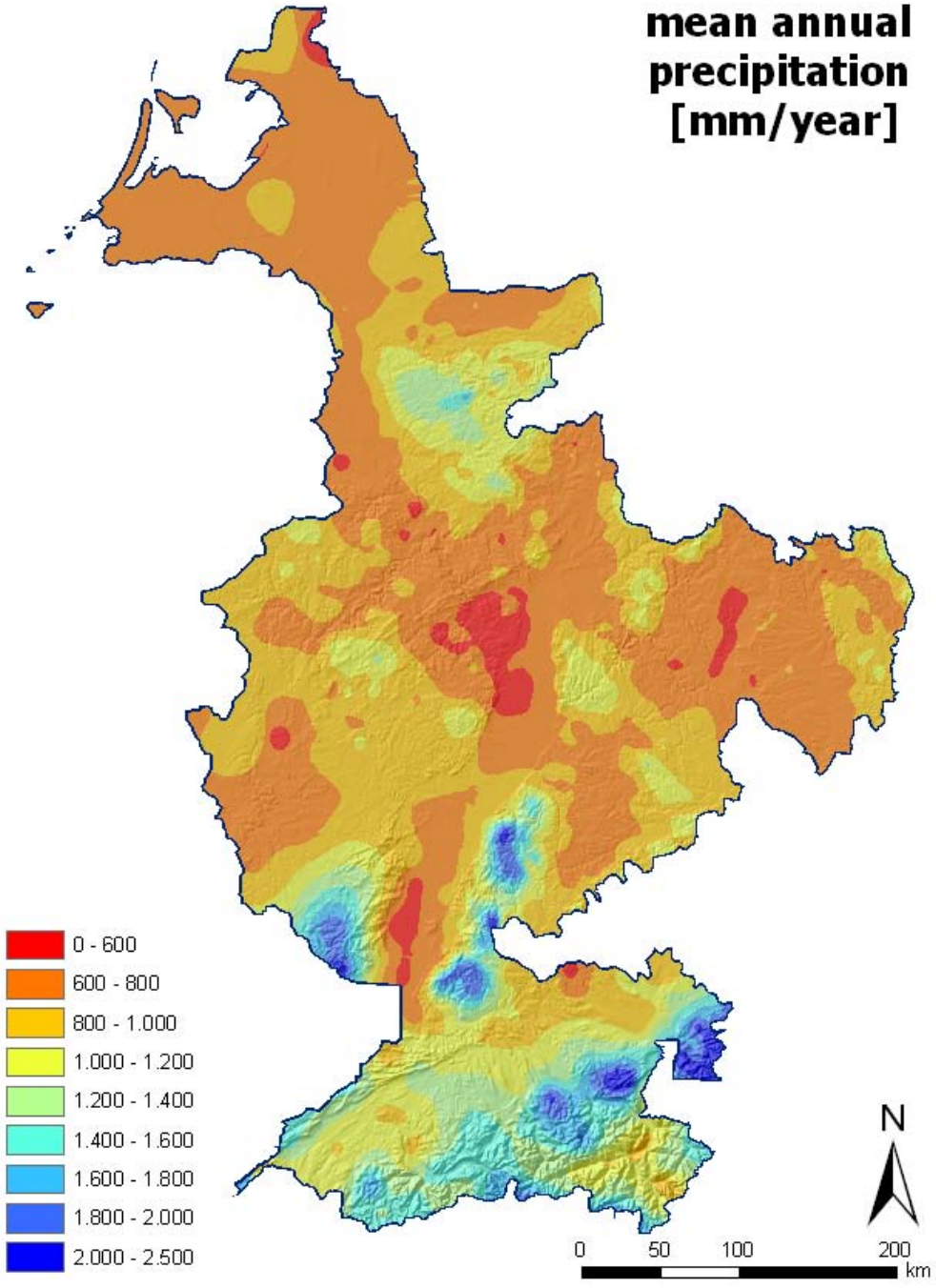

Figure 3.3: Mean annual precipitation in the Rhine catchment (data taken from the RheinGIS compiled by the German Aerospace Center, DLR).

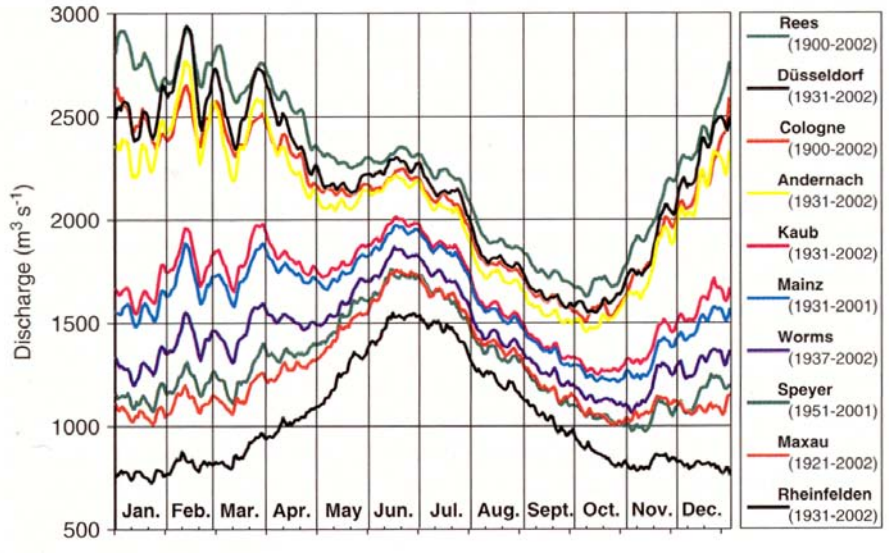

Figure 3.4: Seasonal variation of daily discharge at different gauging stations between Rheinfelden (Switzerland) and Rees (near Dutch-German border), taken from Pinter *et al.* (2006). The hydrographs show the transition from a glacio-nival to a pluvial regime.

Recently, it has been suggested that increased flood frequencies and magnitudes are the results of higher winter rainfall totals, which will increase even more during future climate change. In contrast, agricultural land-use intensification seems to have only limited impacts on the changing flood frequencies (Pfister *et al.*, 2004; Pinter *et al.*, 2006). Additionally, increased flood risk resulted from the human encroachment of flood prone areas along the river, necessitating a sustainable flood risk management in the Rhine catchment as suggested by the results of the IRMA-SPONGE project (Hooijer *et al.*, 2004).

The modern suspended load near the Dutch-German border (at Rees) is 3.15×10^6 to 3.4×10^6 t year^{-1} (Asselman *et al.*, 2003; Kempe & Krahe, 2005). Modern hillslope sediment supply for the non-alpine Rhine catchment has been model-estimated 8.8×10^6 t year^{-1} (Asselman *et al.*, 2003, their Table 5), resembling a mean erosion rate of 0.82 t ha^{-1}year^{-1} (54 mm kyr^{-1}). Modern rates however, not likely represent the Holocene mean, nor presumed Late Holocene agriculture-increased rates, for several reasons. Channelization, embankment, sediment mining and dam construction resulted in decreased sediment exchange of the river channels and neighbouring floodplains in the hinterland. In the delta embankments that influenced sediment

exchange exist since the 12^{th} century AD (Berendsen & Stouthamer, 2001). Widespread reforestation in the last centuries and modern agricultural practice has counteracted the intense erosion associated to earlier agricultural practice.

3.4 Human Impact

The River Rhine basin is one of the most populated areas in the world. Today, about 50 Mio. people (equivalent to a population density of about 250 people/km^2) live in the whole basin (Hofius, 1996, compare Fig. 2.9). However, the population is not evenly distributed across the Rhine basin but is strongly concentrated in industrial agglomerations along the Rhine and its major tributaries (e.g. Rhine-Ruhr agglomeration and the Rhine-Neckar region). As a consequence of the large population and its economic activities, the Rhine catchment has been strongly impacted by agriculture and river engineering. Today, only 36 % of the catchment is covered by forests. Agricultural land (pasture 24 % and arable crop land 28 %) covers the largest part of the catchment area and as much as 6 % is urban area.

Human impact on the Rhine catchment is not limited to the last few hundred years, but already started 7500 years ago[2]. Concerning the river channel, the strong human impact on the Rhine and its tributaries is shown by the ubiquity of bank stabilisation, flood protection (mainly Alpine and Lower Rhine), river regulation (mainly Upper Rhine), navigation improvements (Upper Rhine and Middle Rhine) and hydro-electric power stations (mainly Upper Rhine) (e.g. Kalweit, 1993; Herget *et al.*, 2005). Particularly, the river rectification by Gottfried Tulla since 1815 and the subsequent construction of 12 locks that improved navigation and gained hydro-electric power are often cited as major impacts on the Upper Rhine (Fig. 3.5). Today, the River Rhine is not only one of the most important waterways of the world, with a transport volume of about 290 million tones per year (Wetzel, 1996), but also one of the best studied rivers in the world. The numerous studies from a number of disciplines (amongst others: geology, hydrology, archaeology, climatology and geomorphology) highlight the importance of the Rhine catchment to investigate the LUCIFS objective that is the "Land use and Climate Impact on Fluvial Systems during the period of agriculture".

[2]For a brief introduction to the Holocene history of human impact see Chapter 2.2.2

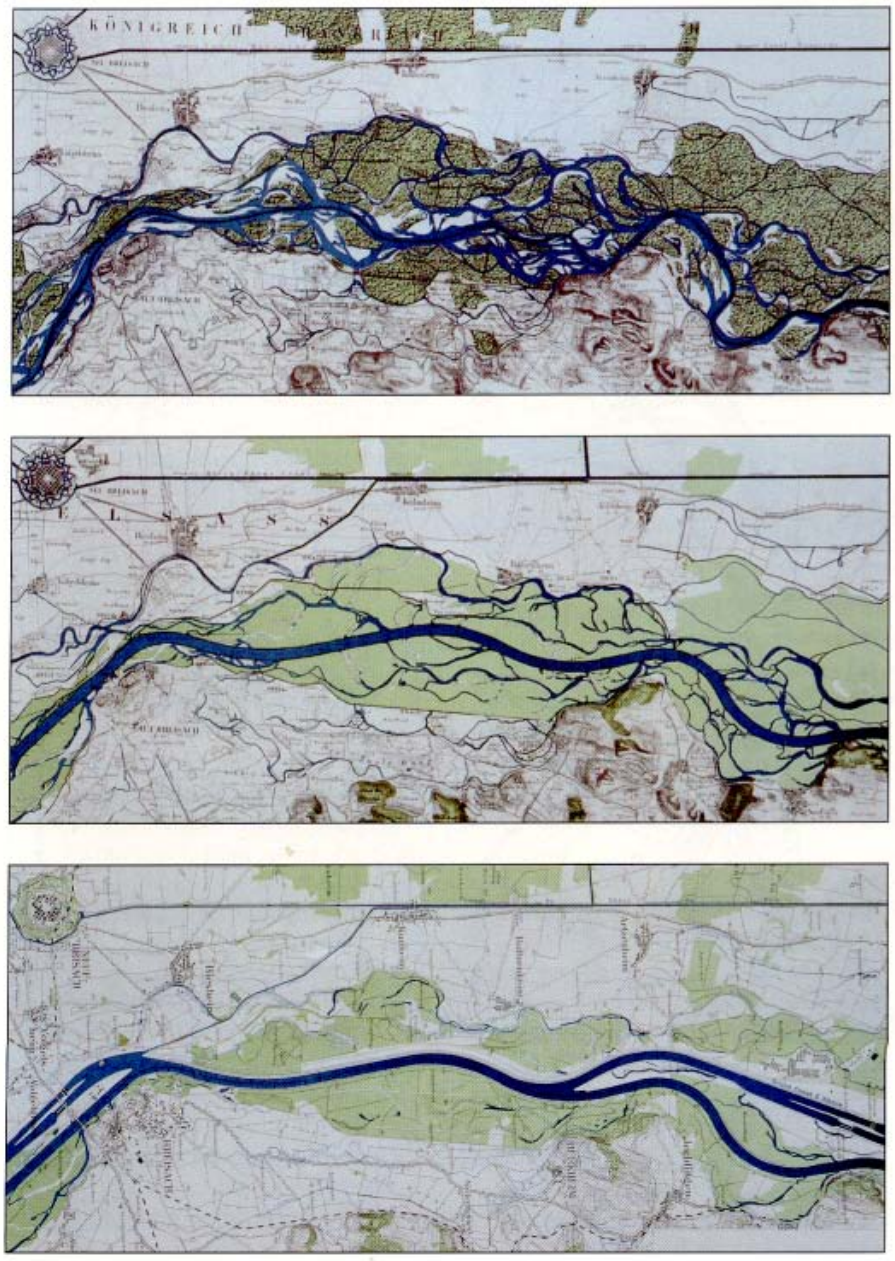

Figure 3.5: Upper Rhine valley near Breisach (Kaiserstuhl). Top: before rectification by Tulla (1828), middle: after rectification by Tulla, bottom: after construction of locks in 1963. Taken from Kalweit (1993).

3.5 Holocene valley development in Central Europe

The Late Quaternary stratigraphical record of the valley floor in the Rhine drainage basin was characterized by Schirmer (1983, 1995) and (Schirmer *et al.*, 2005, Fig. 3.6 and Fig. 2.12). Typically, across most of the valley width the substrate is formed by channel deposits of braided rivers from the last glacial, consisting of sand and gravel. In terms of Schirmer (1995) it is called the *gravel socle* which is build up by V-gravels[3] (Fig. 3.6). The sources of these Pleistocene sand and gravels are hillslope sediments that were released by solifluction and slopewash under periglacial conditions. The Pleistocene deposits are partly dissected and partly overlain by silt, sand and gravel accumulated by meandering rivers since the onset of the Holocene. The channels of these meandering rivers dissected and reworked Pleistocene sands and gravels over part of the valley width (*row terraces* build up by L-gravels[4], see Fig. 3.6). In general, at the transition from the Younger Dryas to the Praeboreal, the rivers incised into the Pleistocene deposits, leaving a terrace (mainly Lower Terrace), which is raised up to 15 m above the Holocene floodplain.

Holocene channel deposits (e.g. forming sand bars) mainly originate from fluvial reworking of pre-Holocene alluvial substratum, and are not considered to originate from hillslope erosion that took place during the Holocene. In contrast, finer sediment covering the sand and gravel (e.g. forming the levees, raising the floodplains) is considered to be the product of Holocene hillslope erosion. A blanket of sandy, silty and clayey sediments (floodplain deposits, mainly flood loams, compare Fig. 3.6) occurs on top of the channel sand and gravels that have been deposited during major floods (with water levels above those of bank full discharge). While some authors claim that the accumulation of the floodplain deposits is mainly controlled by climatic factors (Becker & Schirmer, 1977; Schellmann, 1990; Schirmer, 1995), there is also strong evidence that a major part of the flood loams is deposited during periods of extensive agricultural activity on the hillslopes, and thus may reflect periods of human-enhanced soil erosion (Lang *et al.*, 2003; Niller, 2001; Nolte, 1999; Macklin & Lewin, 2003; Zolitschka *et al.*, 2003).

The valley architecture described above applies to both the smaller upstream valleys and the larger trunk valleys in the channel network. While in

[3]V gravels are deposited by vertical accretion by braiding rivers and are generally horizontally layered

[4]L-gravels are deposited by lateral migration as point bar deposits of meandering rivers. The generally show a layering parallel to the slope of the point par

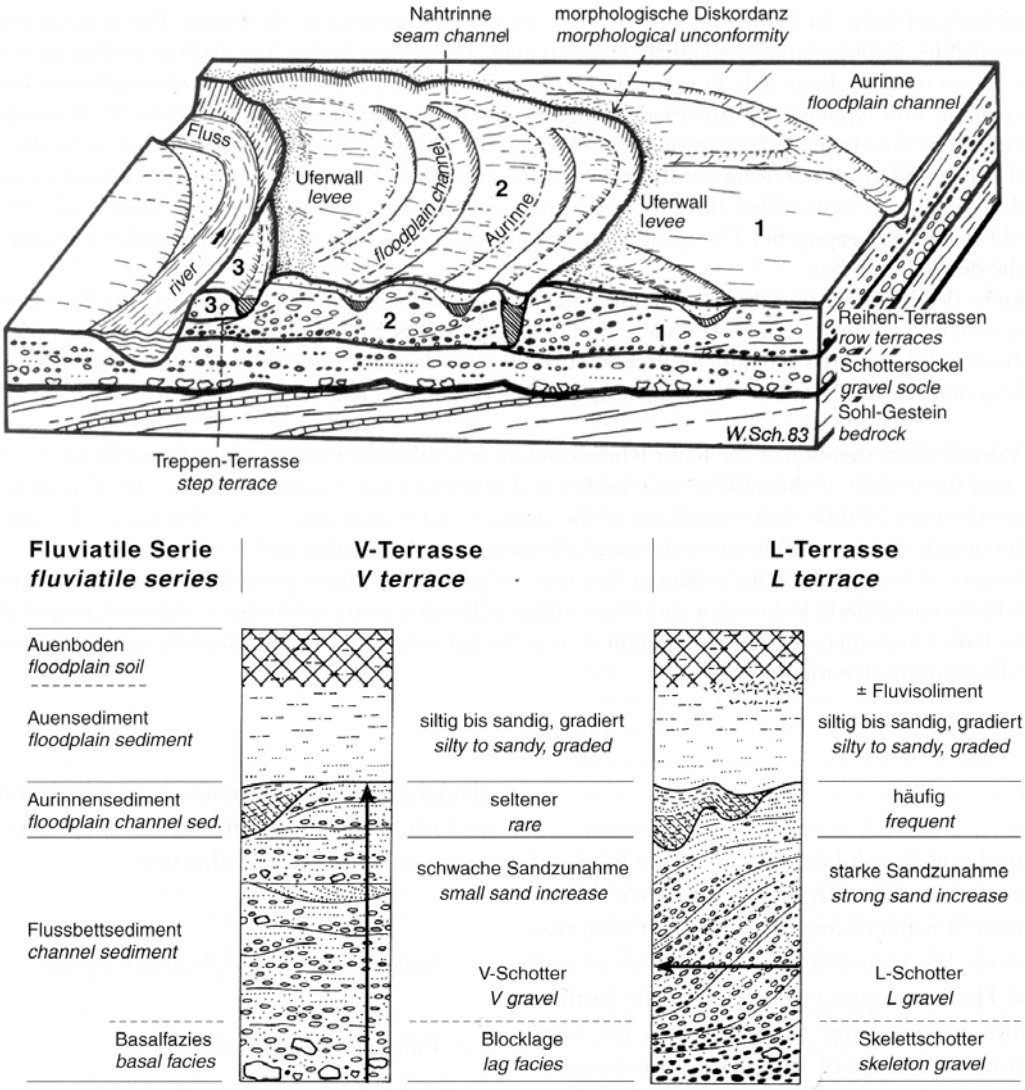

Figure 3.6: Top: block diagramme showing the general picture of valley bottoms in Central Europe. Bottom: Concept of "fluviatile series" of L- and V-gravels. L-gravels are deposited by lateral migration of river meanders at the point bar. In contrast, V gravels are deposited by vertical accretion by braiding rivers. Both figures taken from Schirmer *et al.* (2005).

smaller valleys the majority of floodplain deposits are rather young, considerable amounts of Late Glacial and Earliest Holocene floodplain deposits are preserved in the trunk valleys. In the latter valleys, these commonly form separate terrace surfaces (row terraces according to Schirmer) adjacent to the Holocene channel belt.

At the downstream end of the river system, the Rhine delta in the Netherlands consists of Holocene fluvial deposits up to 20 m thick at the present river mouth. Sedimentation in the delta is accommodated by sea level rise and tectonic subsidence (Cohen, 2005), but is most importantly the product of sediment delivery from the hinterland. The deltaic area has been a near-complete sediment trap for Rhine and Meuse sediments since the onset of deltaic deposition approximately 9000 years ago (Beets & Van der Spek, 2000; Erkens *et al.*, 2006).

3.6 Human impact on sediment fluxes in the Rhine catchment

Agricultural activities in the Rhine drainage basin date back to the Early Neolithic approximately 7500 years ago (Dix *et al.*, 2005; Kalis *et al.*, 2003; Zimmermann, 2003; Zimmermann *et al.*, 2004). Farming activity during the Neolithic was restricted to small areas within the loess-covered area and had limited impact (i.e. only locally) on soil erosion and deposition (Lang *et al.*, 2003; Kalis *et al.*, 2003, Fig 3.7). In the Bronze Age (from 2200 to 800 BC) and Iron Age (from 800 to 1 BC) agricultural areas extended and ploughing techniques changed. There are indications that the major sediment re-distribution due to soil erosion was still limited to the slopes during that time (Lang *et al.*, 2003). Dramatic (episodic) soil erosion and associated deposition of colluvial and alluvial sediments, is known from the Iron Age and from the Roman period (1 - 375 AD). Amongst others Andres (1998), Bibus & Wesler (1995) and Niller (2001) showed that the accumulation of the flood loams started during the Iron Age, which is assumed to relate to intense agricultural activities, widespread deforestation and a growing population density in Central Europe (Zimmermann, 1996). The medieval period (450 - 1450 AD) is characterized by a strongly intensified impact, culminating in heavy gullying during extreme rainfall events in the 14th and 18th centuries with high accumulation rates on hillslopes and floodplain over a significant part of the catchment. The majority of soil-erosion-derived alluvial sediment in upper tributary reaches originates from this period (Lang *et al.*, 2003, Fig 3.7).

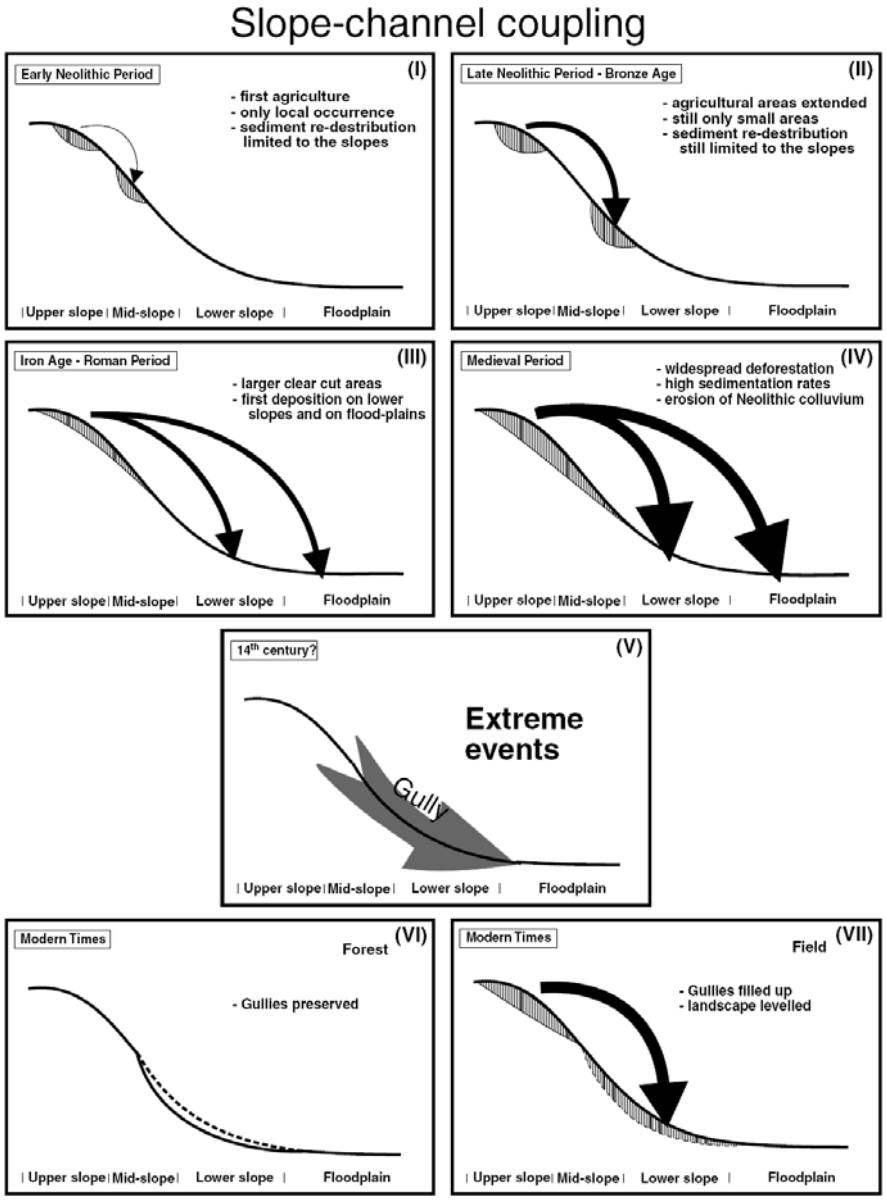

Figure 3.7: Conceptual model of hillslope-channel coupling during the period of agriculture in Central Europe, taken from Lang *et al.* (2003).

Chapter 4

Concept and methods

4.1 Problems, needs and aims

The preceding chapters discussed climate variability at different temporal scales and the general trend of increasing human impact during the Holocene. However, Holocene climate change and human activity did not develop independently but interdependently. In other words there is a causal relationship between climate change and human activity and therefore they change at the same time.

Fluvial systems responded to the complex pattern of land use and climate impact. However, sediment flux in fluvial systems is not only forced by external controls but additionally depends on the systems configuration (internal controls). According to Phillips (2003), fluvial systems show **complex nonlinear dynamics** (CND) that are described in terms of thresholds, storages, buffers, saturation and depletion, negative and positive feedbacks, multiple modes of adjustments, self-organisation and emergence. Consequently, there are considerable time lags between causes and effects and the configurational state in turn is modified by the fluvial processes (feedbacks). Furthermore, the behaviour of fluvial systems is scale dependent in time and space. However, the temporal and spatial scales are not independent from each other but appear to be coupled: i) processes that act at small spatial scales are conditions by the properties of the fluvial system at larger scales and in turn the properties at the larger scale are changed by the cumulative effects at smaller scales; ii) short-term process are connected to the long-term behaviour of the system and in turn long-term trends are influenced by short-term processes. Concerning this behaviour, rivers and their corresponding catchments represent hierarchical systems or in other words "*rivers are physical systems with a history*" (Schumm, 1977).

To understand the behaviour of rivers in the whole range of conditions and processes that controlled and will control their development and to evaluate the importance of their legacy, a long-term perspective at different spatial scales is needed (e.g. Oldfield & Alverson, 2003; Dearing *et al.*, 2006; Dikau, 2006; Gregory *et al.*, 2006). In most (if not in all) cases the record length of direct measurements and monitoring programmes is too short to cover the whole range of Holocene conditions of river response. Therefore, paleoenvironmental reconstructions based on colluvial and alluvial proxies are a necessary prerequisite to understand the relative importance of human and natural drivers on fluvial systems. Floodplains provide a range of potential sites in different stages of development at one time and of different ages that offer paleoecological data (Brown, 1996). Their frequent presence in a large variety of ecological conditions is of great advantage compared to the infrequent distribution of lakes and swamps. In contrast to lakes and swamps,

floodplains do not provide continuous records and often include hiatuses produced by erosional disturbances. The continuity of alluvial records, however, is strongly dependent on the domain of fluvial processes: aggradational rivers are likely to preserve more complete records than rivers dominated by strong channel migration (Lewin & Macklin, 2003). Additionally, nonlinearities and storage effect obscure the direct link between causes and effects in the alluvial record.

Due to the complex and nonlinear nature of rivers, the reconstruction of their history is not possible from single or several drillings or cross sections. In fact approaches that allow the *"...accounting of the sources and disposition of sediment as it travels from its point of origin to its eventual (storage within or) exit from a drainage basin"* (Reid & Dunne, 1996, p.3) are needed. Furthermore, the dynamic character of fluvial systems must be considered, as well as the different interdependent spatial scales. Several methodological implications are made necessary by the large spatio-temporal scale, which is given by the size of the Rhine catchment and the long history of human impact, and the complex nonlinear dynamics of fluvial systems:

1. The size of the Rhine catchment (185 000 km^2) and long history of human impact (7500 years) implies a considerable **historical component** that is necessary explain the fluvial response to land use changes (Schumm, 1991, Fig. 4.1).

2. Concerning the long temporal scale, **palaeogeomorphic, empirical approaches** are necessary (Brown, 1996; Dikau, 2006).

3. Due to considerable time lags between external impacts and fluvial response, **dynamic approaches** are essential to understand cause-effect relationships at different spatiotemporal scales (Wasson, 2002).

4. The failure of reductionist up-scaling approaches that try to explain landform evolution based on small scale, process-based models (Harrison, 2001) suggests a strong focus on a **top-down** approach. This implies that scale-adopted simplified models at large spatio-temporal scales are essential and give the boundary conditions for more complex models at smaller spatio-temporal scales (Fig. 4.2).

These aims are best achieved by a **hierarchy of holistic sediment budget models at different temporal and spatial scales**. It is, however, the main objective of the RheinLUCIFS program to develop a multiscale sediment budget hierarchy and to understand the "Land use and Climate Impacts on the Rhine system, during the period of agriculture".

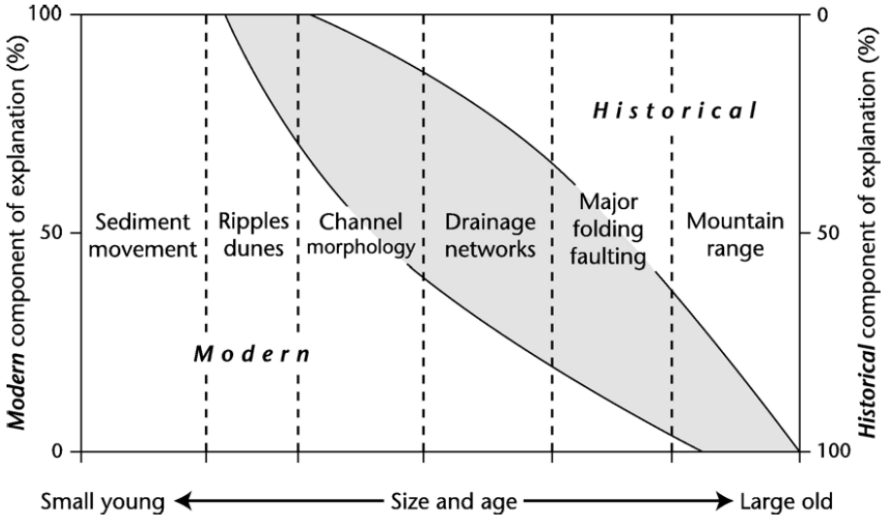

Figure 4.1: The component of historical explanation required to explain geomorphological systems with increasing size and age, taken from Slaymaker (2006), modified after Schumm (1991).

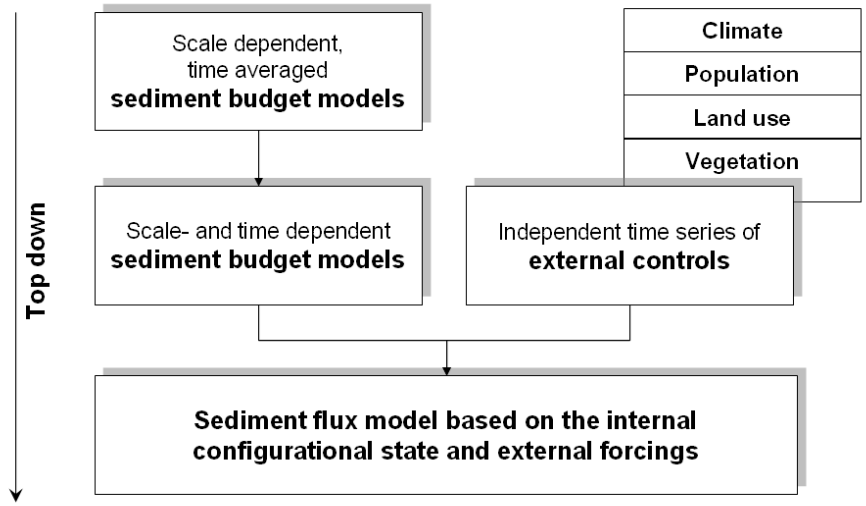

Figure 4.2: Simplified flowchart of the RheinLUCIFS concept, modified after Houben *et al.* (2006).

Sediment fluxes are an important component of biogeochemical cycles (Slaymaker & Spencer, 1998). The understanding of the sediment flux and storage at different spatio-temporal scales, therefore, allows the evaluation of biochemical fluxes that are associated with the sediment transport in the fluvial system. With respect to its effect on the global climate change, the carbon cycle is of special interest. There are numerous geomorphological studies on alluvial and colluvial sediment storage in the River Rhine catchment, which include the measurement of organic carbon content in these storages (e.g. Dambeck, 2005; Dotterweich *et al.*, 2003c; Houben, 2002; Seidel, 2004). However, little is known on long-term carbon storage in these sediments. Until now, the information available from these geomorphological studies has not been exploited in terms of biogeochemical cycles. A combined analysis of organic carbon content in alluvial and colluvial storages with large-scale Holocene sediment budgets can help to understand the long-term effect of sediment storage on the organic carbon cycle (Walling *et al.*, 2006). Due to the close relation of exogenic sediments and the endogenic production of organic matter on floodplains, the seperate analysis of sediment and organic matter on floodplains helps to interpret more accurately the environmental factors controlling the origin of floodplain sediments (Macaire *et al.*, 2006).

Based on the previous considerations, the present thesis will focus on the largest spatial scale of the RheinLUCIFS initiative, which is given by the size of the Rhine catchment, and on the entire period since the onset of agriculture. Therefore, three aims will be followed:

1. The main aim of the thesis is the modelling of a sediment budget of the non-alpine part of the Rhine catchment that integrates the sediment fluxes during the entire Holocene. However, as the focus is driven on the quantification of the floodplain storage it is assumed that floodplains are the major sediment storages at large spatial scales.

2. To evaluate the importance of floodplains as storages of organic carbon within the global carbon cycle, a conceptional fluvial carbon budget model is developed. Therefore, the storage of organic carbon in floodplains of the non-alpine Rhine catchment is estimated and compared to similar studies and short-term carbon yields.

3. To resolve temporal variations of the activity of the Rhine system, a database on ^{14}C-ages taken from colluvial and alluvial sediment storages is compiled and analysed in terms of cumulative frequency distributions and of changing sedimentation rates.

The development of empirical methods, to achieve the presented aims, was adapted to the large spatial and long temporal scale and therefore, focused

on the analysis of existing data. Due to the low data density at these scales, the applied methods provide scale-adapted, rough estimates of i) sediment and carbon storage, ii) soil erosion and iii) temporal activity. Following a top-down approach, the thesis tries to fix boundary conditions for studies at smaller spatial and temporal scales.

4.2 Holocene fluvial sediment budget

In the Rhine system under Holocene climate conditions, relative fine sediment is produced, stored and remobilised on the hillslopes and subsequently transported to the fluvial system (Fig. 4.3). Sediment that is released to the rivers is transported further downstream within river channels. Along the channel, sediment is stored on floodplains, due to vertical accretion during floods. For the sediment budgets, the combined volume of sediment trapped in floodplains in the hinterland and in the Rhine delta is used (Fig. 3.1). The latter area can be considered a near-complete trap since the coastal barrier formed at the beginning of the Middle Holocene (Erkens *et al.*, 2006). Therefore the amounts of Rhine sediment that escaped from the study area have been small and the data comprises a near-complete sediment budget for approximately 125,000 km^2 of Central Europe.

The sediment budget for the alpine part of the Rhine catchment (Fig. 3.1) is excluded in this study for reasons of sediment transfer discontinuity. Lake Constance and smaller lakes in the Swiss alpine foreland function as major sediment sinks. This causes the alpine budget to be effectively decoupled from the downstream Rhine.

Within sediment budget studies, sediment delivery ratios (*SDR*) describe the proportion of sediment leaving an area, relative to the amount of sediment eroded in that area. The proportion of erosion-generated sediment that reaches the river is referred to as the hill slope *SDR* (or *HSDR*). In contrast, the proportion of sediment that reaches the outlet compared to the sediment delivered to the channel is referred to as the channel *SDR*, or *CSDR* (terminology following Asselman *et al.*, 2003). In our calculations, we only assess the *CSDR* of the Rhine catchment, as colluvial sediments that are stored on hill slopes were not recorded in that study.

4.2.1 Estimation of Holocene floodplain volumes

To estimate the sediment storage of Holocene floodplains, the volume S_V was calculated by multiplying the area A_f and the average thickness D_f of Holocene deposits as digitized from maps and queried from borehole data.

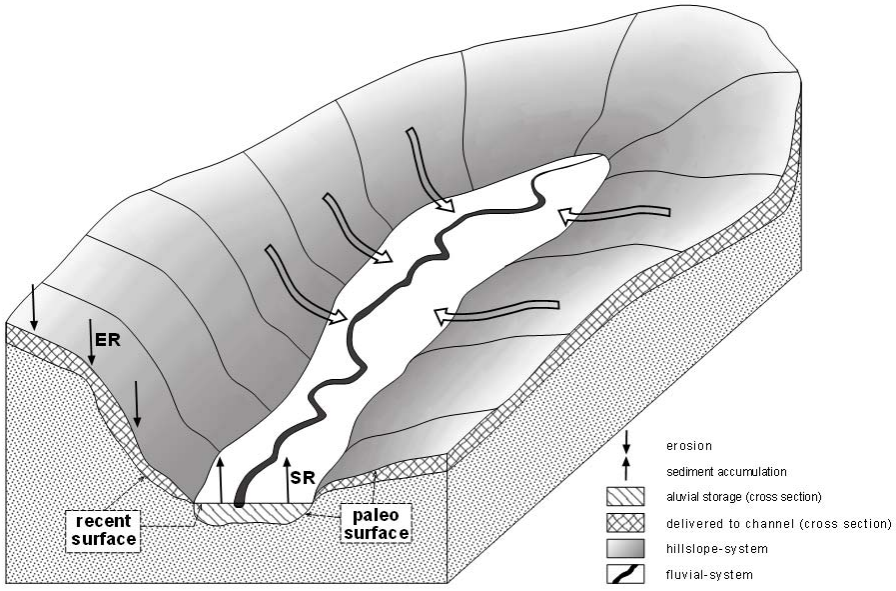

Figure 4.3: Sediment fluxes towards the floodplain storage: schematic representation of the sediment budget approach used in this study.

Due to differences in available data and stratigraphic characteristics the calculation methods differ for the German/French hinterland and the Dutch delta (Fig. 3.1).

4.2.2 Calculation of hinterland volume

Digitised geological maps were used to estimate the **area of the Holocene floodplains** A_f. The GK200 map series (scale 1:200000) used covers approximately 90 % of the study area (Fig. 3.1). The area of Holocene clayey, silty and sandy alluvial sediments was extracted from these maps. Due to the GK200 map scale, narrow floodplains of rivers with small catchments are not resolved. However, the complete floodplain area (even of the smallest floodplains) is assumed to be represented in the geological map series GK25 (scale 1:25000). To estimate the excess amounts of floodplain area, not represented in the GK200, an **up-scaling approach** was used, because the GK25 map series only covers a limited part of the study area. The areal extent of floodplains, as mapped with GK25-resolution, was estimated for the entire catchment, based on floodplain widths extracted from the GK25 (perpendicular to the channels), and the river network derived from the SRTM 3-arcsec. digital elevation model (SRTM-DEM). The up-scaling was done

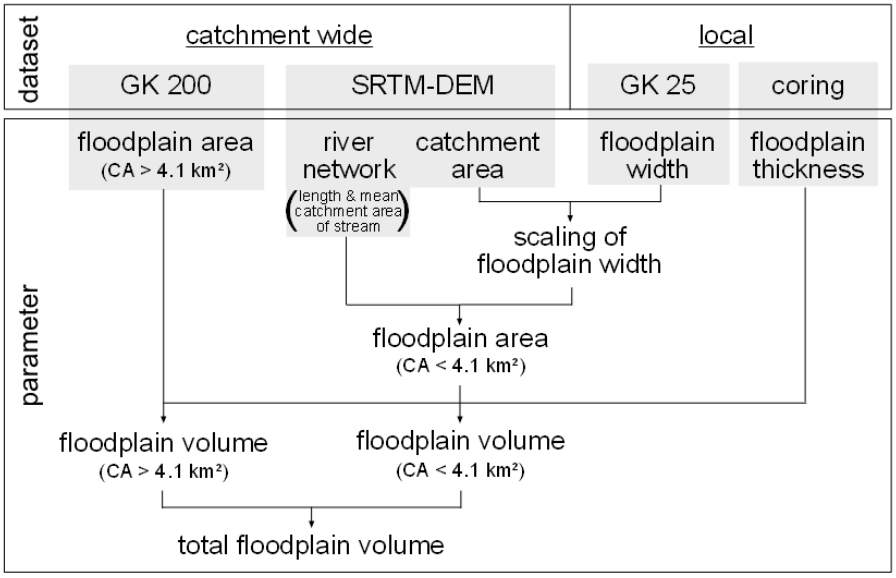

Figure 4.4: Flowchart for calculations yielding the Holocene floodplain fines volume of the Hinterland (Results in Tab. 5.1).

using the following procedure (Fig. 4.4):

- Along 467 cross sections the floodplain width w and catchment area A of the corresponding rivers was measured. This was done using the floodplains extracted from the GK25 and the flow accumulation derived from the SRTM-DEM. The scaling behaviour of the floodplain width was investigated using power law regression of the form:

$$w = a \times A^b \tag{4.1}$$

  with $a = 60.8$ and $b = 0.3$ and a correlation coefficient of $R^2 = 0.5$ (Fig. 4.5).

- The minimum catchment area of floodplains as represented on GK25 and GK200 maps was estimated. The mean values of the minimum catchment area obtained from 534 floodplains of the GK25 and 260 floodplains of the GK200 are 0.3 and 4.1km^2 respectively. This suggests that in catchments with areas between 0.3 and 4.1km^2 floodplains exists, but are not represented in the GK 200.

- The river network was extracted from the SRTM-DEM. The minimum catchment area of streams (0.3km^2) was chosen correspondingly to the

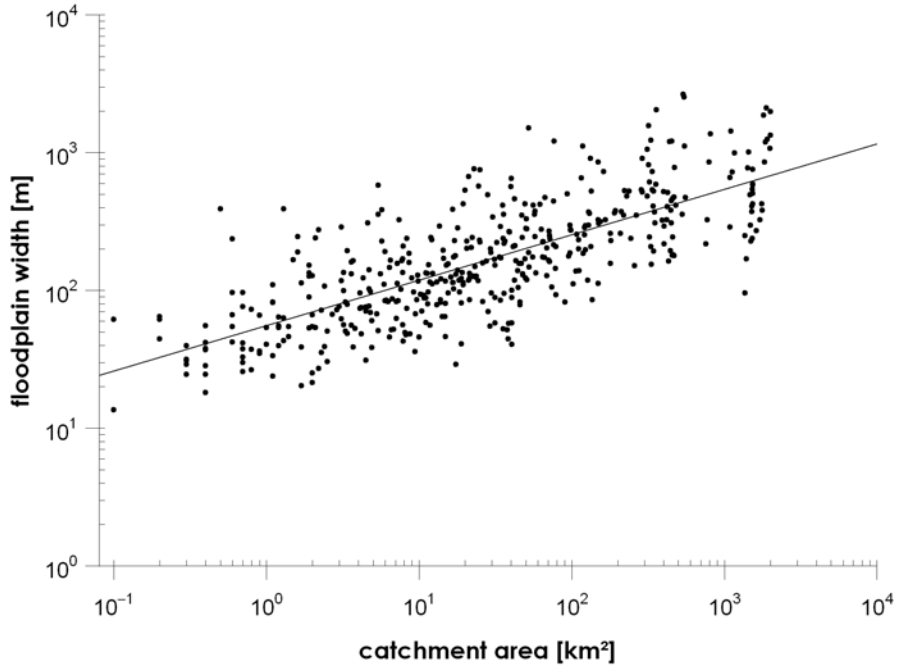

Figure 4.5: Floodplain width (w) vs. upstream catchment area (A_d). Regression calculated for 467 cross-sections combining 1:25,000 geological maps and catchment area extracted from the SRTM 3arcsec digital elevation model: $w = 60.8 \times A_d^{0.3}$ ($R^2 = 0.5$).

minimum catchment area of the floodplains that are represented within the GK25. For every stream segment (that is the river channel between two confluences) the length and mean catchment area was calculated.

- To calculate the floodplain area of channels that is not represented in the GK200 only stream segments with catchment areas smaller than 4.1km^2 were considered. The floodplain width of the remaining stream segments, with catchment areas between 0.3 and 4.1km^2, was calculated using the scaling relation (Eq.4.1). Eventually the floodplain area was estimated based on the floodplain width and the length of the stream segments.

The total floodplain area is the sum of the area derived directly from the GK200 (see column "larger floodplains" in Tab. 5.1) and the excess area calculated using the above up-scaling procedure (column "smaller floodplains" Tab. 5.1). The uncertainty of the areal extend were assumed to be 20% and 50% for the floodplain area extracted from the GK200 and the floodplain

area calculated using the up-scaling approach, respectively.

The **average thickness of floodplain deposits** D_f for the Holocene was estimated based on published core data, from 563 drillings from different locations in various floodplains across the Rhine catchment. A database was set up, to allow for spatial analysis of the core data and assess suitability of the core data for estimating D_f. A large number of core data originate from the work of several German geological surveys (Geologische Landesdienste). The base of Holocene floodplain deposits was queried from the core data. Hereto we used the transition from (dominantly) silty clay / clayey silt to (dominantly) sandy and gravely substrate, corresponding to the transition between overbank deposits and deposits of former river beds. For the area of Holocene floodplains (see above), in our calculations the full thickness of floodplain deposits is attributed a Holocene age. For a selection of boreholes, mainly from the wider trunk valleys (e.g. data from Houben, 2002; Nolte, 1999; Shala, 2001), it is known more exactly what proportion of the thickness is of Holocene age and only that proportion entered the calculations. The resulting data set yielded a mean D_f of 1.6 m, with a standard deviation of 0.4 m. Quantification of the thickness of floodplain deposits is probably less accurate than the floodplain area calculation, because of difficulties differentiating Holocene and Pleistocene sediments, limited availability of core data and consequently a biased and clustered distribution of available data. No significant difference in D_f for different catchments nor a relation between D_f and upstream catchment area A_d were discovered within the dataset (Fig. 4.6). Because floodplain sediment thickness varies over short distances as much as it does over large distances, the average thickness can be used to calculate sediment volumes. Thus we used one value for floodplain thickness for all subcatchments (Tab. 5.1), independent of their size. The relative large number of boreholes considering catchment size, still results in a reasonable estimate of overall mean thickness. For now, an error of 25% of D_f was assigned in the calculations. As part of the sensitivity test, volumes using an extreme thin (1 m) and extreme thick (2 m) floodplain covers were calculated.

The **volume of floodplain deposits** was calculated by multiplying A_f and D_f for all subcatchments (Tab. 5.1), including for error propagations in volume and thickness estimates.

4.2.3 Calculation of the delta volume

To assess floodplain sediment storage in the delta, the starting point was to calculate the total amount of Rhine and Meuse sediment trapped behind the coastal barrier in the Netherlands (Erkens *et al.*, 2006). In contrast to the

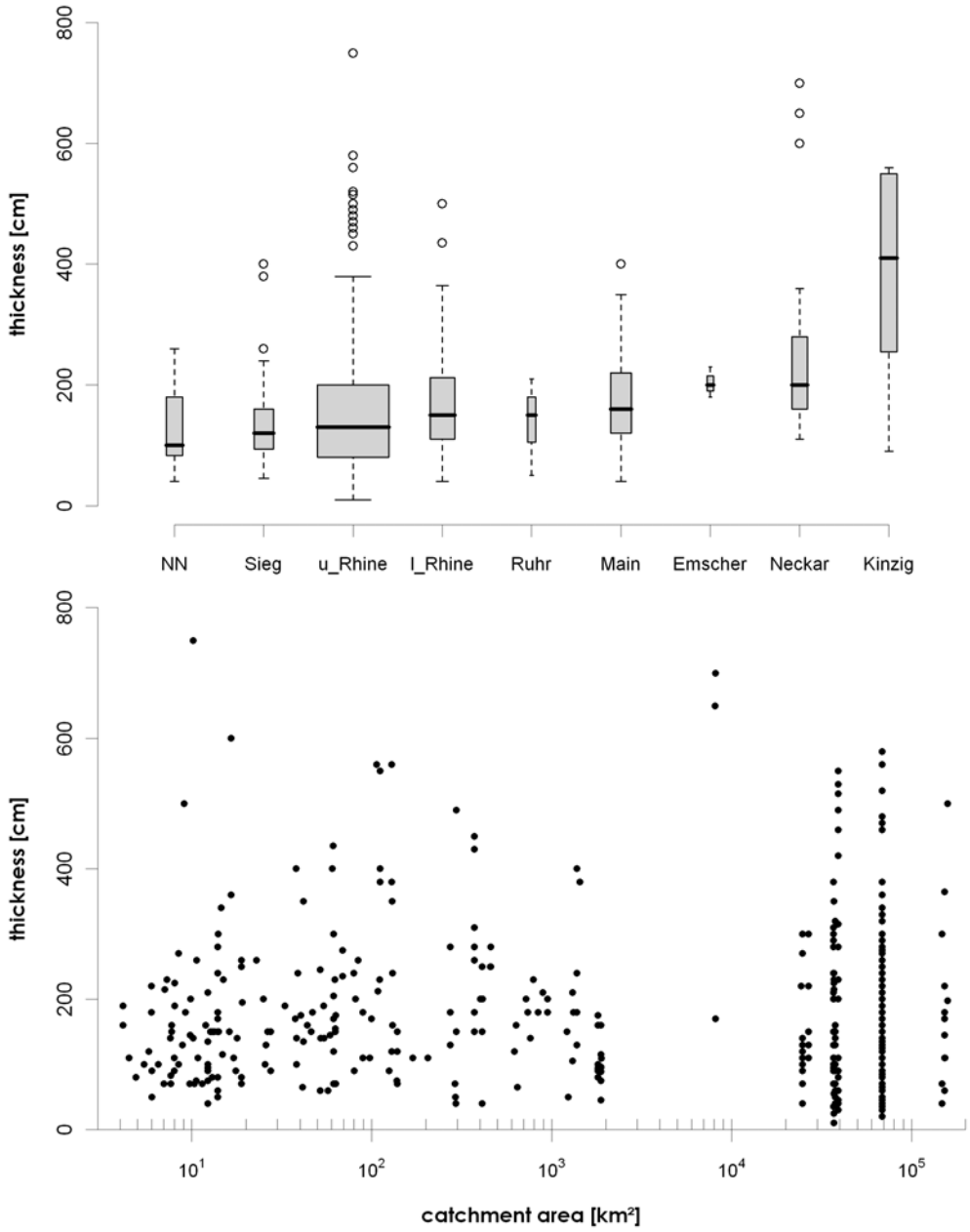

Figure 4.6: Catchment-wide Holocene thickness of floodplain fines. A) Boxplot of Holocene floodplain thickness ordered by subcatchment. Boxes have widths proportional to the number ($\sqrt{N}$) of data points. u_Rhine and l_Rhine correspond to the Upper Rhine and Lower Rhine valley and their smaller tributaries. B) Floodplain thickness vs. catchment size.

upstream valleys where the floodplain cover is of relative constant thickness, the delta volume is wedge or prism shaped. The delta volume is enveloped by the buried surface of the last glacial Rhine palaeovalley and by the modern land surface. Extensive borehole data (Berendsen & Stouthamer, 2001) were used to create a DEM of the Late Pleistocene surface (cell size 250x250 m). A second DEM (same cell size) was created for the modern surface, by resampling a high resolution DEM available from laser altimetry (data from The Netherlands Ministry of Transport, Public Works and Water Management). Calculating their difference yields the thickness of the Holocene deposits for each cell, which after summation gives the total volume of the Holocene prism (Cohen, 2005; Erkens *et al.*, 2006). We defined the northern and southern limits of our prism as the zone where floodplain deposits were less than a meter thick. Palaeogeographical reconstruction (Berendsen & Stouthamer, 2001) has revealed that in the SE of the delta, sediments are derived from the adjacent Meuse catchment. This area was excluded in the volume estimates (Erkens *et al.*, 2006). The Dutch-German border is at the apex of the today's deltaic channels and was taken as an upstream boundary. Downstream towards the modern coast, fluvial delta deposits grade into tidally influenced deposits (estuaries, inlets, lagoons). Fine grained fluvio-lagoonal deposits in the central Netherlands are included in the delta sediment volume, because these are probably all Rhine derived. Sandy channel belts and coastal sands are excluded because these are bed-load derived and do not originate from Holocene erosion of hinterland hillslopes. Peat occurs extensively in central parts of the lagoon, marking an area that was starved from both tidal and fluvial sediments. The western limit of the delta was defined as where peat amounts for a maximum proportion of total Holocene thickness. Because deposition in the delta is limited to the last 9000 years, we multiplied volumes by 10/9 to simulate a 10000 years volume. In additional calculations, we use work on groundwater level rise (Cohen, 2005) to estimate the proportions of the total deltaic volume, associated to shorter timeframes (T=7000, 5000 and 3000 years). This builds upon the insight that sedimentation in the delta was governed by accommodation provided by sea level and groundwater-rise (Tab. 5.2).

4.2.4 Erosion rate calculations

Assuming that large amounts of sediments related to hillslope soil erosion are stored within floodplains, the volume of the accumulated flood loam is a proxy parameter for the sediment volume that has left the hillslope system during the Holocene. Defining hillslope erosion as the amount of material that is delivered to the channel network, the erosion rate E_R can be estimated

based on the sediment volume S_V stored on the floodplains in a time interval T.

Based on the work of Einsele & Hinderer (1998) and Hinderer (2001), we calculate erosion rates E_R^* and E_R (in mm kyr^{-1} and t ha^{-1} year^{-1}, respectively) as:

$$E_R^* = \frac{S_V}{T \times (A_d - A_f)} \times \frac{1}{1 - CSDR} \qquad [LT^{-1}] \qquad (4.2)$$

$$E_R = \rho_B \times E_R^* \qquad [ML^{-2}T^{-1}] \qquad (4.3)$$

with A_f=floodplain area, A_d=catchment area and $A_d - A_f$ = erosive area (that is the catchment area without the floodplains, as quantified in Tab. 5.1) and ρ_B=bulk density of the alluvial sediment. The channel sediment delivery ratio *CSDR* in Eq.4.2 describes the proportion of the eroded material leaving the river at the downstream end of the studied area (as a percentage of the amount of sediment delivered to the channel network over the same timeframe).

The time interval T, over which E_R^* is averaged, is arbitrarily chosen to be 10000 years (i.e. the Holocene from the Boreal chronozone onwards). To resolve the issue of response to growing human impact, we also performed calculations for T=7000, 5000 and 3000 years. The latter calculations explore a hypothesised impact of agriculture-induced leading to gradually increasing rates of sediment supply, by considering a bias in the average age of floodplain sediments towards the younger side, especially in smaller catchments in the hinterland. To evaluate the impact of unknown amount of sediment that has left the Rhine catchment during the Holocene, scenarios of *CSDR*s of 0%, 10%, and 30% were calculated. For all the scenarios, the estimations errors were calculated following Gaussian laws of error propagation.

Colluvial sediment that is still on the slopes has not yet contributed towards the floodplains, and hence is not accounted for by our results. Erosion rates calculated from floodplain volumes therefore are expected to be smaller than erosion rates resulting from e.g. soil profile truncation studies for the same system. The latter method has been widely applied to estimate long-term soil erosion across Rhine tributary catchments (e.g. Bork *et al.*, 1998; Lang *et al.*, 2003; Preston, 2001; Seidel, 2004). In a comparison, our rates should be considered a minimum estimate of total erosion.

Table 4.1: Studied region, number of *TOC* measurements and drill locations and used *TOC* estimation method of analysed publications.

publication	region	***TOC***	drill	Method
Dambeck, 2005	Nothern Upper Rhine	339	25	Wet-comb
Houben, 2001	Wetter	527	7	CHN
Nolte, 1999	Wetter	183	3	CHN
Wunderlich, 1998	Amöneburger Becken	81	2	CHN
Seidel, 2004	Southern Upper Rhine	20	5	CNS
Hilgart, 1995	Altmühl- & Danube-Valley	188	21	Wet-comb
Niller, 1988	around Regensburg	613	95	Wet-comb

TOC = total organic carbon, Wet-comb = Wet-combustion, CHN = CHN element analyser, CNS = CNS element analyser.

4.3 Holocene alluvial *TOC* budget

4.3.1 Data analysis

An organic carbon database was compiled that includes 1948 measurements of organic carbon content from 177 cores in 7 different publications (Dambeck, 2005; Hilgart, 1995; Houben, 2002; Niller, 1998; Nolte, 1999; Seidel, 2004; Wunderlich, 1998, see Tab. 4.1). The data originate from the German parts of the Rhine and the Danube catchments (Fig. 4.7). Besides the total organic carbon (*TOC*) the database contains depth, sedimentary facies, grain size distribution (clay, silt and sand content). If measured, carbonate carbon, calcium carbonate and the ^{13}C of organic carbon was stored in the database as well (but not analysed here). If only organic matter content was reported, the *TOC* was calculated by division with 1.72 (e.g. Boden, 1996; Wunderlich, 1998). *TOC* was measured using a CHN or CNS element analyser (Houben, 2002; Nolte, 1999; Seidel, 2004) or by wet-combustion due to oxidation (Dambeck, 2005; Hilgart, 1995; Niller, 1998).

The *TOC* measurements were classified based on the sedimentary facies that are defined mainly by their depositional environment, genesis, grain size and in the case of carbon rich sediments by their *TOC* content (Tab. 4.2). However, an unequivocal classification was not always possible do to the fact that different authors address similar sediments with different terms. If similar sedimentary facies did not show a significant difference in their mean *TOC* values they were grouped to one facies. This resulted in the large number of sedimentary facies of channel fill deposits, because the used nomenclature on channel fills varies significantly between different authors. Sedimentary facies

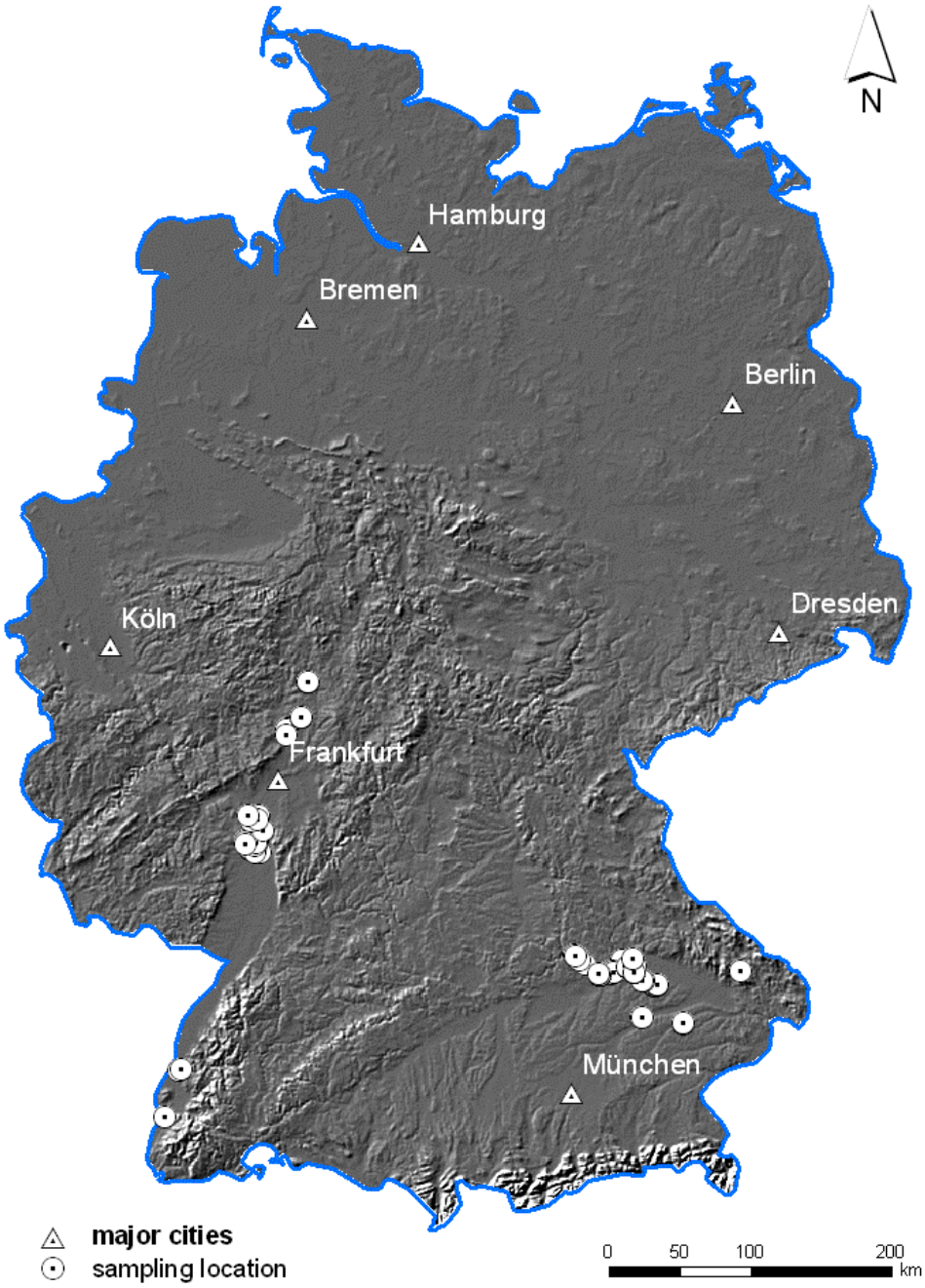

Figure 4.7: Shaded relief map of Germany with *TOC* sampling locations indicated.

Table 4.2: English and German names and abbreviations of sedimentary facies used for the classification of *TOC* measurements.

Facies (english name)	**Facies (german name)**	**Abbreviation**	**Depositional environment**
Flood loam	Auenlehm	FL	Overbank
Younger flood loam	Jüngerer Auenlehm	yFL	deposits
Older flood loam	Älterer Auenlehm	oFL	
Flood sand	Auensand	FS	
Flood clay	Auenton	FC	
Pleistocene/Postglacial overbank deposit	Hochflutsediment	pOB	
Levee deposit	Uferwallsediment	LEV	
Humic basis layer	Humose Basisschicht	HBL	
Black floodplain soil	Schwarzer Auenboden	BFS	
Gyttja	Mudde	F	Channel fill
Minrerogenic gyttja	Minerogene Mudde	Fm	deposits
Silty gyttja	Schluffmudde	Fmu	
Gyttja	Detritusmudde/ Torf	Fhg	
Peaty Gyttja	Torfmudde	Fhh	
Peat	Torf	H	
Channel fill	Rinnenfüllung	CF	
Holocene channel	Holozäne	CBS	Channel bed
bed sediments	Gerinnebettsediment		deposits
Gravels	Schotter	Gf	
(not specified)	(undifferenziert)		
Lower Terrasse gravels	Niederterassenschotter	NT	
Colluvium	Kolluvium	Col	Slope deposits
Loess	Löß	Lo	

were grouped according to their depositional environments into i) overbank deposits, ii) organic rich channel fill deposits, iii) channel bed deposits and iv) slope deposits (compare Tab. 4.2).

In order to test whether fluvial sedimentary facies are a suitable proxy for carbon content, we employed the open source R Project for Statistical Computing (R Development Core Team, 2005). As normal distribution was not given for some subsets, we employed the nonparametric Kruskal-Wallis test to evaluate the significant influence of the sedimentary facies and the depositional environment on *TOC* content. A pairwise Wilcox rank sum test was applied to detect differences of mean *TOC* content between each combination of sedimentary facies and the depositional environment. Additionally, the variation of *TOC* with depth and clay content was estimated. For the

latter, exponential regression of the form

$$TOC = a \times e^{b \times \text{clay}} \tag{4.4}$$

was used.

4.3.2 Conceptual carbon budget model

The carbon budget of fluvial systems is strongly coupled to the flowing water and transported sediments. The hydrologic export of carbon from the hillslope system represents the major input into the channels. This input of allochthonous carbon may be rather large compared with the autochthonous primary production within the aquatic channel system (Cole & Caraco, 2001). In general, large rivers are characterised by the supersaturation of the riverine CO_2 concentrations, which results from the high CO_2 concentrations of the groundwater input and the negative net production within the channels[1]. Due to the CO_2 supersaturation, large rivers are sources of atmospheric CO_2 (Cole & Caraco, 2001; Mayorga *et al.*, 2005).

Regarding the sediment transfer, the effect of rivers on the carbon budget is far less understood. However, the long-term flux of carbon connected to the sediment transfer depends on the aggrading or degrading behaviour of the river system. Deposition acts as a carbon sink because carbon is stored within the fluvial system and decoupled from the hydrologic transport in the channel. Whether erosion is a carbon source or sink depends on the relative CO_2 concentrations in both, the sediment and the water in the channel. If CO_2 concentrations are higher in sediments, erosion may decrease the carbon content of eroded sediments and therefore increase the carbon content of the channel water. In cases of higher CO_2 concentration in the water, sediment may be enriched during the transport, resulting in a carbon sink.

Regarding the net effect of sediment transport on the long-term carbon cycle, the general development of meandering rivers during the Holocene must be considered (Chapter 2.1.3 and 3.5). Meandering channels rework Pleistocene sands and gravels by channel migration during the Holocene. Because no sediment is added to the channel system by channel migration, no change in the carbon surplus takes place. Therefore, the net carbon input into the channel water due to bank erosion of the Pleistocene sands and gravels

[1] According to Cole & Caraco (2001), the negative net production (NEP) results from the large respiration (R) of heterotrophic consumer organisms in rivers that exceeds the amount of organic carbon producted by photosynthesis (Gross Primary Production; GPP) within the river. The negative aquatic production ($NEP = GPP - R < 0$) in the rivers is partly balanced by organic carbon input from the terrestrial ecosystems.

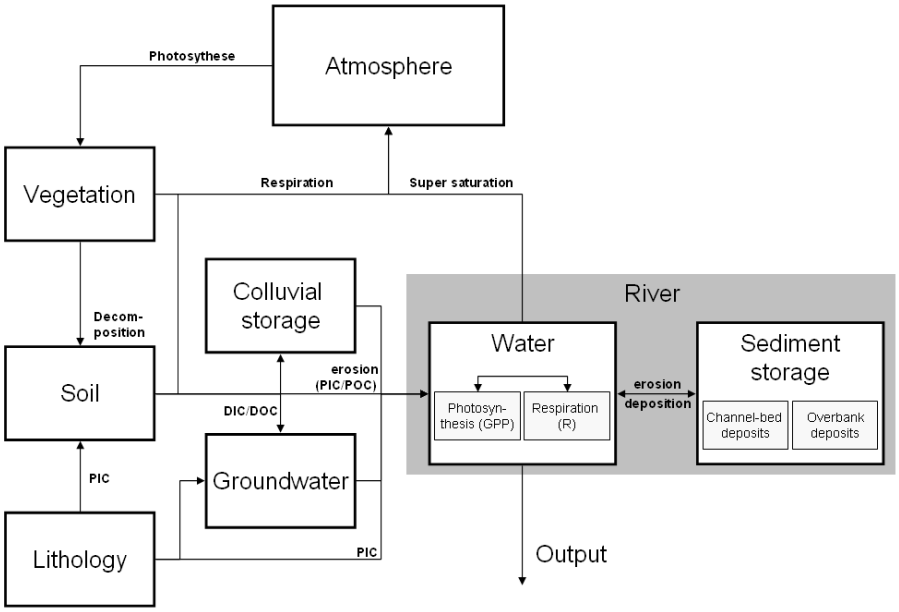

Figure 4.8: C-cycle with focus on the sediment transfer in fluvial systems. PIC = particulate inorganic carbon, POC = particulate organic carbon, DIC = dissolved inorganic carbon, DOC = dissolved organic carbon, GPP = gross primary production, R = heterotrophic respiration.

during the Holocene depends on the difference between the Pleistocene and the Holocene channel bed sediments. As shown by the analysis of the *TOC* content of the different sedimentary facies (Chapter 5.2.2), bank erosion in the Rhine system can be neglected as a source or sink of riverine carbon.

In contrast to the sands and gravels of the channel bed deposits, overbank deposits that result from the vertical accretion on top of channel bed deposits are considered to be the product of Holocene hillslope erosion (compare Chapters 2.1.3 and 4.2). Therefore, vertical accretion results in an increase of *TOC*. In other words, long-term storage on the floodplain lead to carbon sequestration within the fluvial system (Fig. 4.8).

To estimate Holocene *TOC* storage related to overbank and channel fill deposits in the Rhine catchment, it is necessary to know the mass of these deposits. It is likely that channel fill deposits are characterised by significant higher *TOC*-values than overbank deposits. Therefore, the ratio of overbank and channel fill deposits need to be considered. However, the alluvial sediment budget described in Chapter 4.2 results in a cumulative mass of overbank and channel fill deposits and does not consider the relative contributions of these deposits. Thus the relative contributions of overbank

and channel fill deposits was roughly estimated based on nine cross sections along the Wetter (Houben, 2002; Nolte, 1999), one cross section of the Kleine Laaber (Niller, 1998) and along the lower Rhine (pers. comm.. G. Erkens). However, the analysed cross sections are very limited in number and therefore do not represent the entire Rhine catchment. While the cross sections are mainly derived from loess covered areas, cross sections from the Rhenish Slate Massif or the Black Forest are missing. Because the relative contributions of the depositional environments give only rough estimates and not precise numbers, a calculation of different scenarios was performed.

4.4 ^{14}C-database analysis

The sediment and carbon budget of the Rhine catchment integrates the Holocene period and does not consider temporal variations during the Holocene. However, to obtain knowledge of the temporal development of the Rhine basin a ^{14}C-database from ^{14}C samples of colluvial and alluvial sediments in Germany was compiled and analysed in terms of i) cumulative frequency distributions of the ^{14}C ages and ii) changing sedimentation rates on floodplains and in palaeochannels.

The database of 432 published ^{14}C ages contains: depositional environments and facies, catchment area, sampling depth, lab code, type of organic material sampled, ^{13}C values, conventional (as measured) radiocarbon ages and calibrated radiocarbon ages (using INTCAL04 Reimer *et al.*, 2004). The data originates from the German parts of the Rhine, Danube, Weser, and Elbe catchments (Fig. 4.9). The ^{14}C ages range from the Late Pleistocene (max. age 26.000 a BP) to less than 200 a BP. The database and all publication references are available at `www.giub.uni-bonn.de\hoffmann\phd\phd.html`[2] Here only the last 14.000 a cal BP were analysed. To prevent bias towards land use, ^{14}C ages directly correlated with archaeological sites were excluded and only 401 ^{14}C ages of organic remains sampled from alluvial and colluvial sediments are used. Following depositional environments were considered: channel-beds, palaeochannels, floodplains, slopes, gullies, alluvial fans and subrosion depressions (Tab. 4.3). The ^{14}C-ages were classified according to the sedimentary facies:

[2]The login is currently password protected

1. floodplain fines (loam and sand),
2. sands and gravels of meandering and braiding river systems,
3. colluvium,
4. gyttja, organic rich sediments,
5. fossil soils and
6. peat.

4.4.1 Cumulative frequency distributions

To analyse the data in terms of cumulative frequency distributions of fluvial activity they were grouped based on their sedimentary facies. While data from colluvium, floodplain fines, sand and gravels are considered to represent activity phases of colluvial and fluvial systems, ^{14}C data of organic deposits, fossil soils and peat are assumed to represent more stable systems with limited clastic sediment flux. This classification is questionable in places where ^{14}C ages were obtained on gyttja and organic rich sediments sampled from the base of palaeochannel fills. Rather than stability, such ages represent activity transition just after channel abandonment at the beginning of channel infill. Subsequently, these ages (facies 4) will be called "transitional", to distinguish them from clear indicators of activity (facies 1 to 3) or stability (facies 5 and 6).

Based on the sedimentary context, Lewin *et al.* (2005) classify ^{14}C ages as relating to (1) the termination or onset of a fluvial unit or (2) a change in sedimentation rate within a unit. Cases (1) and (2), termed "change date", allow identification of geomorphologically significant changes, and are attributed to major floods. Here, ^{14}C-ages were classified as change data only if the organic remains were sampled near the contact of two sedimentary units. Type (2) change data that mark a change in sedimentation rate (Lewin *et al.*, 2005) where not considered, due to difficulties in establishing changes in sedimentation rates.

For data analysis the grouped ^{14}C data were calibrated using OxCal (V3.10 Bronk Ramsey, 1995, 2001) and the IntCal04 calibration data set (Reimer *et al.*, 2004). All ages are given in calibrated years before 1950 AD. The calibration results in a probability function of each age as shown in Fig. 4.10. Cumulative probability functions (CPFs) were calculated for each group (activity-, stability and transitional ages) by adding the probability density functions of each group. CPFs are not only influenced by the frequency distribution of the ^{14}C data but also by the shape of the calibration curve. Plateau regions in the calibration curve result in relatively higher probabilities in the calibrated data set. This effect is shown in Fig.

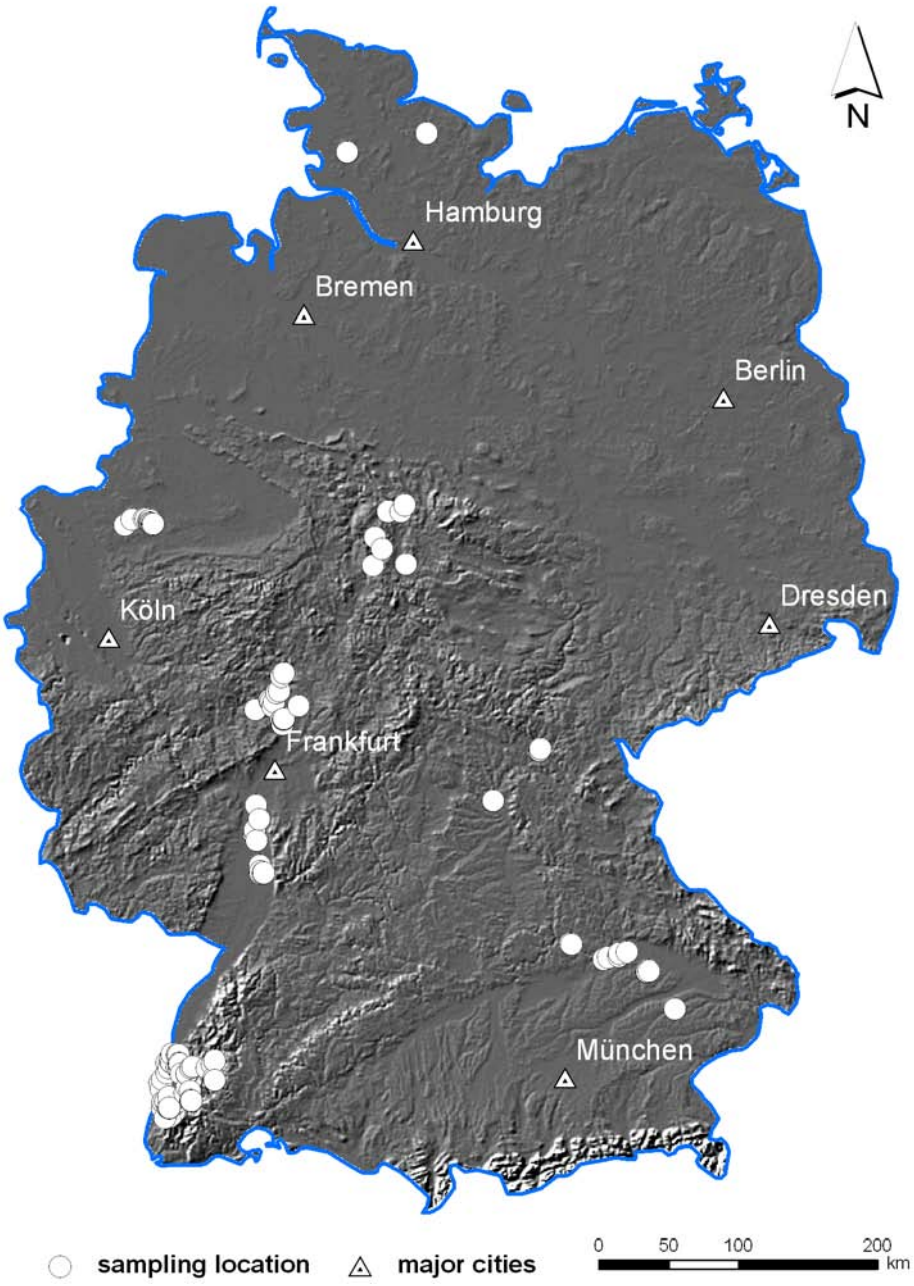

Figure 4.9: Shaded relief map of Germany with ^{14}C sampling locations indicated.

Table 4.3: Number of ^{14}C data taken from different depositional environments (colums) and sedimentary facies (rows). Sedimentary facies are ordered according to activity status.

Facies	**Col**	**Col/FP**	**GF**	**AF**	**FP**	**ACF**	**PC**	**SD**	**AS**	**NN**	$\sum$
Activity											148
FPF				1	46		7				54
CBS					3	19	4				26
Col	38	13	13		4				2		68
Stability											106
BFS		2			12		7				21
FS		1			7				1		9
Peat	12	6		4	23		16	14		1	76
Transitional											155
Gyttja	5	7			28		54	9			103
ORS					3		32	12	5		52
LST					1						1
NN					4	9			8	1	22
$\sum$	53	29	13	5	131	28	120	35	16	2	432

Col = colluvium, Col/FP = interfingering between colluvial and floodplain, FP = floodplain, GF = gullyfill, AF= alluvial fan, ACF = active channelfill, PC = palaeochannel, SD = subrosion depression, AS = archaeological site, NN = unknown, FPF = floodplain fines, CBS = channel bed sediments, BFS = black floodplain soil, FS = fossil soil, ORS = organic rich sediments, LST = Laacher lake tephra.

5.6a as CPF of (n = 140) equally spaced synthetic ^{14}C data. To minimize these effects Lewin *et al.* (2005); Johnstone *et al.* (2006) and Thorndycraft & Benito (2006a,b), subtract the CPF computed from a similar sized set of equally spaced data from the group CPFs. The subtraction resulted in cumulative probability density functions (CPDFs)(Lewin *et al.*, 2005). Besides the effects of the calibration curve, there is typically a strong increase in the probability density towards young ages (see complete dataset in Fig. 5.6b). This results from better preservation of younger materials and higher sampling probability of shallower sediments, and is not necessarily a result of increasing fluvial activity. To eliminate this bias we suggest a normalisation procedure that differs from the one used by Lewin *et al.* (2005). We divide the grouped relative CPFs by the relative CPF of the complete dataset (Fig. 5.6e). This normalisation should eliminate both effects (e.g. wiggles of the calibration curve and the young age bias) at a time.

For comparing the German data set to the results from Great Britain,

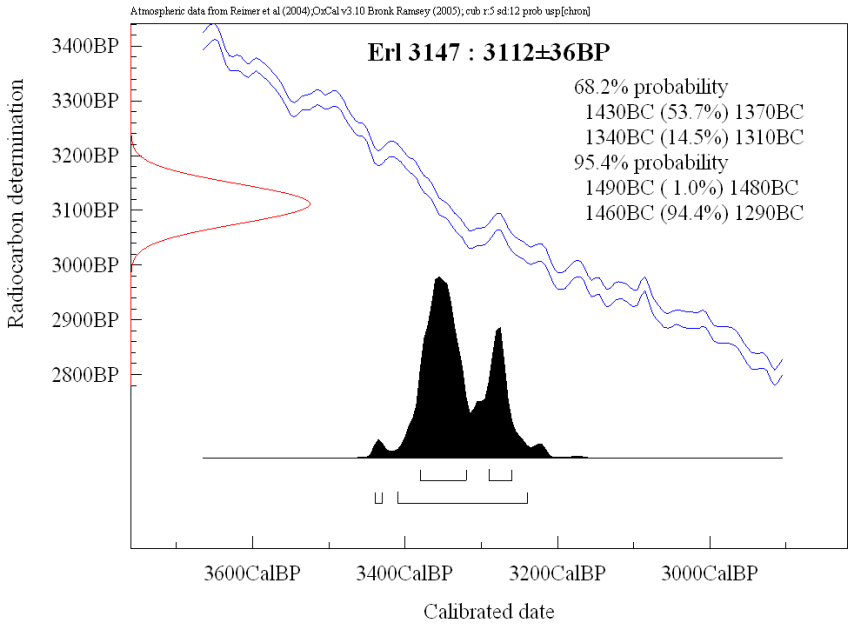

Figure 4.10: Example of ^{14}C-calibration, showing the measured ^{14}C-determination (red), the calibration curve (blue) and the probability density function of the calibrated age (black). The calibration was calculated using OxCal (V3.10 Bronk Ramsey, 1995, 2001)

Poland and Spain, the CPDFs of change dates from GB, Poland and Spain were reanalysed by dividing them by CPFs of equally spaced ages. For this purpose 140 equally spaced ^{14}C ages were used (each with an error of 50 a).

The approach of using the CPFs of activity or stability ages as proxies for widespread geomorphological activity or stability in Germany is limited for several reasons:

1. Potential bias in the ^{14}C ages due to too young radiocarbon ages (e.g. from contamination of organic material with modern carbon) or too old radiocarbon ages (e.g. from contamination of organic material with old carbon like hard water effect, or old-wood effect).

2. Variable precision of ^{14}C determinations: random errors based on AMS ^{14}C measurement are usually much smaller than random errors associated with conventional techniques (e.g. β-counting). Additionally, radiocarbon estimates obtained during the 1960s and 70s are usually less precise than more modern measurements. ^{14}C ages were excluded from the probability analysis when uncertainties where reported.

3. Reworking and redeposition of organic material results in a time lag between the death of the organism (that is determined by ^{14}C dating) and its burial in the fluvial sediments. In strict sense, ^{14}C ages only represent minimum ages for sediment deposition.

4. Sampling bias: Statistical analysis should be based on random samples. In case of the database used here, and in addition to the young-age bias discussed above, it is obvious that many ^{14}C samples were not taken randomly but following specific spatial and temporal preferences of the research agenda a time.

To test the limitations of the dataset and the significance of the finds, statistical tests and sensitivity analysis were employed.

4.4.2 Sedimentation rates

The analysis of CPFs does not allow the calculation of sediment fluxes, erosion or sedimentations rates. However, the integration of the sampling depth in the ^{14}C database does allow the calculation of the sedimentation rate SR:

$$SR_i = \frac{D_i - D_{i-1}}{T_i - T_{i-1}} \tag{4.5}$$

where D_i and T_i are the depth and age of a ^{14}C sample and D_{i-1} and T_{i-1} are the depth and age of the next upper ^{14}C sample. D_i represents the mean value of the 2σ-age range given by the calibrated age. In the case of the upper most ^{14}C sample $i = 1$ and $D_0 = 0$ and $T_0 = 0$. The calculated sedimentation rate SR_i corresponds to the mean rate between to successive ages during the time T_i and T_{i-1}. Due to different sedimentation rates in different depositional environments, sedimentation rates during the last 14 000 years were calculated based on 115 floodplain samples and 104 palaeochannel samples separately. ^{14}C samples with age reversal[3] were excluded from the analysis.

[3]Age reversals are characterised by younger ^{14}C ages below older ages. Age reversals may result from dated material that is older than the deposition ages or from contamination of the dated sample with ^{12}C rich carbon.

Chapter 5

Results

5.1 Holocene fluvial sediment budget

5.1.1 Alluvial sediment storage

The quantification of alluvial sediment storage in the Rhine catchment is summarised in Tab. 5.1. Over all a volume of 37.6 ± 8.3 km^3, corresponding to a total mass of $53.5 \pm 12.4 \times 10^9$ t is stored within the Rhine catchment. These values correspond to an eroded volume of 41.9 ± 9.3 km^3 ($59.5 \pm 13.9 \times 10^9$ t), assuming a channel sediment delivery ratio (*CSDR*) at the river mouth of 10 % and $T = 10\,000$ years. Assuming more extreme values for mean sediment thickness (1-2 m), total amounts vary between 26.5 - 45 km^3 ($37 - 64.6 \times 10^9$ t). Assuming extreme values for *CSDR*s (0 - 30 %), this corresponds to Holocene eroded sediment amounts ranging 26.5 - 64.2 km^3 ($36.9 - 92.3 \times 10^9$ t).

Regarding the hinterland, Tab. 5.1 shows that the amount of sediment trapped in floodplains not resolved by GK200 (9.2×10^9 t) is a significant volume. Quantification of floodplains based only on the GK200 (neglecting narrow floodplains) would have resulted in significant underestimation, missing 31 % of the total of stored sediment. Especially in catchments that are located in the Rhenish Massif (i.e. Ahr, Sieg and Wupper), a large proportion of the sediment storage is not represented in the GK200. In the case of the Ahr catchment, the contribution from the upscaling calculations is even larger than that obtained from the GK200.

In the Rhine delta a volume of 8.1 km^3 or 9.3×10^9 t is estimated for $T = 10\,000$ years. Of this volume, 67 %, 33 % and 25 % had been created since 7000, 5000, 3000 years BP, respectively. In our calculations, these proportions of accommodation space (room for sedimentation) are assumed to apply to 1:1 to deltaic sedimentation (filling with sediment) in Tab. 5.1. Probably that assumption results in underestimation of Late Holocene (since 3000 BP) volumes, because of peat formation, compaction and delayed filling of accommodation space (see Cohen, 2005; Erkens *et al.*, 2006).

Considering the spatial distribution of the sediment storage (Tab. 5.1), roughly 50 % of floodplain sediment is stored in the Rhine trunk valley and delta, highlighting these areas as the major sedimentary sinks. The alluvial sediment volume along the tributaries strongly correlates with catchment size (Fig. 5.4). The Ill catchment has an exceptionally large storage capacity (it hosts 7 % of the total storage, while draining only 3.5 % of the total catchment). This results from its location within the Upper Rhine Graben and confirms the function of the Rhine Graben as a major sedimentary sink.

Table 5.1: Holocene alluvial sediment storage within the Rhine catchment and its tributaries for large and small floodplains.

Rhine and main tributaries	**Catchment Area**			**Large floodplains** subcatchments>4.1km^2 GK200-resolved				**Small floodplains** subcatchments 0.3-4.1 km^2 upscaling approach				**Total floodplain sediment storage**			
	A_d [km^2]	Erosive area $A_d - A_f$ [km^2]	error	Floodplain area A_f [km^2]	error	Sediment volume S_v [km^3]	error	Floodplain area A_f [km^2]	error	Sediment volume S_v [km^3]	error	Sediment volume S_v [km^3]	error	Mass $\rho_B \times S_v$ [10^9t]	error
Wied	744.9	679.4	18.5	30.6	6.1	0.05	0.02	34.9	17.4	0.06	0.03	0.10	0.03	0.16	0.05
Emscher	806.4	686.3	26.4	77.2	15.4	0.12	0.04	42.9	21.4	0.07	0.04	0.19	0.06	0.29	0.08
Wupper	838.0	761.0	21.5	36.5	7.3	0.06	0.02	40.5	20.3	0.06	0.04	0.12	0.04	0.18	0.06
Ahr	910.7	832.9	23.8	31.9	6.4	0.05	0.02	45.9	22.9	0.07	0.04	0.12	0.04	0.19	0.07
Erft	1818.6	1557.6	58.4	164.5	32.9	0.26	0.08	96.5	48.2	0.15	0.09	0.42	0.12	0.63	0.18
Sieg	2870.1	2567.1	76.2	165.9	33.2	0.27	0.09	137.1	68.5	0.22	0.12	0.48	0.15	0.73	0.22
Nahe	4070.0	3581.2	114.9	290.5	58.1	0.46	0.15	198.2	99.1	0.32	0.18	0.78	0.23	1.17	0.35
Ruhr	4476.8	4018.8	118.4	241.9	48.4	0.39	0.12	216.0	108.0	0.35	0.19	0.73	0.23	1.10	0.34
Lippe	4857.6	4183.9	161.3	391.7	78.3	0.63	0.20	282.0	141.0	0.45	0.25	1.08	0.32	1.62	0.48
Ill	4858.1	2918.3	365.4	1785.6	357.1	2.86	0.91	154.3	77.1	0.25	0.14	3.10	0.93	4.66	1.39
Lahn	5916.4	5260.6	161.5	368.2	73.6	0.59	0.19	287.6	143.8	0.46	0.26	1.05	0.32	1.57	0.48
Neckar	13970.8	12223.3	400.4	1070.9	214.2	1.71	0.55	676.6	338.3	1.08	0.61	2.80	0.82	4.19	1.23
Main	27306.6	24077.4	776.3	1868.0	373.6	2.99	0.96	1361.1	680.5	2.18	1.22	5.17	1.55	7.75	2.32
Mosel	28226.6	24580.9	843.4	2208.9	441.8	3.53	1.13	1436.9	718.4	2.30	1.29	5.83	1.71	8.75	2.57
Lower Rhine	2532.1	2119.1	76.7	360.6	72.1	0.58	0.18	52.4	26.2	0.08	0.05	0.66	0.19	0.99	0.29
Middle Rhine	2658.4	2383.9	73.9	137.4	27.5	0.22	0.07	137.2	68.6	0.22	0.12	0.44	0.14	0.66	0.21
Upper Rhine	18863.1	14376.0	833.7	3918.7	783.7	6.27	2.01	568.4	284.2	0.91	0.51	7.18	2.07	10.77	3.11
Hinterland total	125725.1	107297.5	3837.8	12659.3	2531.9	20.25	6.48	5768.3	2884.2	9.23	5.16	29.48	8.29	44.23	12.43
Rhine trunk total	24053.6	18896.4	958.0	4399.3	879.9	7.04	2.25	758.0	379.0	1.21	0.68	8.25	2.35	12.38	3.53

Notes:
Catchment area based on DEM calculations. Large floodplains based on the geological maps (GK200, 1:200 000). Additional area of smaller floodplains based on upscaling approach (see text). Area to volume calculations using mean floodplain thickness $D_f = 1.6 \pm 0.4$ m. Volume to mass using $\rho_B = 1500$ kg m^{-3}. Conservative errors assumed for floodplain areas of larger floodplains: 20 %.; for smaller floodplains: $\pm$ 50 %.

Table 5.2: Total Holocene alluvial sediment storage for different time scenarios.

Time frame	**Delta storage**[1]			**Total storage**[2]	
Duration T (yr)	Volume $S_{V,d}$ [km^3]	%[3]	Mass ($\rho_{B,d}S_V$) [10^9t]	Volume S_V [km^3]	Mass ($\rho_B S_V$) [10^9t]
10 000	8.1 ± 0.8	100%	9.3 ± 0.9	37.6 ± 9.6	53.5 ± 14.4
7000	5.4 ± 0.8	67%	6.2 ± 0.9	34.9 ± 9.6	50.5 ± 14.4
5000	2.7 ± 0.8	33%	3.1 ± 0.9	32.2 ± 9.6	47.3 ± 14.4
3000	2.0 ± 0.8	25%	2.4 ± 0.9	31.5 ± 9.6	46.6 ± 14.4

1. Based on Erkens *et al.* (2006): bulk density $\rho_{B,d} = 1150$ kg m^{-3}.
2. Total storage = Hinterland storage + Delta storage
   Volume: $S_V = S_{V,d} + S_{V,hl}$ ($S_{V,hl}$ =29.5 ± 8.3 km^3)
   Mass: $\rho_b S_V = \rho_{B,d}S_{V,d} + \rho_{B,hl}S_{V,hl}$ ($\rho_{B,hl}S_{V,hl}$ =44.2 ± 12.4 × 10^9 t)
3. % of total accommodation created after time T (obtained from Cohen, 2005). Yields minimum estimate for sedimentation volume.

5.1.2 Holocene erosion rates

Estimated mean erosion rates are presented for a set of different assumptions (Tab. 5.3). Using the most reasonable set of assumptions ($CSDR$ = 10 %, ρ_B = 1500 kg m^{-3} and D_f = 1.6 m) catchment wide denudation of 0.4 m in the last 10 000 yrs corresponds to an erosion rate of 0.55 ± 0.16 t ha^{-1}year^{-1} (38.9 ± 10.8 mm kyr^{-1}). More extreme rates of catchment wide erosion follow from varying (i) D_f between 1 and 2 m; (ii) $CSDR$ between 0 and 30 %; (iii) ρ_B between 1300 and 1700 kg m^{-3} (for hinterland) and (iv) the duration of deposition attributed to the of hinterland alluvial sediments to 3000, 5000, 7000 and 10 000 years. Resultant extreme minima and maxima for erosion rates are 0.3 and 2.9 t ha^{-1}year^{-1} or 25 - 173 mm kyr^{-1}.

For all parameters in Equations 4.2 and 4.3, we evaluated the effects of uncertainty in their quantification in a sensitivity analysis (Tab. 5.3). The $CSDR$ was varied between 0 and 30 % to range its sensitivity in the estimates. This results in an erosion rate between 0.5 and 0.71 t ha^{-1}yr^{-1} (38.9 - 50 mm/kyr), keeping other parameters constant (compare line 4 and 5 in Tab. 5.3). Uncertainty in bulk densities ρ_B (1200 to 1700 kg m^{-3}) results in erosion rates between 0.46 - 0.64 t ha^{-1}yr^{-1} as shown in Tab. 5.3 (lines 6 and 7). Variation of the bulk density changes only the erosion rate E_R, while E_R^* is independent of ρ_B and therefore does not change. Variation of the timeframe between 3000 and 10 000 years (while keeping other parameters constant) results in erosion rates between 0.55 and 1.61 t ha^{-1}year^{-1} (line 8 to 11 in Tab. 5.3).

Table 5.3: Quantification of erosion and erosion rates based of different scenarios for the input parameters.

	Calculation parameters				Alluvial storage								Catchment wide erosion[3]					
					Hinterland floodplains[1]				Hinterland + Delta[2]				Denudation		Erosion rate			
Nr.	D_f	ρ_B	*CSDR*	*Time*	*Volume*		*Mass*		*Volume*		*Mass*				E_R^*		E_R	
	[m]	[kg/l]	[%]	[yr]	[km^3]	error	[10^{9}t]	error	[km^3]	error	[10^{9}t]	error	[m]	error	[mm/kyr]	error	[t/ha/yr]	error
Most reasonable values *and extremes*																		
1	1.6	1500	10	10 000	29.5	9.6	44.2	14.4	37.6	9.6	53.5	14.4	0.39	0.10	38.9	10.8	0.55	0.16
2	2	1700	30	3000	36.9	10.6	62.7	18.1	38.9	10.6	65.0	18.1	0.52	0.14	172.6	74.7	2.88	1.26
3	1	1200	0	10 000	18.4	8.3	22.1	10.0	26.5	8.3	31.4	10.0	0.25	0.08	24.7	8.2	0.29	0.10
Sensitivity test (CSDR, Density)																		
4	1.6	1500	0	10 000	29.5	9.6	44.2	14.4	37.6	9.6	53.5	14.4	0.35	0.09	35.0	9.7	0.50	0.14
5	1.6	1500	30	10 000	29.5	9.6	44.2	14.4	37.6	9.6	53.5	14.4	0.50	0.13	50.0	13.8	0.71	0.21
6	1.6	1200	10	10 000	29.5	9.6	35.4	11.5	37.6	9.6	44.7	11.5	0.39	0.10	38.9	10.8	0.46	0.13
7	1.6	1700	10	10 000	29.5	9.6	50.1	16.3	37.6	9.6	59.4	16.3	0.39	0.10	38.9	10.8	0.62	0.18
Time frame scenarios																		
8	1.6	1500	10	10 000	29.5	9.6	44.2	14.4	37.6	9.6	53.5	14.4	0.39	0.10	38.9	10.8	0.55	0.16
9	1.6	1500	10	7000	29.5	9.6	44.2	14.4	34.9	9.6	50.5	14.4	0.36	0.10	51.6	16.1	0.75	0.24
10	1.6	1500	10	5000	29.5	9.6	44.2	14.4	32.2	9.6	47.3	14.4	0.33	0.10	66.6	24.0	0.98	0.36
11	1.6	1500	10	3000	29.5	9.6	44.2	14.4	31.5	9.6	46.6	14.4	0.33	0.10	108.8	49.3	1.61	0.73

1. From Tab. 5.1
2. From Tab. 5.2
3. For the non-alpine part of the catchment upstream from the Dutch-German border $A_d - A_f = 107300 \pm 3838 km^2$
4. D_f = floodplain thickness, ρ_B = bulk density of overbank fines, *CSDR* = Channel sediment delivery ratio

5.2 *TOC* storage in floodplains

Table 5.4 lists the number of 1948 TOC measurements and the measured sedimentary facies. 767 measurements were taken from overbank deposits, 373 from channel fill deposits, 327 from channel bed deposits and 489 measurements originate from slope deposits (Tab. 5.4). The spatial distribution of the measurements is illustrated in Fig. 4.7. The data are not evenly distributed but show strong clusters i) around Freiburg in the Black Forest and the southern Upper Rhine Graben, ii) around Frankfurt in the Nidda Catchment, the Amöneburger Becken and in the northern Upper Rhine Graben and iii) at the Altmühl and Danube rivers close to Regensburg.

5.2.1 Sample depth and clay content

The relation of the *TOC* content to the sample depth and the clay content is shown in Fig. 5.1 and Figure 5.2, respectively. While there is no correlation between *TOC* and sample depth, *TOC* exponentially increases with increasing clay content except for the dataset of Niller (1998). The strongest correlation and largest increase is shown in the dataset of Dambeck (2005) with a correlation coefficient $R^2 = 0.45$ and an exponent $b = 0.052$ followed by the dataset of Houben (2002) with $R^2 = 0.31$ and $b = 0.042$ and Seidel (2004) with $R^2 = 0.32$ and $b = 0.035$ (compare Figure 5.2). The datasets from the Danube catchment (Hilgart, 1995; Niller, 1998) show no or only a weak correlation.

In general, *TOC* increases linearly with clay content at regional and global scales (Parton *et al.*, 1993; Schimel *et al.*, 1994). The observed weak or absent correlation between clay and *TOC* content could be due to a differing clay mineral composition (Rasmussen *et al.*, 2005). In the Danube catchment, clay mineral distribution is strongly influenced by kaolinitic weathering residues from the adjacent limestone ridge.

5.2.2 Depositional environment and sedimentary facies

The results of the statistical analysis of the *TOC* versus sedimentary facies and depositional environment are shown in Fig. 5.3 - 5.5. The boxplots and the results of the Kruskal-Wallis tests, which are summarized in Tab. 5.5, suggest a significant influence of the sedimentary facies and the depositional environments on the *TOC* content for the entire dataset as well as for each subset at 1%-significance level. Furthermore, the result of the pairwise Wilcox test suggests that the mean *TOC* values of each combination of paired

Table 5.4: Number of *TOC* measurements taken from different publications (column) and sedimentary facies (rows). For facies names see Tab. 4.2

depo.	facies	dataset (publication)							
env.		Dam	Hil	Hou	Nil	Nol	Sei	Wun	$\sum$
I	FL	0	29	0	90	0	8	14	141
	yFL	12	20	93	0	68	0	0	193
	oFL	0	11	0	0	0	0	0	11
	FS	14	2	0	18	0	0	0	34
	FC	14	0	0	0	0	0	0	14
	pOB	68	34	154	0	0	3	0	259
	LEV	0	0	22	0	0	0	0	22
	HBL	0	0	0	28	0	0	0	28
	BFS	0	5	21	0	20	9	10	65
II	F	0	11	12	4	0	0	3	30
	Fhg	0	0	0	0	0	0	23	23
	Fhh	6	0	0	0	24	0	5	35
	Fm	7	0	0	0	26	0	17	50
	Fmu	24	0	0	0	0	0	0	24
	H	7	0	0	14	0	0	3	24
	CF	96	0	80	8	0	0	0	184
III	CBS	51	3	111	0	12	0	0	177
	Gf	22	10	0	23	4	0	2	61
	NT	0	21	34	0	29	0	0	85
IV	Col	12	20	0	322	0	0	4	366
	Lo	0	20	0	103	0	0	0	123
$\sum$		339	188	527	610	183	20	81	1948

Depo.env. = depositional environment
I = overbank deposits
II = channel fills
III = channel bed deposits
IV = slope deposits.

Datasets: Dam = Dambeck (2005), Hil = Hilgart (1995), Hou = Houben (2002), Nil = Niller (1998), Nol = Nolte (1999), Sei = Seidel (2004), Wun = Wunderlich (1998)

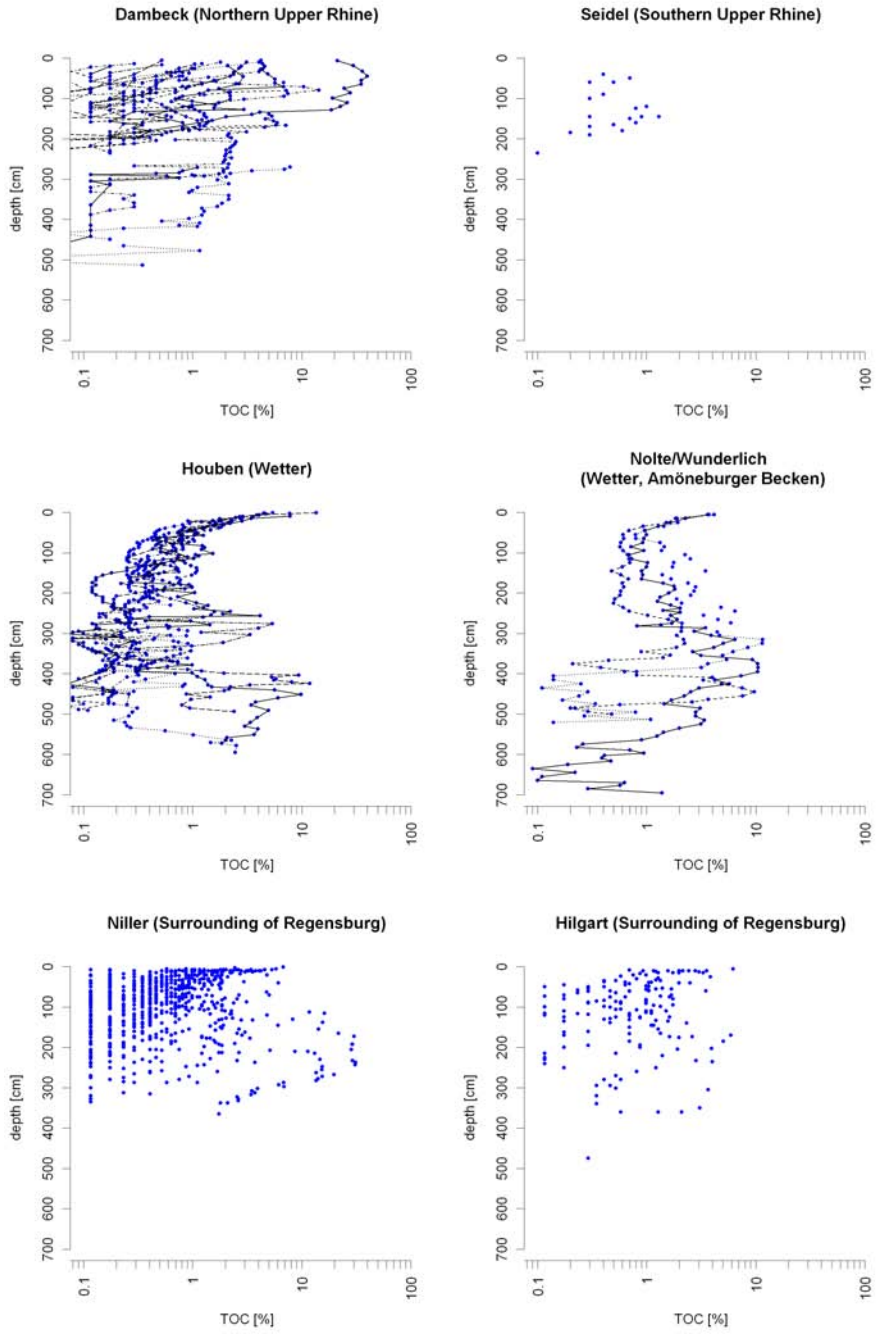

Figure 5.1: *TOC* content versus depth for analysed publications. The lines connect measurements from a certain drilling (datasets of Dambeck, 2005; Houben, 2002 and Nolte, 1999/Wunderlich, 1998 only).

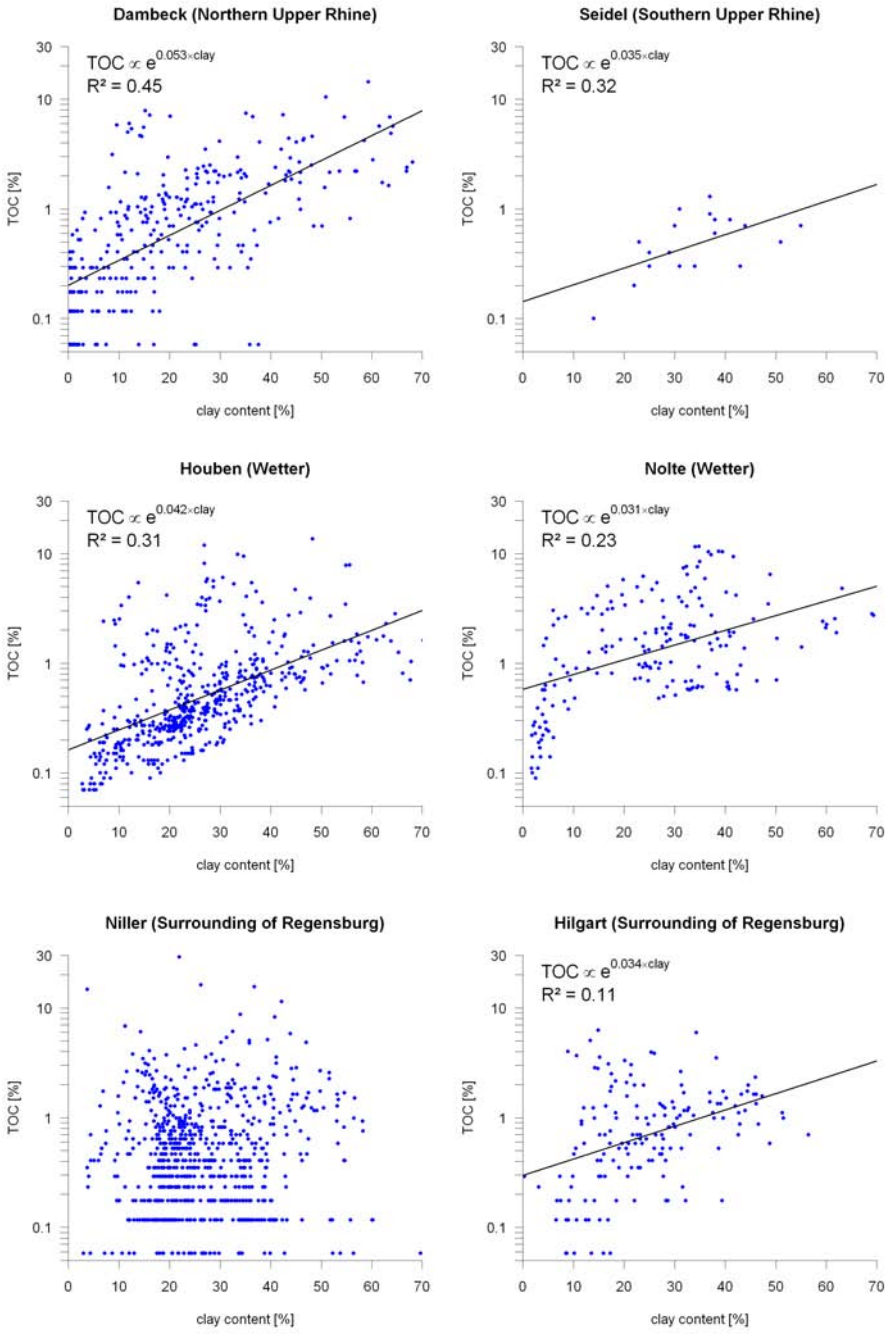

Figure 5.2: Clay content versus *TOC* content based on the analysed publications. The lines represent results of the exponential regression: $TOC = a \times e^{b \times \text{clay}}$.

Table 5.5: Results of Kruskal-Wallis test of *TOC* in different sedimentary facies and depositional environments for analysed publications and for the complete dataset.

	Sedimentary facies			Depositional environment		
Data	χ^2	df	p	χ^2	df	p
Dambeck, 2005	243.2	11	$< 2.2 \times 10^{-16}$	180.6	3	$< 2.2 \times 10^{-16}$
Houben, 2002	203.3	8	$< 2.2 \times 10^{-16}$	20.2	2	$4.2\ 10^{-05}$
Hilgart, 1995	91.9	11	7.08 10-15	54.4	3	$9.3\ 10^{-12}$
Niller, 1998	283.6	9	$< 2.2 \times 10^{-16}$	170.6	3	$< 2.2 \times 10^{-16}$
Nolte, 1999	119.3	6	$< 2.2 \times 10^{-16}$	80.9	2	$< 2.2 \times 10^{-16}$
Seidel, 2004	8.95	2	0.01	only overbank deposits		
Wunderlich, 1998	62.6	9	4.2 10-10	29.1	3	2.2 10-06
complete dataset	909.9	22	$< 2.2 \times 10^{-16}$	442.2	3	$< 2.2 \times 10^{-16}$

depositional environments differs even though there is a large variation of the *TOC* content within the depositional environment. For example, the mean *TOC* content in channel fill deposits ranges from 1 to 55 % as shown in Fig. 5.4. In general, the *TOC* contents increase significantly from channel bed deposits, slope deposits and overbank deposits to channel fill deposits (Fig. 5.3).

The large variation of *TOC* concentration within the depositional environment is partly explained by the variation between the different sedimentary facies of a depositional environment (Fig. 5.4). Pairwise comparisons of the mean *TOC* using Wilcox rank sum test (Tab. 5.6) show that sedimentary facies with the same depositional environment may significantly differ from each other (e.g. flood loams FL and levee deposits LEV). In contrast, sedimentary facies in two different depositional environments can be similar concerning their mean *TOC* concentration (e.g. unspecified channel fill CF and flood loams FL). Especially, the majority of sedimentary facies from channel fill deposits show significant differences between each other. Furthermore, colluvial deposits and loess, which make up the studied slope deposits, are significant different regarding the median *TOC*. Considering the channel bed deposits, the differences between each combination of the channel bed facies are not significant at the 5% level (Tab. 5.6). However, there is a small increase of *TOC* from gravels via lower terrace sediments to unspecified channel bed deposits (Fig. 5.4).

Focusing on overbank deposits, there is a general increase of *TOC* with age. Therefore, Pleistocene overbank deposits (pOB) show significantly smaller

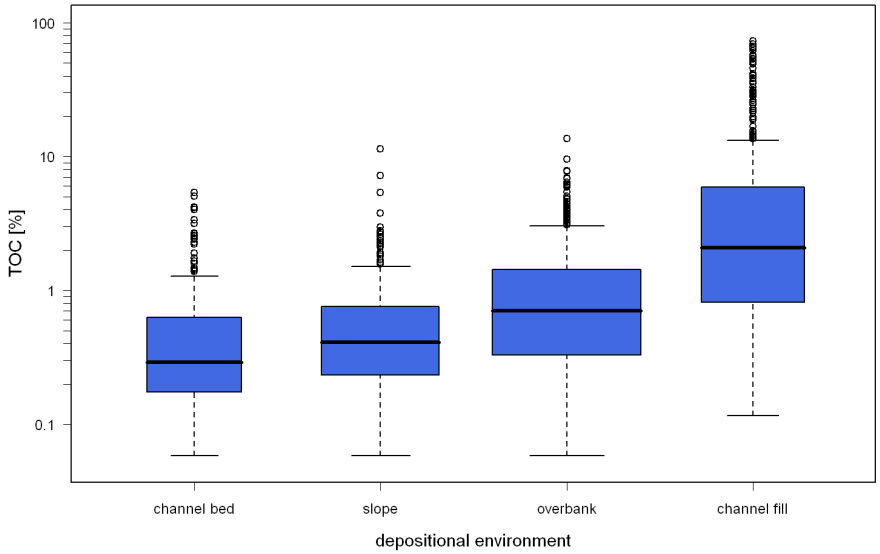

Figure 5.3: *TOC* versus depositional environment (number of measurements = 1948). Boxes have widths proportional to the number ($\sqrt{N}$) of data points in each box.

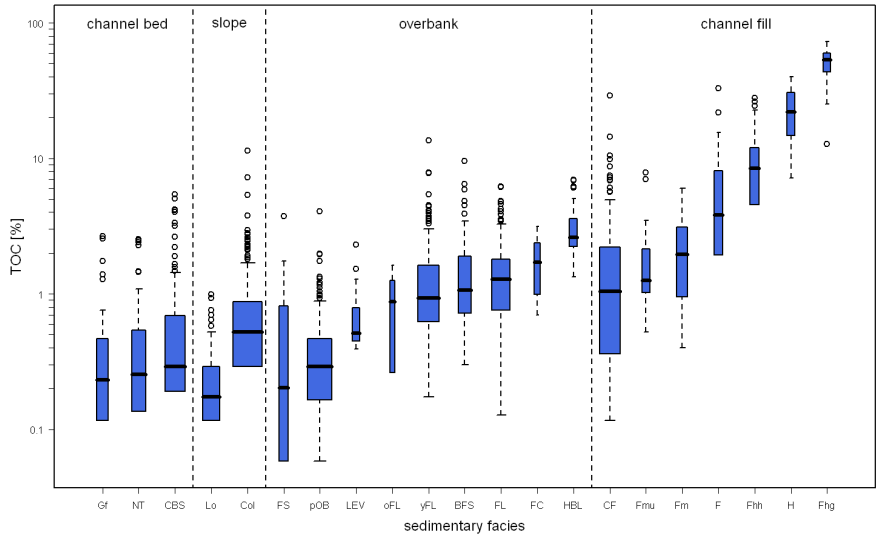

Figure 5.4: *TOC* versus sedimentary facies (number of measurements = 1948). Boxes have widths proportional to the number ($\sqrt{N}$) of data points in each box. For abbreviation of the sedimentary facies see Tab. 4.2.

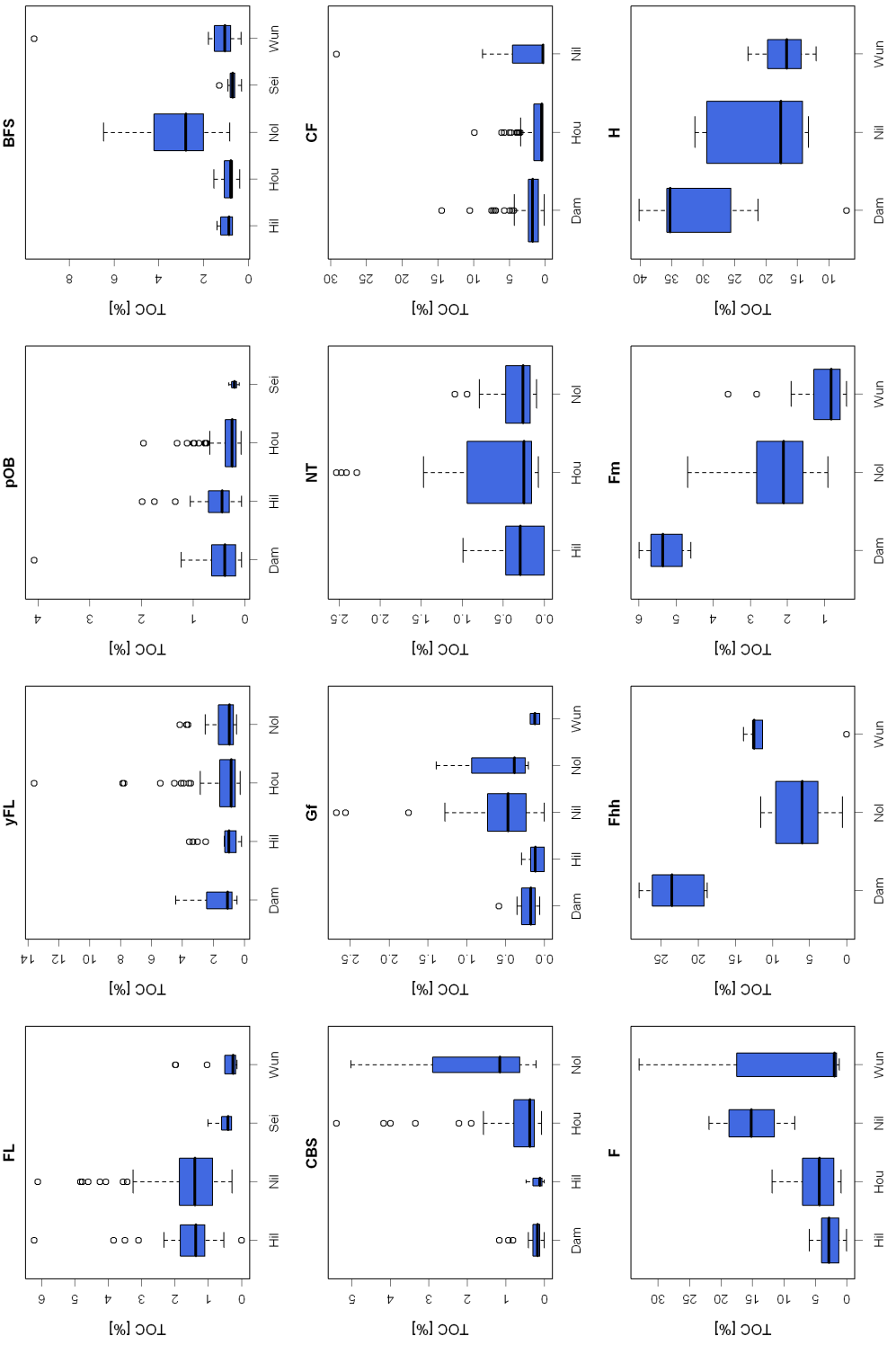

Figure 5.5: Comparison of *TOC* content of sedimentary facies (abbreviations see Tab. 4.2) in different dataset / publications: Dam = Dambeck (2005), Hil = Hilgart (1995), Hou = Houben (2002), Nil = Niller (1998), Nol = Nolte (1999), Sei = Seidel (2004), Wun = Wunderlich (1998).

Table 5.6: Comparison of TOC-means in different sedimentary facies (abbreviations see Tab. 4.2) based on the pairwise Wilcox test of the complete dataset. Values in the table represent the significance level (p-values). Dark shaded numbers highlight differences of the TOC means at a 1% significance level. Light shaded numbers highlight differences of the TOC means at 5% significant level. Non shaded numbers represent non significant differences (=equality) of TOC means.

	FS	pOB	LEV	oFL	yFL	BFS	FL	FC	HBL	CF	Fmu	Fm	F	Fhh	H	Fhg	Gf	NT	CBS	Lo
pOB	1.00	-	-	-	-	-	-	-	-	-	-	-	-	-	-	-	-	-	-	-
LEV	0.29	0.00	-	-	-	-	-	-	-	-	-	-	-	-	-	-	-	-	-	-
oFL	1.00	1.00	1.00	-	-	-	-	-	-	-	-	-	-	-	-	-	-	-	-	-
yFL	0.00	0.00	0.02	1.00	-	-	-	-	-	-	-	-	-	-	-	-	-	-	-	-
BFS	0.00	0.00	0.00	1.00	1.00	-	-	-	-	-	-	-	-	-	-	-	-	-	-	-
FL	0.00	0.00	0.01	0.94	1.00	1.00	-	-	-	-	-	-	-	-	-	-	-	-	-	-
FC	0.00	0.00	0.00	0.44	0.46	1.00	1.00	-	-	-	-	-	-	-	-	-	-	-	-	-
HBL	0.00	0.00	0.00	0.00	0.00	0.00	0.00	0.10	-	-	-	-	-	-	-	-	-	-	-	-
CF	0.00	0.00	1.00	1.00	1.00	1.00	1.00	1.00	0.00	-	-	-	-	-	-	-	-	-	-	-
Fmu	0.00	0.00	0.00	0.44	0.20	1.00	1.00	1.00	0.00	1.00	-	-	-	-	-	-	-	-	-	-
Fm	0.00	0.00	0.00	0.05	0.00	0.31	0.04	1.00	0.24	0.03	1.00	-	-	-	-	-	-	-	-	-
F	0.00	0.00	0.00	0.01	0.00	0.00	0.00	0.37	1.00	0.00	0.06	0.18	-	-	-	-	-	-	-	-
Fhh	0.00	0.00	0.00	0.00	0.00	0.00	0.00	0.00	0.00	0.00	0.00	0.00	0.27	-	-	-	-	-	-	-
H	0.00	0.00	0.00	0.00	0.00	0.00	0.00	0.00	0.00	0.00	0.00	0.00	0.00	0.00	-	-	-	-	-	-
Fhg	0.00	0.00	0.00	0.00	0.00	0.00	0.00	0.00	0.00	0.00	0.00	0.00	0.00	0.00	0.00	-	-	-	-	-
Gf	1.00	1.00	0.01	1.00	0.00	0.00	0.00	0.00	0.00	0.00	0.00	0.00	0.00	0.00	0.00	0.00	-	-	-	-
NT	1.00	1.00	0.01	1.00	0.00	0.00	0.00	0.00	0.00	0.00	0.00	0.00	0.00	0.00	0.00	0.00	1.00	-	-	-
CBS	1.00	1.00	0.02	1.00	0.00	0.00	0.00	0.00	0.00	0.00	0.00	0.00	0.00	0.00	0.00	0.00	1.00	1.00	-	-
Lo	1.00	0.00	0.00	0.46	0.00	0.00	0.00	0.00	0.00	0.00	0.00	0.00	0.00	0.00	0.00	0.00	0.45	0.43	0.00	-
Col	0.08	0.00	1.00	1.00	0.00	0.00	0.00	0.00	0.00	0.00	0.00	0.00	0.00	0.00	0.00	0.00	0.00	0.00	0.00	0.00

TOC values than older (oFL) and younger flood loam (yFL). However, even though the median *TOC* of older flood loams is smaller than that of the younger flood loam (Fig. 5.4), the difference is not significant (Tab. 5.6). The increasing trend of *TOC* with decreasing grain size is also shown in the sequence of flood sand (FS), to flood loams (FL) and flood clay (FC). Again, due to the large variation of the *TOC* content in these facies the difference between flood loams and flood clay is not significant (Tab. 5.6).

The variation of the *TOC* within sedimentary facies can partly be explained by regional and methodological differences that results from the different datasets (Fig. 5.5). While overbank and channel bed deposits in different subsets show very similar *TOC* contents (esp. FL, yFL, pOB, Gf and NT), the variation of *TOC* in channel fills deposits (esp. F, Fhh, Fm, H) is rather large. This may result from the different methodology and terminologies used to measure and describe the channel fill deposits even though the channel fill facies are amongst others defined based on the content of organic carbon (Boden, 1996).

5.3 Holocene alluvial *TOC* budget

5.3.1 *TOC* flux related to channel bed erosion and deposition

To evaluate the influence of sediment storage in fluvial systems on the long-term (Holocene) organic carbon budget, differences in *TOC* between Pleistocene (mainly NT) and Holocene (CBS) channel bed deposits and the overall *TOC* in overbank deposits must be considered. Regarding the complete dataset, the median *TOC* increases from facies Gf, Nt and CBS, even though the differences are not significant (compare Fig. 5.4 and Tab. 5.6). This may result from the large variation of *TOC* measurements due to the large regional differences of the different subsets. At a regional scale, the comparison between Pleistocene and the Holocene channel bed deposits is only possible at the Wetter (Houben, 2002; Nolte, 1999), where both facies were measured at one location. The dataset of Nolte (1999) as well as Houben (2002) show significantly higher *TOC* values in Holocene than in Pleistocene deposits as suggested by the regional Wilcox rank sum tests (Tab. 5.7). Therefore, the remobilisation of Pleistocene deposits and the subsequent deposition in the channel bed acts as a carbon sink in the carbon cycle of fluvial systems. However, as the study sites of Nolte (1999) and Houben (2002) are located a small distance of 15 km, it is questionable if the difference is representative for the entire Rhine catchment. Due to the fact that i) the differences

between Pleistocene and Holocene channel beds are not large and not well defined and ii) a budget of the stored mass of Holocene channel bed sediment for the entire Rhine catchment is still missing, *TOC* fluxes due to the remobilisation of Pleistocene channel bed sediments are not taken into account in this study.

5.3.2 *TOC* storage related to overbank deposition

In total $53.5 \pm 14 \times 10^9$ t of Holocene floodplain sediment is stored in the non-alpine part of the Rhine catchment (Tab. 5.1). Based on the analysed cross sections 85 % (with an assumed range of 70 - 95 %) of the Holocene floodplain sediments correspond to overbank deposition and 15 % (with an assumed range of 5 - 30 %) to channel fills. The mean *TOC* values of these depositional environments 1.1 % and 7.5 % (with 95 % confidence intervals of 1.0 - 1.2 % and 6.1 - 8.9 %, respectively), resulting in a stored *TOC* mass of 0.5×10^9 t and 0.6×10^9 t, respectively (Tab. 5.8). Even though the sediment mass of channel fill deposits is much smaller than that of the overbank deposits, they store almost the same amount of *TOC*, due to their higher *TOC*. Therefore, 1.1×10^9 t *TOC* is sequestered by the non-alpine Rhine catchment within floodplains during the period of floodplain deposition. Considering the minimum and maximum values of the stored sediment masses and the 95 % confidence intervals of the *TOC*-measurements, *TOC* storage in the floodplains may range between 0.7 and 1.6×10^9 t. Corresponding Holocene mean sequestration rates range from 3.4 to 25.4 g m^{-2} $year^{-1}$, depending the used time scenario (10 000, 7000, 5000 and 3000 years) since floodplain deposition started.

When comparing the *TOC* content of alluvial sediments to colluvial deposits, the processes leading to sedimentation need to be considered. Alluvial sediments may have been subjected to prolonged transport in rivers leading to graded texture; colluviation may lead to poorly graded deposits, although easily eroding texture classes dominate. Furthermore, colluvial deposits generally originate from humus rich topsoil while alluvial deposits may be traced back to different types of soils or sediment. Despite potentially high mineralization rates of soil organic matter during the erosion process (Beyer *et al.*, 1993), fresh colluvial deposits can be expected to have higher *TOC* contents than recent alluvial deposits. The degree of in situ C accumulation depends on relief position (Glatzel & Sommer, 2005) and conditions of aerobic mineralization. According to calculations by Glatzel & Stahr (2002), riparian colluvial deposits in a south-west German phragmition store 39 g C cm^{-2} due to waterlogged conditions.

Table 5.7: Wilcox test on NT and CBS facies of the dataset obtained from Houben (2002) and Nolte (1999).

facies		**Houben 2002**	**Nolte 1999**
NT	Median	0.245	0.26
	Conf. Interval	0.19	2.23
CBS	Median	0.37	1.16
	Conf. Interval	0.02	0.3
	p-value	0.016	2×10^{-3}
	Location difference	0.1	0.75

Table 5.8: *TOC* budget of the Rhine catchment based on floodplain (overbank and channel fill) deposition with minimum and maximum scenarios.

sediment	**%**[1]			**mass** [10^9 **t**][2]		
mass	mean	min	max	mean	min	max
Overbank	85	95	70	45.5	27.7	64.1
channel fill	15	5	30	8.0	2.0	20.3
Sum	100			53.5	39.5	67.5

TOC	**%**[3]			**mass** [10^9 **t**][2]		
	mean	min	max	mean	min	max
Overbank	1.11	1.02	1.20	0.50	0.28	0.77
channel fill	7.52	6.12	8.92	0.60	0.12	1.81
Mean/Sum	2.07	1.79	2.36	1.11	0.71	1.59

1. proportion of overbank and channel fill sediments is taken from cross section analysis.
2. total mass of alluvial sediment stored in the Rhine catchment ($53.5 \pm 14 \times 10^9$ t) is taken from Tab. 5.1.
3. Mean *TOC* content is taken from statistical analysis of 1948 TOC-measurements. Minimum and maximum values are the lower and upper limit of the 95 % confidence interval.

5.4 ^{14}C-database analysis

5.4.1 Cumulative frequency distributions

The number of ^{14}C-data from fluvial deposits in Germany is listed in Tab. 4.3 according to the depositional environments and sedimentary facies from which the organic material was retrieved. The largest number of data is derived from floodplains (N = 131) and palaeochannels (N = 120). The sedimentary facies used most frequently are gyttja (N = 103), peat (N = 76) and colluvium (N = 68). Based on the different facies, 148 ^{14}C-data are classified as activity ages, 106 as stability ages and 155 as transitional ages. The spatial distribution of the 432 ^{14}C-data is illustrated in Fig. 4.9. The data are not evenly distributed throughout Germany but show strong clusters i) around Freiburg in the Black Forest and the southern Upper Rhine Graben, ii) around Frankfurt in the Nidda Catchment, the Amöneburger Becken and in the northern Upper Rhine Graben, iii) at the Danube river close to Regensburg, iv) at the Weserbergland and v) at the Lippe valley.

The CPF analysis is presented in Fig. 5.6. In Fig. 5.6a the CPF of 140 synthetic equally spaced ^{14}C-ages (assumed uncertainty of $\pm$100 years for each datum) is shown. The shape of the CPF results mainly from the shape of the ^{14}C calibration curve. The CPF of the complete set of 432 ^{14}C-data is shown in Fig. 5.6b, and the CPF of the ^{14}C-ages taken to represent activity in Fig. 5.6c. Different ways of data treatment are depicted in Fig. 5.6d and 5.6e: The CPDF of all activity data divided by CPF of the equally spaced data is shown in Fig. 5.6d and the CPF of all activity data divided by the CPF of the complete dataset is shown in Fig. 5.6e. The results indicate successful rectification of the young age bias using the proposed normalisation procedure. Compared to Fig. 5.6d in Fig. 5.6e the probabilities are more uniformly distributed during the last 14 000 years and should provide a more accurate picture.

The normalised CPFs that were constructed by dividing the CPF of a data subset by the CPF of the full dataset, and that were used for further analysis and interpretation, are shown in Fig. 5.7: Radiocarbon ages representing activity in Fig. 5.7a, stability in Fig. 5.7b and transition in Fig. 5.7c. Following Macklin *et al.* (2005) phases of increased flooding are represented by 'change dates'. In the Rhine dataset 127 'change dates' were identified and the resulting CPF is plotted in Fig. 5.7d.

Periods where the relative probabilities are larger than the mean relative probability and that indicate phases of increased geomorphic activity or stability are shaded in gray in Fig. 5.7. The results of the probability frequency analysis suggest a tendency towards stable fluvial and colluvial systems dur-

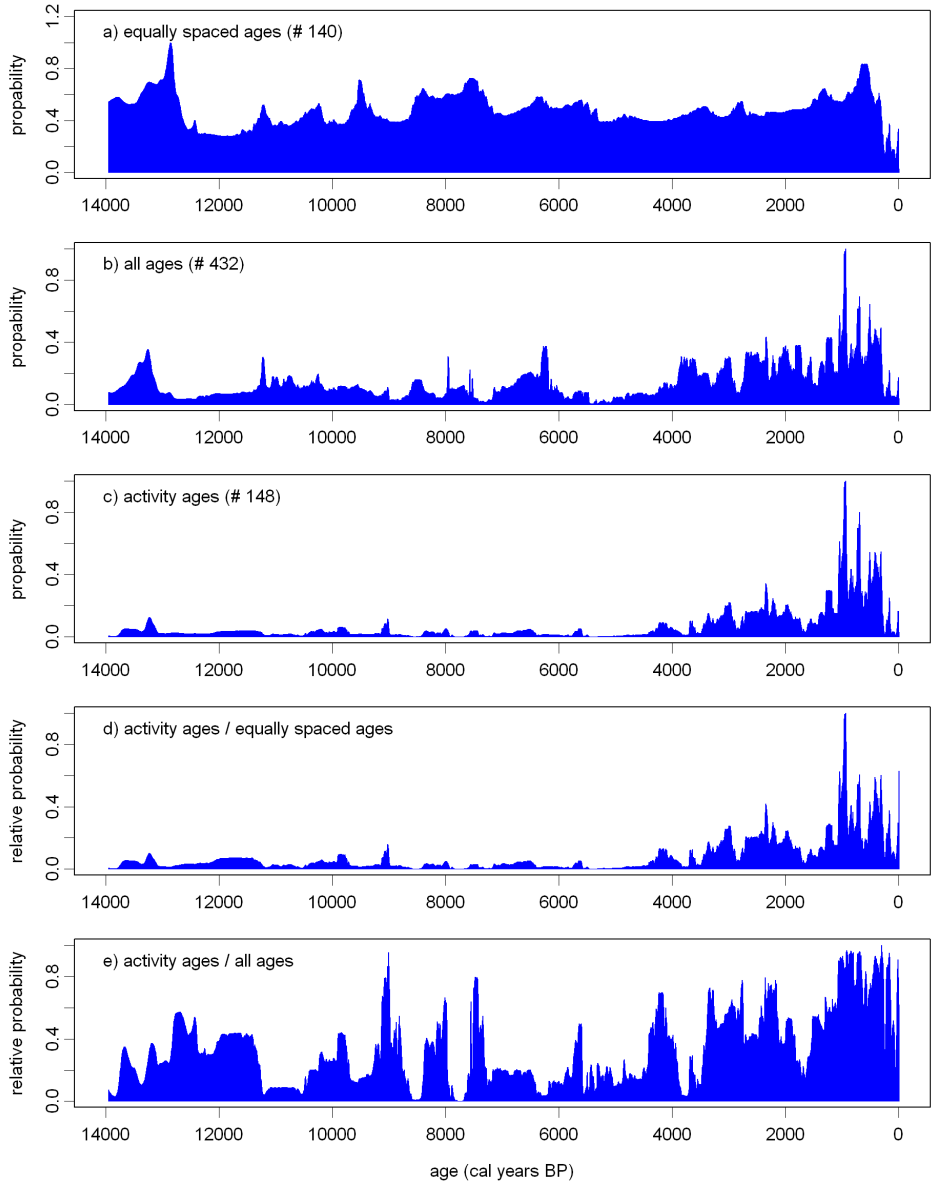

Figure 5.6: a) CPF of 140 synthetic equally spaced ^{14}C-data (error of each age was set to 100 years). b) CPF of the complete dataset (413 ^{14}C-data). c) CPF of the 134 ^{14}C-data representing activity. d) CPF of activity data divided by CDF of equally spaced ^{14}C-data. e) CPF of activity data divided by CPF of the complete dataset.

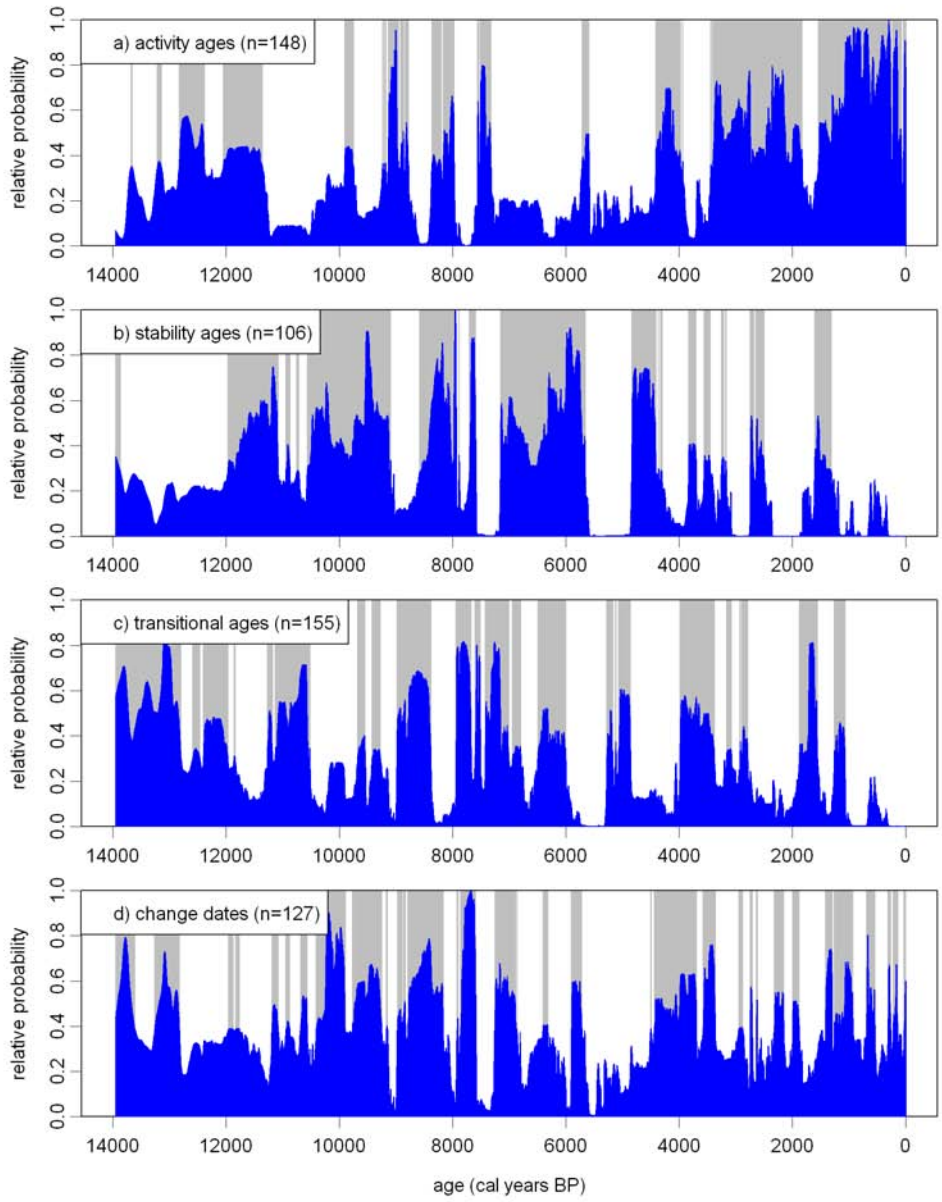

Figure 5.7: CPFs of 134 activity (a) and 68 stability (b) ages. c) CPF of 103 ^{14}C-ages of transitional status (gyttja and organic rich sediment). d) 127 'change data' reflecting phases of increased flooding (Macklin *et al.*, 2005). Gray shaded areas mark phases were the CPF is larger than the mean probability of the corresponding CPF.

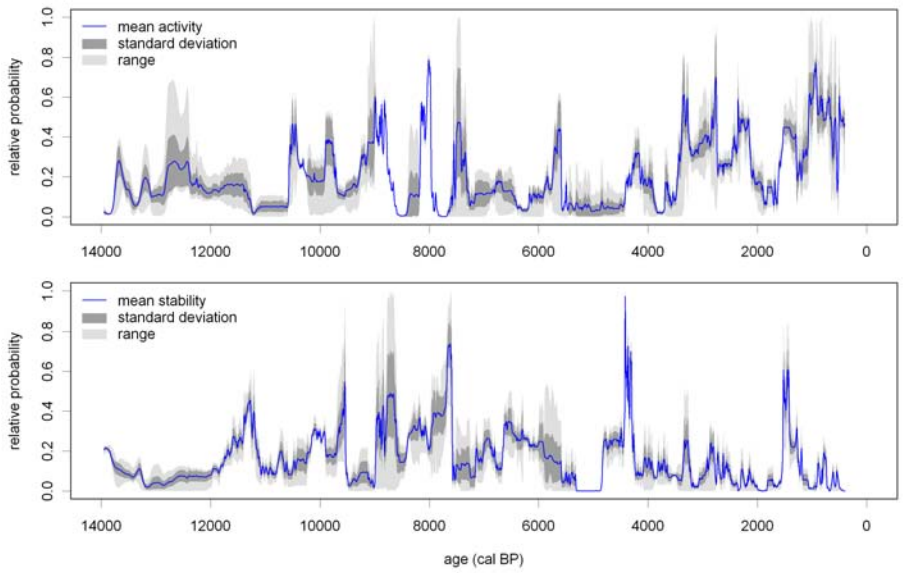

Figure 5.8: Sensitivity analysis of activity and stability CPFs. The black line represents the mean probability based on 4 CPFs calculated from randomly chosen subsets containing 50 % of the activity or stability data. The dark and light grey areas represent the standard deviation and range of the 4 CPFs.

ing the early and middle Holocene and increased activities during the Late Pleistocene and the last 4000 years in Germany. Single peaks of increased activity during the last 9 kyr are located at 9.0 kyr, 8.2 kyr, 7.5 kyr, 5.6 kyr, 4.2 kyr, 3.3 kyr, 2.8 kyr, 2.3 kyr and 1.1 kyr. In general, phases of increased activity coincide with phases of decreased stability (and vice versa) suggesting a homogenous response of the studied system to external forcing. In contrast, phases of increased stability that coincide with phases of increased activity may result from regionally different responses to external and/or internal forcing.

To test the significance of the results a sensitivity analysis was carried out. Eight data subsets were chosen randomly: four containing 50 % of the activity data each and four containing 50 % of stability data each. The resulting probability ranges and their standard deviations are depicted in Fig. 5.8. It is shown that the increased activity at 9.0-8.5 kyr and 8.2-8.0 kyr and the increased stability around 4.3 kyr are of highest significance, as indicated by the small standard deviation and range of CPFs of the randomly chosen subsets. Even though, the remaining peaks and trends are of lower significance, they are still visible in all 4 subsets as indicated by the standard

deviation and range (grey shaded areas in Fig. 5.8), which closely follow the trend of the mean values (blue line in Fig. 5.8).

5.4.2 Sedimentation rates

The calculated sedimentation rates of 115 floodplain and 104 palaeochannel samples range between 0.02 and 9 mm year^{-1} (Fig. 5.9). The large scatter certainly results from the large spatial scale (compare Fig. 4.9) and the large small scale variation that influences the floodplain deposition. Even though there is a large scatter of three orders of magnitude, the data reveal three phases of changing sedimentation during the last 14 000 years:

1. During the Late Glacial / Early Holocene (e.g. from 14 000 to ≈ 8000 years BP) sedimentation rates range between 0.1 and 1.0 mm year^{-1}. Palaeochannel data show slightly higher sedimentation rates than floodplain samples.

2. From ≈ 8000 to ≈ 4000 years BP sedimentation rates slight decrease. In the case of the floodplain samples, the decrease is more pronounced by the lower boundary (lower dashed line in Fig. 5.9 top). The palaeochannel data are characterised by a stronger decrease of the high sedimentation rates (upper higher dashed line in Fig. 5.9 bottom). In general, this phase coincidences with the Holocene climatic optimum.

3. From 4000 years BP onwards, sedimentation rates strongly increase up to 9 mm year^{-1}. In contrast to the preceding decline, the increase is shown by the lower and upper limit of the range. However, the increase is more distinct in the case of the floodplain samples than the palaeochannel data.

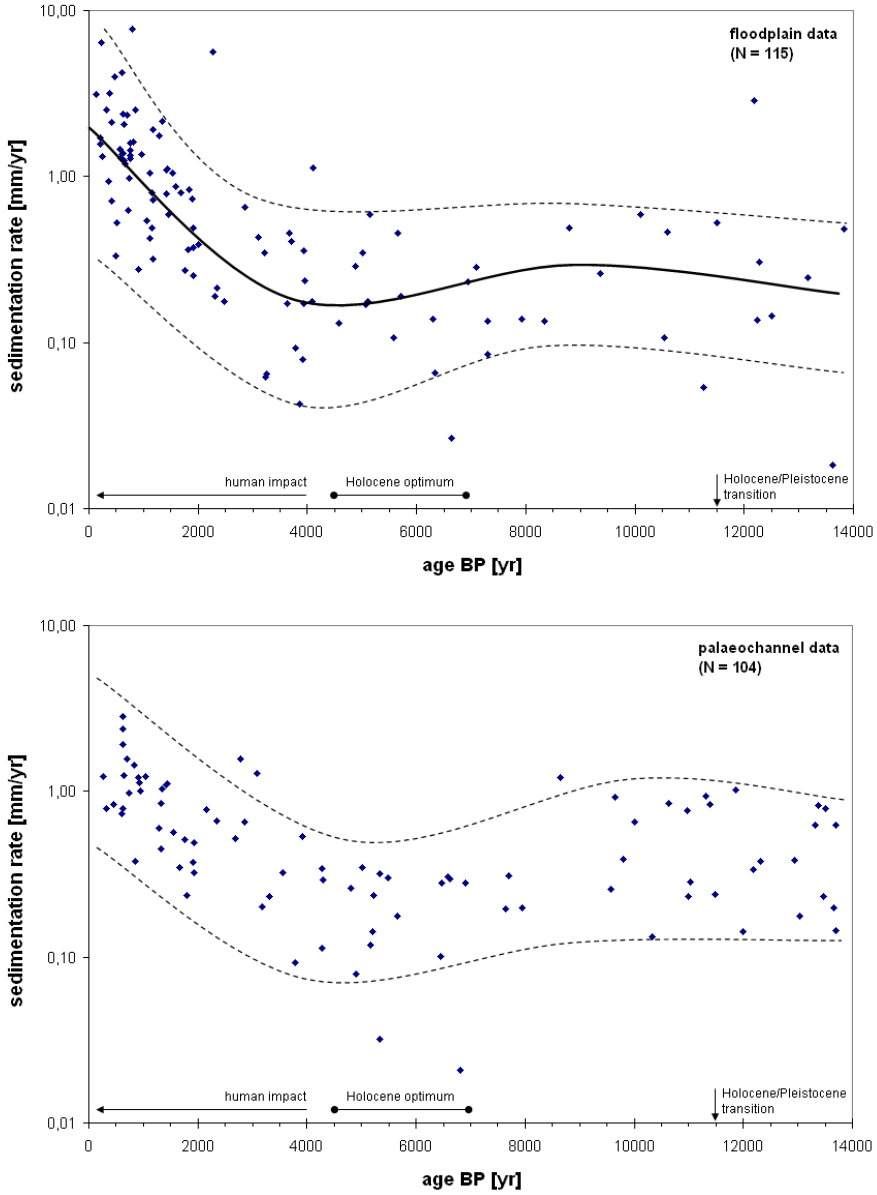

Figure 5.9: Sedimentation rates of floodplains (top) and palaeochannels (bottom) calculated based on ^{14}C sample depth and age (Eq. 4.5). Dashed lines indicates the envelope of measured sedimentation rates (drawn manually).

Chapter 6

Discussion

6.1 Holocene fluvial sediment budget

6.1.1 Quantification of sediment storage

For the first time, Holocene floodplain sediment storage within the Rhine catchment is quantified for its entire non-alpine part. The large size of the study area had several implications for quantifying the total sediment volume and applying the budget approach. First, issues of mapping resolution affecting the areal extent of floodplains were circumvented. These were solved using an upscaling approach combining data of different resolution and coverage as shown in Fig. 4.4. Second, validation of the results using 'all-available' data is not possible until now. Therefore, we assumed rather large errors on our volume estimates, particularly for the contribution derived from the upscaling procedure, because we did not validate the upscaling results until now with independent data. For now the results can only be validated using internal consistency checks and comparison with other studies that quantified hillslope erosion for parts of the catchment.

The results in Tab. 5.1 and Fig. 6.1 suggest that the sediment storage of the tributaries of the Rhine increase with catchment size, as expected. However, the heterogeneous Rhine catchment has large sinks along its trunk river that do not apply to this rule (Upper Rhine valley, Lower Rhine valley, Rhine delta). The Upper Rhine valley stores a volume that is in the same order of magnitude as the Lower Rhine valley and Rhine delta further downstream. It provides a huge storage along the river by trapping a large part of the sediments yield from southern Germany. Therefore, significant amounts of Holocene-eroded sediments do not reach the Middle and Lower Rhine at short-terms and at the Holocene timescale. So apart from the de-coupled Alpine sediment budget, also the sediment budget of the Upper Rhine is partly de-coupled from the Middle and Lower Rhine (at least when regarding interglacial suspended sediment loads, including human impact).

To further reduce the uncertainty of the calculated floodplain volumes and associated erosion rates, breakdown of the Rhine catchment into spatial entities of similar topography, lithology and history of human impact is necessary. That would enable to consider spatial variation in various steps of our methodology, such as (i) the scaling behaviour of the floodplain width, (ii) variation of mean thicknesses of floodplain deposits, (iii) aspects of drainage density and (iv) variations in the onset and duration of human impact.

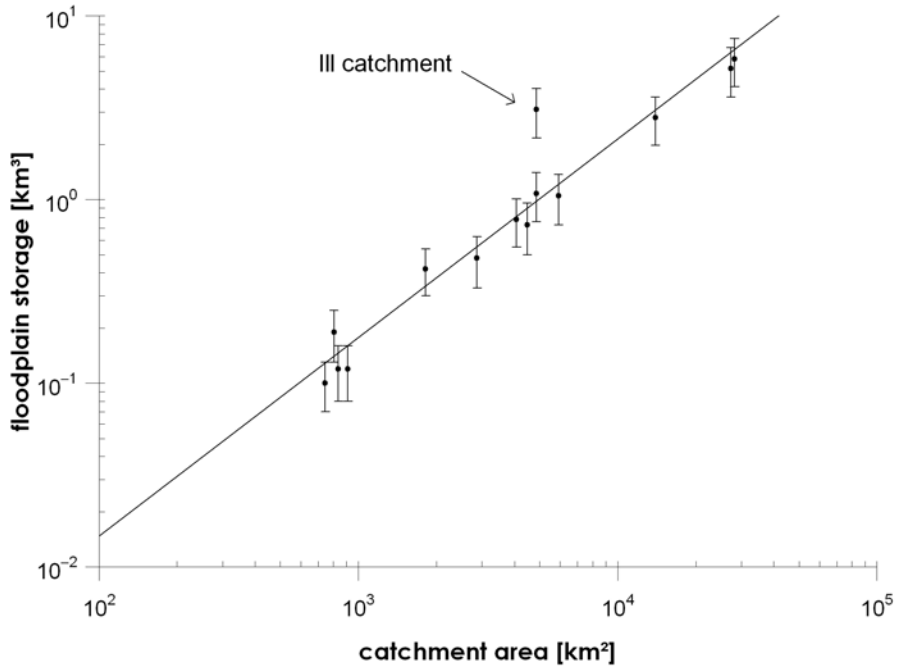

Figure 6.1: Size of Holocene alluvial sediment storages vs. subcatchment area (Tab. 5.1). The regression lines calculated is based on a power law: $S_V = 7 \times 10^{-5} A_d^{1.13} (R^2 = 0.93)$

6.1.2 Quantification of mean Holocene erosion rate

The sediment budget approach was used to calculate the Holocene erosion rates for the non-alpine Rhine catchment. Most reasonable calculations yield a mean erosion rate of 0.55 ± 0.16 t ha^{-1}yr^{-1} (38.5 ± 10.7 mm kyr^{-1}), averaged over the last 10 000 years. Mean Holocene erosion rates calculated from equations 1 and 2 are, based on (1) quantified alluvial sediment volumes S_V, (2) the time T attributed to deposition of this volume, (3) assumed *CSDR* of the river system and (4) the bulk density ρ_B of the sediment. All these parameters are estimated or assumed with some uncertainty. The applied sensitivity analysis allowed evaluating the influence of the uncertainties to the calculated erosion rate (Tab. 5.3). The erosion rate linearly depends on the sediment volume. Therefore, the uncertainty of the calculated sediment volume ($\approx$ 30 %) accounts for an uncertainty of 30 % of the calculated erosion rate. However, this value does not account for the neglected colluvial storage. Similar, the uncertainty of the bulk density ($\approx$ 13 %) accounts for an uncertainty of 13 % of the calculated erosion rate. The large variation of

the *CSDR* between 0 and 30 % results in an uncertainty of only 16 % of the erosion rate, due to the nonlinear effect of *CSDR* in Eq. 4.2. The variation of time between 3000 and 10 000 yrs. results in an uncertainty of the erosion rate of approximately 50 %.

To summarise, the sensitivity analysis showed that the largest uncertainty of the erosion rate results from the large uncertainty of the timing of floodplain deposition, followed by the uncertainty of the alluvial sediment volume. Therefore, timing is the most critical factor in the calculation of mean erosion rates. However, considering the neglected amount of colluvial storage, which was not considered in the sensitivity analysis, the uncertainty of the sediment storage may be even bigger. Though the *CSDR* is varied for a large range its impact on the uncertainty of the erosion rate rather low.

The large uncertainty in the onset of the timing of floodplain deposition, especially in the tributary valleys in the hinterland, follows from the fact that floodplain thicknesses were estimated based on the lithological boundary from sand/gravel to fines. The beginning of the Holocene sedimentation, which is marked by this lithological boundary, may strongly vary within the Rhine catchment, leading to highly variable sedimentation rates. The Pleistocene-Holocene transition had a major impact on river systems in central Europe, and the top of Pleistocene deposits is well resolved. However, it is debatable whether Holocene floodplain sediment accumulation was rather steady throughout the last 10 000 years (as appears the case in the large sinks along the trunk valley) or is a matter of mainly Late Holocene sedimentation (as appears to be the case for in the smaller tributary catchments). The maximum duration of 10 000 years results in a rather low erosion rate and is a rather safe estimate for minimum mean rates of erosion/sediment delivery. Considering the increasing erosion rates towards the Late Holocene (e.g. Lang *et al.*, 2003), most floodplain sediments are assumed to be younger.

An important parameter controlling the magnitude of the erosion estimate is the *CSDR*. Including the hinterland and the delta, our *CSDR* applies to the present river mouth (at the Dutch coast) at which location it could be considered small. Asselman *et al.* (2003) in their modelling of the modern situation consider the *CSDR* at the Dutch-German border (the delta apex) for which they derive a value of approx. 36 % (calculated over the non-alpine Rhine catchment; 27 % including the Alpes). We can use this to assess our estimate of the *CSDR* at the river mouth, assuming that the delta-apex *CSDR* under modern conditions is at the upper end of the delta apex *CSDR* range when averaged over the Holocene (because of river 'normalisation' measures for navigational and flood management purposes; see introduction). If the delta apex *CSDR* was 36 % or less during the Holocene, this implies that the delta mouth *CSDR* (i.e. full Rhine catchment *CSDR*) ranged between 0

and 30 %. This underpins our choice of *CSDR* ranges in Tab. 5.3. From the calculations, we conclude that the delta volume is somewhat underestimated: likely clayey tidal-lagoonal and estuarine deposits that occur adjacent to the fluvial delta within the Dutch coastal wedge should also be considered Rhine derived. We consider a river mouth *CSDR* of 10-20 % most realistic, when considering the volumes in Tab. 5.2. If additional ('tidal Rhine alluvium' Erkens *et al.*, 2006) volumes are added to the budget analysis, the *CSDR* further drops.

6.1.3 Comparison of the erosion rate with other studies

To evaluate the mean Holocene erosion rate derived for the Rhine catchment, it is compared with results obtained for different temporal and spatial scales, from different catchments across Central Europe (Fig. 6.2). The data set in Fig. 6.2 is cross-correlated, which introduces a bias in Fig. 6.2B: short-term erosion rates have been obtained for smaller catchments, whereas long-term rates have been obtained from larger catchments. Furthermore, the estimates are obtained using different methods, which has introduced additional variance. Nevertheless, the declining trends of the erosion rate for increasing time frame, have been attributed to (human-induced) increasing soil erosion towards the present (Bork *et al.*, 1998; Dotterweich, 2005; Lang & Honscheidt, 1999; Thiemeyer *et al.*, 2005). The reduction of erosion rates with increasing catchment size may partly reflect the reduction in mean slope for larger catchments (as an additional effect next to the increase over time), but that effect cannot be differentiated in the current dataset. We derive (roughly 50 %) lower erosion rates (Fig. 6.2A), than studies based on at-the-site-of-erosion measurements (e.g. truncated soil profiles), and attribute the difference to the colluvial storage. Comparing the calculated erosion rates with those obtained in other studies (Fig. 6.2B), the $T = 7000$ scenario fits best into the declining trend of erosion rates with increased catchment size. However, as the colluvial storage is neglected (reducing the calculated erosion rate), the $T = 10\,000$ scenario may yield better estimates for the 10 000 year averaged-rate for sediment reaching rivers.

To further improve quantifications of erosion rates building upon the sediment budget approach described above, uncertainties in the timing of the onset of sediment erosion and floodplain deposition across the hinterland should be reduced through better floodplain chronologies. Additionally, colluvial storage must be considered to evaluate possible effects of relative changes in the exchange between hillslope and channel systems. Spatially

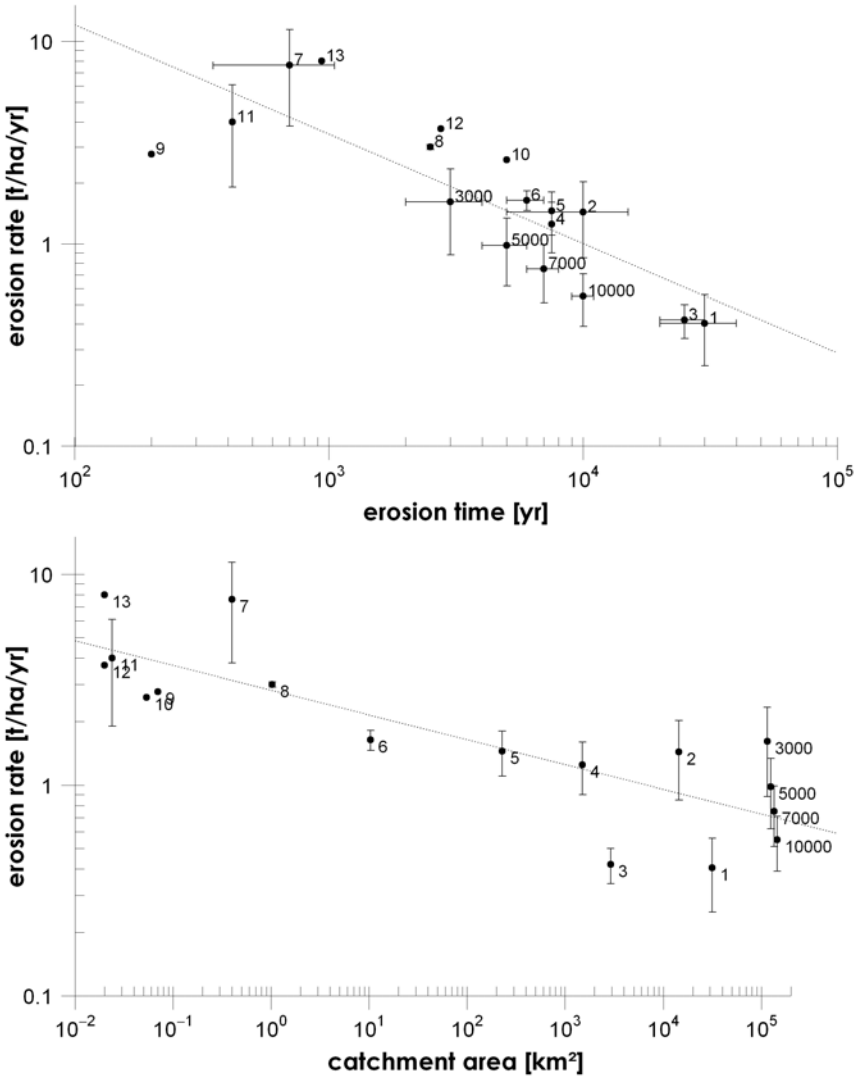

Figure 6.2: Comparison of estimates of long-term erosion rates (spanning over 250 yr), as published for catchments across Central Europe. Horizontal and vertical lines mark the error ranges of the estimates. A) Erosion rate plotted vs. averaged erosion time; B) erosion rate vs. catchment size. [1-3] Schaller *et al.* (2001); [4-6] Houben *et al.* (2006); [7] Dotterweich (2005); [8] Rommens *et al.* (2005); [9] Dotterweich *et al.* (2003a); [10] Preston (2001); [11] Schmidtchen (2003). [12] Dotterweich *et al.* (2003b); [13] Schmidtchen *et al.* (2003). [3000, 5000, 7000, 10,000] this study, time scenarios in Tab. 5.3.

disaggregating the calculations can further constrain estimates. Such would allow quantifying and dating increased floodplain deposition, and assess the spatial and temporal variation of the *CSDR*. Future research should thus include colluvial storage and focus on resolving erosion and deposition within the floodplains over Holocene timescales, to obtain better grip on changing intensities of erosion on the hillslopes. Such can further validate the estimates of effective erosion rates of this paper.

6.2 Holocene alluvial carbon budget

The results presented here are the first steps towards the utilization of the wealth of organic measurements available from case studies focusing on the Holocene dynamics of geomorphological systems in Germany. The approach classifies the *TOC* measurements based on depositional environments and sedimentary facies, which both have a significant influence on the *TOC* content.

6.2.1 Limitations and uncertainties

The approach is limited by the uncertainties caused by the spatial clustering of the *TOC* sampling sites, the measurement of *TOC* and the unambiguous terminology used to describe sedimentary facies in geomorphological systems. The *TOC* sites are strongly clustered at loess covered areas, the Northern Upper Rhine Graben and the area around Regensburg. Upland areas (e.g. Rhenish Slate Massif, Black Forest) are missing in the compiled database. As there are no data from these areas up to now the effects of this spatial bias can not be discussed. *TOC* measurements from the "missing" areas are clearly required in order to establish a more representative picture of *TOC* storage and the carbon sequestration on floodplains in the Rhine catchment.

As the *TOC* concentrations, which are compiled in this study, are measured by different methods, it must be considered that *TOC* content obtained by wet-combustion generally result in smaller values than those obtained with element analysers due to incomplete carbon oxidation (Schlichting *et al.*, 1995). In order to limit uncertainties due to different techniques of carbon combustion (Niller, 1998; Nolte, 1999; Seidel, 2004), we did not include loss on ignition measurements in our analysis. Still, *TOC* concentrations of organic samples were determined by combustion at 550 to 600°C. Therefore, mineral samples were oxidized by $K_2CR_2O_7$ and colorimetric determination of Cr^{3+} or by spectrometric analysis of CO_2. The applied measurements differ especially for sediments with high *TOC* values (e.g. channel fills) and for

clay rich samples, which may release crystal water. However, it is assumed that the errors are smaller than the local variability and are therefore not discussed further (Nolte, 1999; Seidel, 2004).

6.2.2 Significance and perspective

In a first approach, the analysed *TOC* measurements are used to calculate the *TOC* mass stored within floodplain deposits. The calculation is based on a simplified carbon budget and a Holocene sediment floodplain storage budget for the non-alpine Rhine catchment. Overall 1.1×10^9 t (with min. and max. values ranging between 0.7 and 1.6×10^9 t) *TOC* is stored by the non-alpine Rhine catchment within floodplains since the beginning of floodplain deposition of overbank fines and channel fills. Therefore, mean Holocene sequestration rates range between 0.07 and 0.53×10^6 t year^{-1} or 3.4 to 25.4 g m^{-2}year^{-1}.

To the authors knowledge this is the first estimate of carbon sequestrations rates obtained for floodplains in Germany. Interestingly, these values are in the same order of magnitude as the modern *TOC* transport at 0.65×10^6 t year^{-1} of the river Rhine measured at the gauging station at Lobith from 1975 to 1978 (Kempe *et al.*, 1991; Kempe & Krahe, 2005). Although the values obtained from the long-term *TOC* storage are smaller than the modern *TOC* export, they suggest the major importance of the floodplain storage for the fluvial carbon cycle (Fig. 4.8). Concerning the increased modern soil erosion and floodplain deposition compared to mean Holocene rates (Tab. 5.3) and considering the different temporal scales (modern vs. Holocene) the importance of *TOC* storage within the floodplains may even increase further.

The long-term sequestration rates from the Rhine catchment can be compared with the few data available on carbon sequestration on floodplains (Noe & Hupp, 2005; Walling *et al.*, 2006). Walling *et al.* (2006) estimated carbon sequestration rates along six rivers in southern England based on *TOC* measurements and sedimentation rates obtained from ^{137}Cs measurements. The estimated values, which range between 69.2 and 114.3 g m^{-2}year^{-1}, correspond to mean values since 1963. Noe & Hupp (2005) measured the carbon sequestration along three rivers within the Atlantic Coastal Plain (USA) using feldspar marker horizons over a period of 3-6 years. The carbon accumulation rates reported for the different sites ranged from 61 to 212 g m^{-2}year^{-1}. The estimated sequestration rates reported from the UK and USA are both an order of magnitude larger than those presented here. However, the values given by Noe & Hupp (2005) and Walling *et al.* (2006) could be expected to be higher than those reported in this paper, since the former represent recent values that correspond to increased recent soil erosion and

floodplain accumulation rates compared to mean Holocene rates (see above). To investigate the controls of carbon sequestration in more detail, a spatially and temporally resolved C-budget is necessary. Additionally, the integration of colluvial budgets is necessary to evaluated the impact of soil erosion on the global carbon cycle (Lal, 2005; Walling *et al.*, 2006).

6.3 ^{14}C-database analysis

6.3.1 Cumulative frequency distributions

The results presented here are the first step towards an utilization of the wealth of radiocarbon data available from case studies focused on the Holocene dynamics of geomorphological systems in Germany. The technique used to construct frequency distributions of ^{14}C-ages by dividing the relative CPFs of the subsets by the relative CPF of the complete dataset allows reducing ambiguities originating from ^{14}C calibration curve wiggles and the sampling bias towards younger ^{14}C-ages (Fig. 5.6d and 5.6e).

The approach is limited by the uncertainties involved with radiocarbon dating and the assumptions underlying the use of ^{14}C-probabilities as a proxy of fluvial activity or stability. Issues associated include reworking of organic sediments and erroneous ^{14}C-analysis. Especially for periods of strong human impact reworking of charcoal and other organic remains is commonplace (Lang & Honscheidt, 1999; Edwards & Whittington, 2001). Due to the large number of ages included in the analysis the impact of erroneous ^{14}C-analysis are probably negligible: The sensitivity analysis (Fig. 5.8) suggests that general trends of the calculated CPFs are significant. The interpretation of narrow peaks in the CPFs should be undertaken with care as they may result from a small number of ^{14}C-ages only and may therefore represent exclusively local events. Sensitivity analysis are especially important if small data sets are to be analysed, as e.g. for regional CPFs used to unravel regionally different response to external forcing (Macklin *et al.*, 2005). Smaller numbers of ^{14}C-ages increase the weight of a single measurement and may bias the results towards incorrect ages. At present it is unclear to which level the assumptions of large number statistics can be relaxed (the minimum number of data points needed) to still obtain significant results. The sensitivity analysis of the 106 stability ages shows that significant results can be obtained using approx. 100 ^{14}C-ages only. The effects of spatial heterogeneities for the analysis are also still difficult to judge. Therefore, further work must be carried out to expand the ^{14}C-database at the national scale and to fill the gaps between the regional clusters.

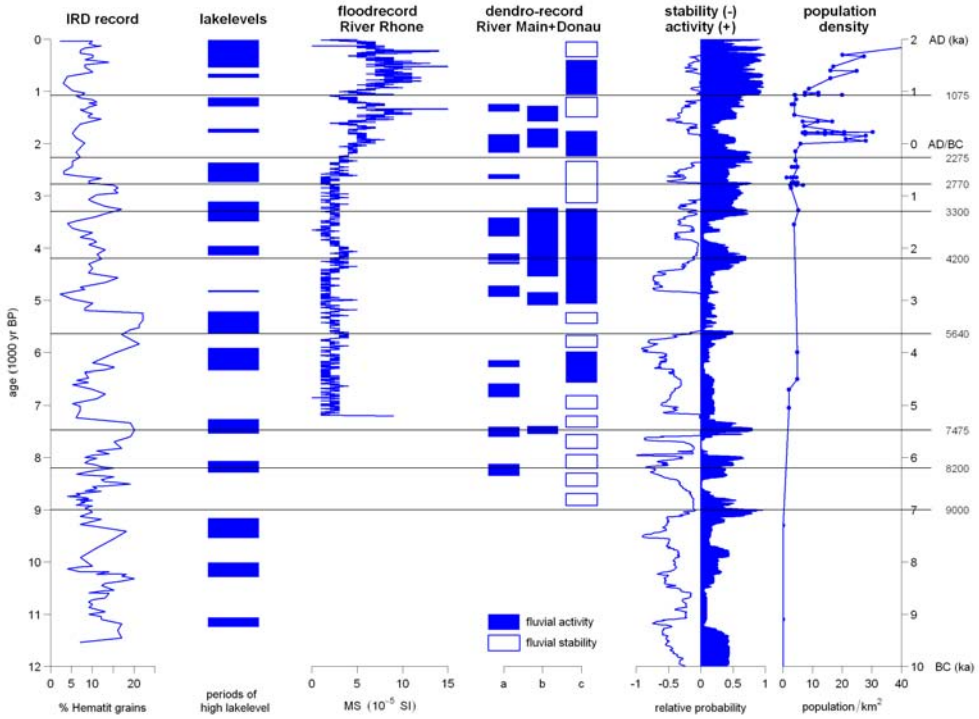

Figure 6.3: Activity and stability CPFs (column 6) plotted alongside independent palaeohydrological indicators (columns 1-5) and population data (column 7). Column 1) Ice rafted debris (IRD) record after Bond *et al.* (2001). High Hematite grain content correlates with the southwards advection of North Atlantic drift Ice and therefore with Holocene cooling phases in the North Atlantic and in Europe. Column 2) Phases of higher lake levels reconstructed from Jura, French Pre-Alps and Swiss Plateau (Magny, 2001, 2003). Column 3) Flood record of river Rhone based on magnetic susceptibility (MS) measurements on a sediment core from Lake Le Bourget, France (Arnaud *et al.*, 2005). High MS values correspond to high sediment discharge of the Rhone River to Lake Le Bourget. Column 4) Dendrochrological record of fluvial activity of a) the Main River and b) the Danube River. Phases of fluvial activity and stability (c) are based on Becker & Schirmer (1977). Column 5) Geomorphic activity (positive probability values) and stability (negative probability vales) based on CDPF analysis (this study). Column 6) Population density in Central Europe reconstructed based on archaeological finds (Zimmermann, 1996).

Comparison to other archives of Holocene environmental change

To evaluate the relative importance of climate and land use change (LUCIFS) the ^{14}C chronology of fluvial activity and stability is compared with independent archives of Holocene environmental change (Fig. 6.3). For the comparison following archives and proxy data for climate and human impact in Central Europe were chosen: the ice drifted debris record (IRD) from the North Atlantic (Bond *et al.*, 2001), lake levels in the northern Alps (Magny, 2001), floods of the alpine Rhone river (Arnaud *et al.*, 2005), fluvial activity of the Danube and the Main rivers reconstructed from a subfossil oak[1] chronology (Becker & Schirmer, 1977) and the population density (Zimmermann, 1996). Even though very different in nature, the archives are believed to represent the most reliable and complete reconstructions of climate and human impact during large parts of the Holocene in Central Europe.

Unfortunately, not all archives cover the same time span. Especially for the period before BC 7000 the activity/stability record can only be compared to IRD and lake levels (Fig. 6.3). With the exception of the 9 kyr BP peak, all activity peaks (at around 8.2 kyr, 7.5 kyr, 5.6 kyr, 4.2 kyr, 3.3 kyr, 2.7 kyr, 2.3 kyr and after 1.1 kyr) coincide with changing environmental conditions recognized at least in one alternative recorded. The prominent cooling at 8200 year BP (e.g. Alley *et al.*, 1997; Prasad *et al.*, 2006) that started at around 8600 years and ended after 8000 years (Rohling & Palike, 2005) is clearly seen by increased probability densities of the activity data as well as in the dendrochronological record of the Main (Becker & Schirmer, 1977) and higher lake levels in the alpine foreland (Magny, 2001). The following phase of increased activity reaches its maximum at 7475 years and again correlates with higher lake levels and Rannen-deposits. In contrast to the 8200 years BP event, the 7475 years BP event is also characterised by high percentages of Hematite grains of the IRD-record (Bond *et al.*, 2001), suggesting a cooler climate during that phase. The increased activity at around 5640 years BP may result from cooler and/or wetter climate conditions as evidenced by the IRD and lake level records as well as by the flood record of the River Rhone (Arnaud *et al.*, 2005). Another prominent event of cooler and wetter climatic conditions following the Holocene Climatic Optimum can be recognized in all palaeohydrological records: The increased geomorphic activity that started at around 4400 years and ended approximately at 3900

[1]Subfossil oaks that were frequently found in gravel bed deposits of Central European rivers are called Rannen. Using dendrochronological techniques, the Rannen were dated and their ages were analysed in terms of frequency distributions by Becker & Schirmer (1977). Times with high frequencies of Rannen deposits are generally interpreted as phases of increased river activity.

years BP coincidences with higher lake levels, increased flood activity and a high number of deposited Rannen in the Main and Donau catchments.

Wide spread human impact occurred for the first time during the Bronze Age. The activity maximum at 3300 years BP coincides with cooler/wetter climatic conditions (e.g. high percentages of hematite grains, high lake levels, increased flooding of the Rhone and a large number of deposited Rannen in the Donau catchment) and falls in a period that is associated with growing population densities (Fig. 6.3), changing agricultural practices and increased arable land use (Zimmermann, 1996)). Deciphering the relative role of climatic variability and human impact during that period is rather difficult. For example, the small peak at 2770 years coincides with increased population density and agricultural activity as well as a cold phase at 2650 a (Van Geel *et al.*, 1998) that resulted in a marked glacier advance in the European Alps from 2800 a to 2600 years (Holzhauser *et al.*, 2005). A differing pattern can be seen for the broad peak of fluvial activity at 2275 years (ranging from 2300-2100 years BP). This maximum does not coincide with a change in climate or population density but coincides with a shift in landuse techniques during the pre-Roman Iron Age.

Increasing probabilities in the activity record after 1075 years seem to be associated with the rising population density that resulted in enhanced agricultural activities. This correlates with the general increasing trend in the flood record of the River Rhone, which is interpreted to results from growing sediment yield due to increasing human impact since at least the Iron Age (Arnaud *et al.*, 2005).

To summarise, before 4200 years BP, events of fluvial activity are mainly coupled with wetter and/or cooler climatic phases. Due to the growing population and intensified agricultural activities from the Bronze ages onwards, the increase in geomorphologic activity between 3300 years and 2770 years BP can not unequivocally be related to climate. From approximately 1075 years BP onwards the growing population density and the associated changes in land use are considered as the major external forcing of river activity. The human impact significantly increased the sensitivity of the fluvial systems to climatic events so that even relatively low intensity rainfalls result in sever flooding.

Comparisons of change data

To evaluate the concept of 'change data' and their CPDF as a proxy of past hydrological events (Macklin *et al.*, 2006), the CPFs of change data from the German database are compared to the records from Poland, Great Britain and Spain (Macklin *et al.*, 2006, Fig. 6.4).

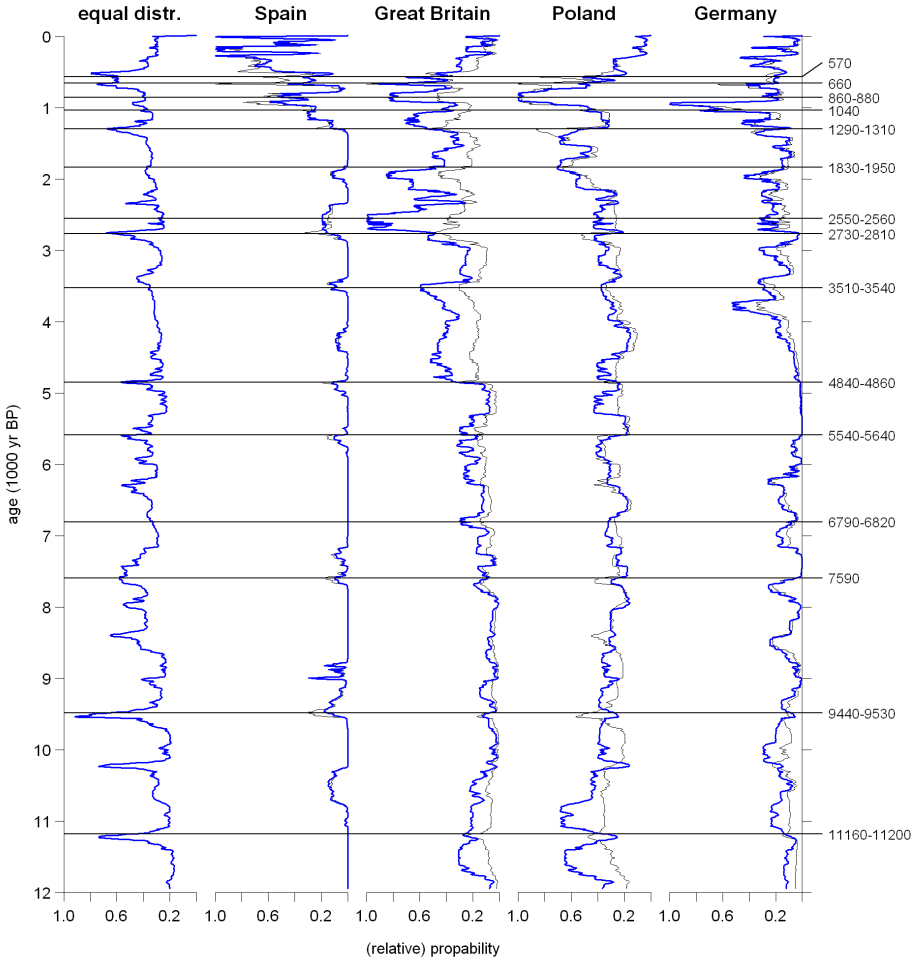

Figure 6.4: Comparing CPF of 140 equally distributed ^{14}C-ages (every 50 years with an 1σ-error of 50 years) and reanalysed CPDFs of 'change dates' from Greate Britain, Spain and Poland and the newly compiled CPF from Germany. Thin black line: CPF of change ages (not normalised). Thick blue line: reanalysed, normalised CPF of change dates: non-normalised CPF of change ages divided by CPF of 140 equally spaced ^{14}C-ages. Episodes of European flooding taken from Macklin *et al.* (2006) are listed on the left axis and are shown by the horizontal lines.

In Fig. 6.4 the CPF of the 140 equally distributed ages (left graph) is plotted along with the normalised CPFs (thick lines) of changes dates from Spain, Greate Britain, Poland and Germany. Thin lines represent non-normalised CPFs of the change ages. Episodes of European flooding taken from Macklin *et al.* (2006) are listed on the right-hand axis and are shown by horizontal lines. It must be considered that episodes of European flooding are reconstructed by Macklin *et al.* (2006) based on the probability differences as described above. As can be seen from the comparison with the CPDF of equally spaced ^{14}C-ages, periods of major flooding in Europe [2] are associated with plateaus of the ^{14}C calibration curve (peaks in the CPDF of the equally spaced ages) (Fig. 6.4). Thus, the calculation of probability difference curves based on Macklin *et al.* (2006) seems not to fully remove influences from variations in atmospheric ^{14}C. The approach used here based on dividing the relative CPFs of change data by the relative CPFs of equally spaced ^{14}C-ages seems mathematically more sound compared to the analysis of (Macklin *et al.*, 2006). Concerning the reanalysed data, which are not influenced by the form of the calibration curve, the correlation between the datasets is questionable. Except for the 7.5 kyr BP event, there are no major peaks in the CPFs that coincide in more than two countries. Therefore, synchronous response of the fluvial systems in the four different countries to large-scale climatic change can not be detected. The results obtained from the analysis of the CPDFs of the change data challenges the major findings by Macklin *et al.* (2006). The CPDF-concept is not suitable to reconstruct major periods of flooding. In fact, the change in sedimentation style, which is analysed by the change date concept, does not correlated to periods of major flooding. It is stated that change in sedimentation style is dominantly controlled by internal forcing and not by major flooding. Furthermore, the 'change date' concept uses only 50 % of the data in each database, while the above described approach of activity and stability data uses as much information of the database as possible.

6.3.2 Sedimentation rates

The estimated range of sedimentation rates between 0.01 and 10 mm year^{-1} agrees well with rates estimated from similar floodplain environments in different parts of the Earth (Walling *et al.*, 1998; Rumsby, 2000; Knox, 2006, compare also Chapter 2.1.3). However, the values are an order of magnitude smaller than those estimated for the Yellow River in China (Xu, 1998,

[2]Periods of major flooding are defined by flood events that occur in more than one country (Macklin *et al.*, 2006)

compare also Fig. 2.13).

The large scatter of the sedimentation rates, however, is the result of i) the complex configuration of floodplains with a large spatial variability of the depositional environment, ii) the large spatial scales that is covered by the compiled ^{14}C-database and iii) the problems that correspond to the ^{14}C-dating of fluvial sediments.

Despite the large scatter, three phases can be assigned regarding the changes in floodplain and palaeochannel sedimentation, during the last 14 000 years: i) the Late Glacial-Holocene with medium sedimentation rates, ii) Holocene Climatic Optimum with a slightly decreasing rates and iii) the last 4000 years, which are characterised by a remarkable increase in sedimentation rates. In general, the results agree with the model of Holocene floodplain developments explained by Brown (1996). Therefore, the slightly increased sedimentation rates before approximately 8000 years BP coincide with the disequilibrium and colonization of the early Holocene floodplains that result from the rapid climate change during the Late Glacial-Holocene transition of European floodplains (Brown, 1996). The equilibrium and stability of the middle Holocene floodplains is shown by decreasing sedimentation. Due to the large scatter, the differences between these two phases are only very limited and must be carefully discussed. The results, therefore, suggest only a minor change of floodplain sedimentation due to the natural environmental change. The last 4000 years, however, are characterised by a significant increasing rate that is caused by strong human impact on floodplain sedimentation.

For the first time, the wealth of radiocarbon data available from floodplain deposits in Germany is utilized to show the increasing floodplain deposition during the last 4000 years. It appears to be a large-scale signal, which occurred in almost all floodplains in the Rhine and neighbouring catchments. Similar results were obtained from the Yellow River in China (Xu, 1998), where the transformation of the natural vegetation at the start of the Sui Dynastie (at approx AD 581) caused human induced acceleration of the floodplain deposition by an order of magnitude from approximately 0.5 cm year^{-1} to more than 9 cm year^{-1}. However, the sedimentation rates are an order of magnitude larger than those reported here, resulting from the large extend of erodable loess areas in the Yellow River catchment.

In the case of the Mississippi (Knox, 2006), the increasing floodplain deposition due to human impact started much later and turn out to be much smaller (max. rates are smaller than 2.2 mm year^{-1}). Additionally, there is a general increase of floodplain deposition during the last 8000 years, which is dominantly caused by climate shift during the Holocene. The Mississippi data suggest a less significant human impact but a more pronounced climate

impact than inherent in the data obtained from Germany and the Yellow River.

Chapter 7

Conclusion and Perspectives

7.1 Holocene fluvial sediment budget

For the first time a Holocene-averaged sediment budget for the Rhine catchment is presented. This provides useful information on the efficiency of floodplains as major sedimentary sinks along the drainage network of large catchments. To quantify the sediment stored in the fluvial system, a multi-scale budgeting approach was used. Therefore, average thickness of floodplain sediment accumulations were calculated across the catchment. Furthermore, an upscaling method was developed to deal with partial data coverage regarding maps that resolve the spatial extent of smaller sediment storages. The results were used as complementary data to larger floodplains that had been mapped catchment wide at lower resolution maps. By including the volumes trapped in the Rhine delta at the downstream end of the system, problems of sediment loss and unclosed budgets were minimized, although still 10-20 % of the total eroded volume can be considered to be yielded to the North Sea during the Holocene.

The sediment budget resulted in a total mass of Holocene alluvial sediments of $58.9 \pm 13.7 \times 10^9$ t, corresponding to a mean erosion rate of 0.55 ± 0.14 t $ha^{-1}year^{-1}$ (38.9 ± 10.8 mm kyr^{-1}), averaged over last 10 000 years. This value is low compared to other estimates of long-term erosion rates across Central Europe, for several reasons: (1) the quantification excludes colluvial storage on hillslopes, (2) a linear average was calculated whereas erosion rates and accumulation of floodplain sediments were most probably increasing over the Holocene. To account the problems of timing several time scenarios were explored.

7.2 Holocene alluvial *TOC* budget

To the authors' knowledge, for the first time mean Holocene carbon sequestrations rates were estimated for floodplains of the Rhine catchment. The sequestration rates were calculated based on the Holocene alluvial sediment storage of the Rhine. This provides useful information on the coupling of carbon flux to sediment transfers in fluvial systems and the efficiency of floodplains as major carbon sinks along the drainage network of large catchments. The estimated total Holocene carbon sequestration rate ranges between 3.4 to 25.4 g m^2 $year^{-1}$ with more reasonable values between 5.3 to 17.7 g m^2 $year^{-1}$. Compared to recent particulate carbon export, these values are in the same order of magnitude but somewhat smaller indicating that approximately the same amount of the exported carbon may be stored in floodplains. However, compared to carbon sequestration rates obtained

elsewhere, the presented values are at the lower limit, corresponding to the lower mean Holocene soil erosion and floodplain accumulation rates.

7.3 ^{14}C-database analysis

For the first time, a database of 506 fluvial and colluvial ^{14}C-ages from Germany is complied and analysed to reconstruct phases of geomorphic activity and stability. 8 periods of activity are identified (peaking at 8.2 kyr, 7.54 kyr, 5.6 kyr, 4.2 kyr, 3.3 kyr, 2.8 kyr, 2.3 kyr and since 1075 years BP) and are compared with climatic, palaeohydrological and human impact proxy data. Until 4200 years BP, events of geomorphic activity are mainly coupled to wetter and/or cooler climatic phases. Due to growing population and intensive agricultural activities during the Bronze ages the increased geomorphologic activity between 3300 and 2770 years cannot unequivocally be related to climate. Since 1075 years the growing population density is considered as the major external forcing.

Concerning the changing sedimentation rates on floodplains and in palaeochannels, three phases were identified, during the last 14 000 years: i) the Late Glacial-Holocene with medium sedimentation rates, ii) Holocene Climatic Optimum with a slightly decreasing rates and iii) the last 4000 years, which are characterised by increasing sedimentation rates. The results are in good correspondence with a conceptual model of the Holocene floodplain development in Europe.

Work is continued, to further expand the database and to test the effects of the spatial clustering of sampling localities. In the future, the database should allow analysing fluvial system response (1) within sub-catchments of similar physiographic setting or land use history and (2) across rather homogeneous sub-catchments. This should allow an improved understanding of forcing - response relationships and will form an important step towards a temporally resolved sediment budget for the Rhine.

7.4 Concluding summary and perspectives

To understand the relative importance of land use and climate impacts on fluvial systems during the period of agriculture is the main objective of the PAGES Focus 5 - LUCIFS. In this context, the modelling of the Holocene sediment budget of the Rhine systems is the major concern of this thesis, which contributes to the German RheinLUCIFS initiative. The main aim was to test whether the numerous small scale geomorphological studies can

be used in combination with nationwide geological maps to provide new information of the large scale Rhine system. Therefore the focus was driven towards:

1. the spatially distributed modelling of the mean Holocene sediment and carbon storage in floodplain deposits of the non alpine part of the Rhine catchment and

2. the temporal variable activity status of geomorphological systems in Germany and the changing floodplain sedimentation rates.

The results show the great potential of scale-related approaches that are based on numerous available data from the Rhine catchment. However, focusing at large systems it must be considered that uncertainties increase with catchment size. Therefore, a detailed error analysis and/or the modelling of scenarios are/is essential when working at these scales. In the case of the spatial budgeting of sediment and carbon, this was done by estimating the uncertainties of the data and assumptions and by calculating the error propagation. To estimate the uncertainties of the ^{14}C-chronology, a sensitivity analysis was applied to test the significance of the results. Synthetic ^{14}C-dataset constructed fluvial landform evolution models (e.g. CEASAR, CHILD)[1] and with well defined boundary conditions can be used to further test the assumptions made.

Considering the LUCIFS objectives, it is now necessary to model spatially distributed and dynamic sediment budgets. Time dependent sediment budget models are a necessary prerequisite to understand the nonlinear behaviour of fluvial systems (Wasson, 2002). Only, when independent time series of external controls and time dependent sediment fluxes are known, is it possible to estimate the time lag between cause and effect and the changes of fluvial systems that are caused by internal feedback.

Concerning time-dependent sediment budgets at smaller spatial scales, Erkens *et al.* (2006) and Houben (2006) developed promising approaches for the Rhine Delta and a small catchment in the Hessian Basin, respectively. It is planned to extend the work of Erkens *et al.* (2006) to the German part of the Lower Rhine Embayment. Therefore, first time-dependent sediment budget analyses were already started by the author, which are based on the extensive database of the Geological Service of North Rhine-Westphalia.

[1]The CEASAR model is developed by Coulthard *et al.* (1999); Coulthard & Macklin (2001) to model long-term sediment fluxes in fluvial systems. The latest version (Coulthard & Van De Wiel, 2006) includes a module that allows the modelling of meander migration and therefore of floodplain evolution. Similar, the CHILD model is developed to model long-term landform evolution with a strong focus on the fluvial component (Tucker *et al.*, 2001)

The estimation of time-dependent erosion rates has always been a critical component of long-term sediment budgets. In most sediment budgets erosion is estimated based on the corresponding sediment depositions assuming a linear correlation between erosion and deposition. Recently, terrestrial cosmogenic nuclides (TCN, especially ^{10}Be and ^{26}Al) were applied to directly estimate hillslope erosion (for reviews see Cockburn & Summerfield, 2004; von Blanckenburg, 2006).

Additionally, the quantification of long-term, dynamic sediment budgets benefits from the development of new dating methods. Recently, optically stimulated luminescence dating (OSL) has been successfully applied to fluvial deposits over the Holocene and Pleistocene periods (see e.g. Wallinga *et al.*, 2001). Using OSL, it is for the first time possible to estimate the time of sediment deposition and therefore relax the limitations of the ^{14}C-technique[2]

To model time-dependent sediment budgets, the spatial and temporal approaches, which were applied in this thesis, need to be coupled. Based on the discussion above, this can be achieved by:

1. focusing on smaller spatial scales (up to a few 1000 km^2) at which better dating control is possible

2. including missing components of the sediment budget (e.g. independent estimates of soil erosion and colluvial storage)

3. combining classical sediment budgets with new techniques (e.g. OSL and ^{10}Be)

4. evaluating the impacts of soil erosion and colluvial sediment storage on the long-term carbon cycle in fluvial systems

5. constructing regional ^{14}C-chronologies for different depositional environments

6. constructing scale-dependent ^{14}C-chronologies (e.g. the grouping of activity ages based on their contributing catchment size)

The erosion measurements based on TCN in combination with sediment budget approaches and new dating techniques provide a powerful tool to model dynamic, time-dependent sediment budget of fluvial systems.

[2]Using ^{14}C-dating the time of death of the dated sample is estimated and not the time since deposition.

Bibliography

Aalto, R., Maurice-Bourgoin, L., Dunne, T., Montgomery, D. R., Nittrouer, C. A., & Guyot, J. L. (2003). Episodic sediment accumulation on Amazonian flood plains influenced by El Nino/Southern Oscillation. *Nature*, **425**(6957), 493–497.

Adams, J., Maslin, M., & Thomas, E. (1999). Sudden climate transitions during the Quaternary. *Progress in Physical Geography*, **23**(1), 1–36.

Allen, J. R. L. (1965). A review of the origin and characteristics of recent alluvial sediment. *Sedimentology*, **5**, 89–191.

Alley, R. B. & Agustsdottir, A. M. (2005). The 8k event: cause and consequences of a major Holocene abrupt climate change. *Quaternary Science Reviews*, **24**(10-11), 1123–1149.

Alley, R. B., Mayewski, P. A., Sowers, T., Stuiver, M., Taylor, K. C., & Clark, P. U. (1997). Holocene climatic instability: A prominent, widespread event 8200 yr ago. *Geology*, **25**(6), 483–486.

Andres, W. (1989). The Central German Uplands. In F. Ahnert (Hrsg.), *Landorms and landform evolution in West Germany*, pp. 25–44. Catena Supplement 15.

Andres, W. (1998). Terrestrische Sedimente als Zeugen natürlicher und anthropogener Umweltveränderungen seit der letzten Eiszeit. In R. Dikau, G. Heinritz, & R. Wiessner (Hrsg.), *Global Change - Konsequenzen für die Umwelt*, pp. 118–133. Steiner, Stuttgart.

Andres, W., Bos, J. A. A., Houben, P., Kalis, A. J., Nolte, S., Rittweger, H., & Wunderlich, J. (2001). Environmental change and fluvial activity during the Younger Dryas in central Germany. *Quaternary International*, **79**, 89–100.

Arnaud, F., Revel, M., Chapron, E., Desmet, M., & Tribovillard, N. (2005). 7200 years of Rhone river flooding activity in Lake Le Bourget, France: a high-resolution sediment record of NW Alps hydrology. *Holocene*, **15**(3), 420–428.

Asselman, N. E. M. (1999). Suspended sediment dynamics in a large drainage basin: the River Rhine. *Hydrological Processes*, **13**(10), 1437–1450.

Asselman, N. E. M. (2000). Fitting and interpretation of sediment rating curves. *Journal of Hydrology*, **234**(3-4), 228–248.

Asselman, N. E. M. & Middelkoop, H. (1995). Floodplain sedimentation: quantities, patterns and processes. *Earth Surface Processes and Landforms*, **20**, 481–499.

Asselman, N. E. M., Middelkoop, H., & van Dijke, P. (2003). The impact of changes in climate and land use on soil erosion, transport and deposition of suspended sediment in the River Rhine. *Hydrological Processes*, **17**, 3225–3244.

Auerswald, K. & Dikau, R. (2006). Review of erosion measurements.

Bak, P. (1988). Self-organized criticality. *Physical Review A*, **38**(1), 364–374.

Bak, P. (1996). *How nature works: the science of self organized criticality.* Springer-Verlag, New York.

Becker, B. & Schirmer, W. (1977). Palaeoecological study on the Holocene valley developement of the River Main, Southern Germany. *Boreas*, **6**, 303–321.

Beets, D. & Van der Spek, A. (2000). The Holocene evolution of the barrier and the back-barrier basins of Belgium and the Netherlands as a function of late Weichselian morphology, relative sea-level rise and sediment supply. *Netherlands Journal of Geosciences*, **79**, 3–16.

Behrmann, J. H., Ziegler, P. A., Schmid, S. M., Heck, B., & Granet, M. (2005). The EUCOR-URGENT Project. Upper Rhine Graben: evolution and neotectonics. *International Journal of Earth Sciences*, **94**(4), 505–506.

Benedetti, M. M. (2003). Controls on overbank deposition in the upper Mississippi River. *Geomorphology*, **56**(3-4), 271–290.

Berendsen, H. & Stouthamer, E. (2001). *Palaeogeographical development of the Rhine-Meuse delta, The Netherlands.* Van Gorcum, Assen.

Beyer, L., Fründ, R., Schleuss, U., & Wachendorf, C. (1993). Colluvisols under Cultivation in Schleswig-Holstein .2. Carbon Distribution and Soil Organic-Matter Composition. *Zeitschrift für Pflanzenernährung und Bodenkunde*, **156**(3), 213–217.

Bibus, E. & Wesler, J. (1995). The middle Neckar as an example of fluviomorphological provesses during the Middle and Late Quaternary period. *Zeitschrift für Geomorphologie N.F., Suppl.-Bd.*, **100**, 15–26.

Boardman, J. & Favis-Mortlock, D. (1999). Frequency-magnitude distributions for soil erosion, runoff and rainfall - a comparative analysis. *Zeitschrift für Geomorphologie N.F., Suppl.-Bd.*, **115**, 51–70.

Boden, A. (1996). *Bodenkundliche Kartieranleitung*. Schweizerbartsche Verlagsbuchhandlung, Hannover, 4 edition.

Bogaart, P. W., Van Balen, R. T., Kasse, C., & Vandenberghe, J. (2003). Process-based modelling of fluvial system response to rapid climate change II. Application to the river Maas (the Netherlands) during the Last Glacial-Interglacial Transition. *Quaternary Science Reviews*, **22**(20), 2097–2110.

Bond, G., Showers, W., Cheseby, M., Lotti, R., Almasi, P., deMenocal, P., Priore, P., Cullen, H., Hajdas, I., & Bonani, G. (1997). A pervasive millennial-scale cycle in North Atlantic Holocene and glacial climates. *Science*, **278**(5341), 1257–1266.

Bond, G., Kromer, B., Beer, J., Muscheler, R., Evans, M. N., Showers, W., Hoffmann, S., Lotti-Bond, R., Hajdas, I., & Bonani, G. (2001). Persistent solar influence on north Atlantic climate during the Holocene. *Science*, **294**(5549), 2130–2136.

Bork, H.-R. & Lang, A. (2003). Quantification of past soil erosion and land use / land cover changes in Germany. In A. Lang, K. Hennrich, & R. Dikau (Hrsg.), *Long Term Hillslope and Fluvial System Modelling. Concepts and Case Studies from the Rhine River Catchment*, Lecture Notes in Earth Sciences, pp. 231–240. Springer, Heidelberg.

Bork, H.-R., Bork, H., Dalchow, C., Faust, B., Piorr, H.-P., & Schatz, T. (1998). *Landschaftsentwicklung in Mitteleuropa*. Klett-Perthes, Gotha, Stuttgart.

Bremer, H. (1989). On the geomorphology of the South German scarplands. In F. Ahnert (Hrsg.), *Landorms and landform evolution in West Germany.*, pp. 45–68. Catena Supplement 15.

Bridge, J. (2003). *Rivers and Floodplains*. Backwell, Malden.

Brierley, G. & Fryirs, K. (2005). *Geomorphology and River Management. Applications of the River Styles Framework*. Blackwell, Malden.

Bronk Ramsey, C. (1995). Radiocarbon Calibration and Analysis of Stratigraphy: The OxCal Program. *Radiocarbon*, **37**, 425–430.

Bronk Ramsey, C. (2001). Development of the Radiocarbon Program OxCal. *Radiocarbon*, **43**, 355–363.

Brown, A. & Quine, T. (1999). Fluvial Processes and Environmental Change: An Overview. In A. Brown & T. Quine (Hrsg.), *Fluvial Processes and Environmental Change*, pp. 1–27. John Wiley & Sons Ltd.

Brown, A. G. (1996). Floodplain environments. In M. G. Anderson, D. E. Walling, & P. Bates (Hrsg.), *Floodplain Processes*, pp. 95–138. John Wiley & Sons Ltd., Chichester.

Brown, A. G. (2002). Learning from the past: palaeohydrology and palaeoecology. *Freshwater Biology*, **47**, 817–829.

Brunsden, D. & Thornes, J. (1979). Landscape sensitivity and change. *Transactions Institute of British Geographers (New Series)*, **4**(4), 463–484.

Burt, T. (1996). Linking Hillslopes to Flooplains. In M. G. Anderson, D. E. Walling, & P. Bates (Hrsg.), *Floodplain Processes*, pp. 461–492. John Wiley & Sons Ltd., Chichester.

Chorley, R. & Kennedy, B. (1971). *Physical geography - A systems approach*. London.

Chorley, R., Schumm, S., & Sugden, D. E. (1984). *Geomorphology*. Methuen, London, New York.

Church, M. & Slaymaker, O. (1989). Disequilibrium of Holocene sediment yield in glaciated British Columbia. *Nature*, **337**(2), 452–454.

Church, M., Ham, D., Hassan, M., & Slaymaker, O. (1999). Fluvial clastic sediment yield in Canada: scaled analysis. *Canadian Journal of Earth Sciences*, **36**(8), 1267–1280.

Cockburn, H. A. P. & Summerfield, M. A. (2004). Geomorphological applications of cosmogenic isotope analysis. *Progress in Physical Geography*, **28**(1), 1–42.

Cohen, K. (2005). 3D Geostatistical interpolation and geological interpretation of paleo-groundwater rise in the Holocene coastal prism in the Netherlands. In L. Giosan & J. Bhattacharya (Hrsg.), *River Deltas - Concepts, models, and examples. SEPM Special Publication*, **83**, pp. 341–364.

Cole, J. J. & Caraco, N. F. (2001). Carbon in catchments: connecting terrestrial carbon losses with aquatic metabolism. *Marine and Freshwater Research*, **52**(1), 101–110.

Coulthard, T. J. & Macklin, M. G. (2001). How sensitive are river systems to climate and land-use changes? A model-based evaluation. *Journal of Quaternary Science*, **16**(4), 347–351.

Coulthard, T. J. & Van De Wiel, M. (2006). A cellular model of river meandering. *Earth Surface Processes and Landforms*, **31**, 123–132.

Coulthard, T. J., Kirkby, M., & Macklin, M. (1999). Modelling the Impacts of Holocene Environmental Change in an Upland River Catchment, Using Cellular Atomaton Approach. In A. Brown & T. Quine (Hrsg.), *Fluvial Processes and Environmental Change*, pp. 31–46. John Wiley & Sons Ltd.

Crutzen, P. J. & Stroemer, E. (2000). The Anthropocene. *IGBP Newsletter*, **41**, 12.

Dambeck, R. (2005). *Beiträge zur spät- und postglazialen Fluß- und Landschaftsgeschichte im nördlichen Oberrheingraben*. Dissertation, Johann Wolfgang Goethe-University.

Daniels, J. M. & Knox, J. C. (2005). Alluvial stratigraphic evidence for channel incision during the Mediaeval Warm Period on the central Great Plains, USA. *Holocene*, **15**(5), 736–747.

Dansgaard, W., Johnsen, S., Clausen, H., Dahl-Jensen, D., Gundestrup, N., Hammer, C., Hvidberg, C., Steffensen, J., Sveinbjörnsdttir, A., Jouzel, J., & Bond, G. (1993). Evidence for general instability of past climate from a 250 kyr ice-core record. *Nature*, **264**, 218–220.

Dearing, J. A. & Jones, R. T. (2003). Coupling temporal and spatial dimensions of global sediment flux through lake and marine sediment records. *Global and Planetary Change*, **39**(1-2), 147–168.

Dearing, J. A., Battarbee, R. W., Dikau, R., Larocque, I., & Oldfield, F. (2006). Human-environment interactions: learning from the past. *Regional Environmental Change*, **6**(1-2), 1–16.

Dedkov, A. (2004). The relationship between sediment yield and drainage basin area. *IAHS Publ.*, **288**, 197–204.

deMenocal, P. B. (2001). Cultural responses to climate change during the Late Holocene. *Science*, **292**(5517), 667–673.

Diamond, J. (2005). *Collapse. How Societies Choose to Fail or Succeed.* Penguin Group, New York.

Dikau, R. (2006). Oberflächenprozesse - ein altes oder neues Thema? *Geographica Helvetica*, **61**(3), 170–180.

Dikau, R., Herget, J., & Hennrich, K. (2005). Land use and climate impacts on fluvial systems during the period of agriculture in the river Rhine catchmen (RhineLUCIFS) - An introduction. *Erdkunde*, **59**(3/4), 177–183.

Dix, A., Burggraaff, P., Kleefeld, K.-D., Küster, H., Schirmer, W., & Zimmermann, A. (2005). Human impact and vegetation change as triggers for sediment dynamics in the river Rhine catchment. *Erdkunde*, **59**(3/4), 276–293.

Dotterweich, M. (2005). High-resolution reconstruction of a 1300 year old gully system in northern Bavaria, Germany: a basis for modelling long-term human-induced landscape evolution. *Holocene*, **15**(7), 994–1005.

Dotterweich, M., Schmitt, A., Bork, H., & Schmidtchen, G. (2003a). Jungholozäne Bodenerosion und Kerbenbildung im Wolfsgraben bei Bamberg. *Forschungen zur Deutschen Landeskunde*, **253**, 129–164.

Dotterweich, M., Haberstroh, J., & Bork, H. (2003b). Mittel- und jungholozäne Siedlungsentwicklung, Landnutzung, Bodenbildung und Bodenerosion an einer mittelalterlichen Wüstung bei Friesen, Landkreis Kronach in Oberfranken. *Forschungen zur Deutschen Landeskunde*, **253**, 17–56.

Dotterweich, M., Schmitt, A., Schmidtchen, G., & Bork, H.-R. (2003c). Quantifying historical gully erosion in northern Bavaria. *Catena*, **50**, 135–150.

Downs, P. & Gregory, K. J. (2004). *River Channel Management. Towards sustainable catchment hydrosystems.* Arnold, London.

Edwards, K. J. & Whittington, G. (2001). Lake sediments, erosion and landscape change during the Holocene in Britain and Ireland. *Catena*, **42**(2-4), 143–173.

Einsele, G. & Hinderer, M. (1998). Quantifying denudation and sediment-accumulation systems (open and closed lakes): basic concepts and first results. *Palaeogeography Palaeoclimatology Palaeoecology*, **140**(1-4), 7–21.

Erkens, G., Cohen, K. M., Gouw, M., Middelkoop, H., & Hoek, W. (2006). Holocene sediment budgets of the Rhine delta (the Netherlands): A record of changing sediment delivery. *IAHS Publ.*, **206**, 406–415.

Erskine, W. & Warner, R. (1999). Significance of river bank erosion as a sediment scource in the alternating flood regimes of South-eastern Australia. In A. Brown & T. Quine (Hrsg.), *Fluvial Processes and Environmental Change*, pp. 139–164. John Wiley & Sons Ltd.

Evans, R. (1990). Soil erosion: its impacts on the English and Welsh landscape since woodland clearance. In J. Boardman, I. Foster, & J. Dearing (Hrsg.), *Soil Erosion on Agricultural Land*, pp. 232–254. John Wiley & Sons Ltd., Chichester.

Favis-Mortlock, D., Boardman, J., & Bell, M. (1997). Modelling long-term anthropogenic erosion of a loess cover: South Downs, UK. *Holocene*, **7**(1), 79–89.

Fonstad, M. & Marcus, W. A. (2003). Self-organized criticality in riverbank systems. *Annals of the Association of American Geographers*, **93**(2), 281–296.

Glaser, R., Ammann, B., Brauer, A., Heiri, O., Jacobeit, J., Lotter, A., Luterbacher, J., Maisch, M., Magny, M., Pfister, C., Tinner, W., Veit, H., & Wanner, H. (2005). Palaeoclimate within the River Rhine catchment during Holocene and historic times. *Erdkunde*, **59**(3/4), 251–275.

Glatzel, S. & Sommer, M. (2005). Colluvial soils and landscape position: field studies on greenhouse gas exchange and related ecologfical characteristics. *Zeitschrift für Geomorphologie N.F., Suppl.-Bd.*, **139**, 87–99.

Glatzel, S. & Stahr, K. (2002). The greenhouse gas exchange of a pond margin in South Germany. In G. Broll, W. Merbach, & E. Pfeiffer (Hrsg.), *Wetlands in Central Europe. Soil Organisms, soil ecological processes and trace gas emissions*, pp. 215–233. Springer, Stuttgart.

Gomez, B., Phillips, J. D., Magilligan, F. J., & James, L. A. (1997). Floodplain sedimentation and sensitivity: summer 1993 flood, Upper Mississippi River Valley. *Earth Surface Processes and Landforms*, **22**(923-936).

Gregory, K., Benito, G., Dikau, R., Golosov, V., Johnstone, E., Jones, J., Macklin, M. G., Parsons, A., Passmore, D. G., Poesen, J., Soja, R., Starkel, L., Thorndycraft, V. R., & Walling, D. E. (2006). Past hydrological events and global change. *Hydrological Processes*, **20**, 199–204.

Gregory, K. J. (2006). The human role in changing river channels. *Geomorphology*, **79**, 172–191.

Harrison, C. G. A. (2000). What factors control mechanical erosion rates? *International Journal of Earth Sciences*, **88**(4), 752–763.

Harrison, S. (2001). On reductionism and emergence in geomorphology. *Transactions of the Institute of British Geographers*, **26**(3), 327–339.

Hay, W. W. (1998). Detrital sediment fluxes from continents to oceans. *Chemical Geology*, **145**(3-4), 287–323.

Herget, J. (2000). Holocene development of the River Lippe Valley, Germany: A case study of anthropogenic influence. *Earth Surface Processes and Landforms*, **25**(3), 293–305.

Herget, J., Bremer, E., Coch, T., Dix, A., Eggenstein, G., & Ewald, K. (2005). Engeneering impact on river channels in the Rhine catchment. *Erdkunde*, **59**(3/4), 294–319.

Hilgart, M. (1995). *Die geomorphologische Entwicklung des Altmühl- und Donautales im Raum Dietfurt-Kelheim-Regensburg im jüngeren Quartär. Forschungen zur Deutschen Landeskunde*, **242**. Selbstverlag, Trier.

Hinderer, M. (2001). Late Quaternary denudation of the Alps, valley and lake fillings and modern river loads. *Geodinamica Acta*, **14**, 231–263.

Hofius, K. (1996). The River Rhine: Geography and its catchment area. In IHP/OHP (Hrsg.), *The River Rhine - Developement and Management*, pp. 3–12. Koblenz.

Holzhauser, H., Magny, M., & Zumbuhl, H. J. (2005). Glacier and lake-level variations in west-central Europe over the last 3500 years. *Holocene*, **15**(6), 789–801.

Hooijer, A., Klijn, F., Pedroli, B., & Van Os, A. (2004). Towards sustainable flood risk management in the Rhine and the Meuse River basins: synopsis of the findings of the IRMA-SPONGE. *River Research and Applications*, **20**(3), 343–357.

Hooke, J. (2003). River meander behaviour and instability: a framework for analysis. *Transactions Institute of British Geographers (New Series)*, **28**, 238–253.

Houben, P. (2002). *Die räumlich-zeitlich veränderte Reaktion des fluvialen Systems auf jungquartäre Klimaänderungen. Eine Fallstudie aus der Hessischen Senke.* Dissertation, Universität Frankfurt.

Houben, P. (2006). A Holocene sediment budget for Rockenberg catchment. Fieldguid to the Open LUCIFS Workshop may 11, 2006.

Houben, P., Hoffmann, T., Zimmermann, A., & Dikau, R. (2006). Land use and climatic impacts on the Rhine system (RheinLUCIFS): Quantifying sediment fluxes and human impact with available data. *Catena*, **66**, 42–52.

Houghton, J., Ding, Y., Griggs, D., Noguer, M., van der Linden, P., Dai, X., Maskell, K., & Johnson, C. (2001). *Climate change 2001: The Scientific Basis: Contribution of the Working Group I to the Third Assessment Report of the IPCC, 2001.* University Press, Cambridge.

Huntley, B., Baillie, M., Grove, J., Hammer, C., Harrison, S. P., Jacomet, S., Jansen, E., Karlen, W., Koc, N., Luterbacher, J., Negendank, J. F. W., & Schibler, J. (2002). Holocene palaeoenvironmental changes in Nort-West Europe: Climatic implications and the human dimension. In G. Wefer, W. Berger, K.-E. Behre, & E. Jansen (Hrsg.), *Climate Development and History of the North Atlantic Realm*, pp. 259–298. Springer, Berlin.

Johnstone, E., Macklin, M. G., & Lewin, J. (2006). The development and application of a database of radiocarbon-dated Holocene fluvial deposits in Greate Britain. *Catena*, **66**, 14–23.

Kalis, A., Merkt, J., & Wunderlich, J. (2003). Environmental changes during the Holocene climatic optimum in central Europe - human impact and natural causes. *Quaternary Science Reviews*, **22**, 33–79.

Kalweit, H. (Hrsg.) (1993). *Der Rhein unter der Einwirkung des Menschen: Ausbau, Schiffahrt, Wasserwirtschaft.* Lelystadt.

Kemp, J. (2004). Flood channel morphology of a quiet river, the Lachlan downstream from Cowra, southeastern Australia. *Geomorphology*, **60**(1-2), 171–190.

Kempe, S. & Krahe, P. (2005). Water and biogeochemical fluxes in the river Rhine catchment. *Erdkunde*, **59**, 216–250.

Kempe, S., Pettine, M., & Cauwet, G. (1991). Biogeochemistry of European Rivers. In E. Degens, S. Kempe, & J. E. Richey (Hrsg.), *SCOPE 42: Biogeochemistry of Major World Rivers*, pp. 169–212. John Wiley & Sons, Chichester.

Kesel, R. H. (2003). Human modifications to the sediment regime of the Lower Mississippi River flood plain. *Geomorphology*, **56**(3-4), 325–334.

Kirchner, J. W., Finkel, R. C., Riebe, C. S., Granger, D. E., Clayton, J. L., King, J. G., & Megahan, W. F. (2001). Mountain erosion over 10 yr, 10 k.y., and 10 m.y. time scales. *Geology*, **29**(7), 591–594.

Kirkby, M. (1999a). Landscape Modelling at Regional to Continental Scales. In S. Hergarten & H. J. Neugebauer (Hrsg.), *Process Modelling and Landform Evolution. Lecture Notes in Earth Sciences*, **78**, pp. 189–204. Springer-Verlag, Heidelberg.

Kirkby, M. (1999b). Towards an Understanding of Varieties of Fluvial Form. In A. Miller & A. Gupta (Hrsg.), *Varieties of Fluvial Form*, pp. 507–514. John Wiley & Sons Ltd., Chichester.

Knighton, A. D. (1998). *Fluvial forms and processes*. Arnold, London.

Knorr, W., Prentice, I., House, J., & Holland, E. (2005). Long-term sensitivity of soil carbon turnover to warming. *Nature*, **433**, 298–301.

Knox, J. C. (2000). Sensitivity of modern and Holocene floods to climate change. *Quaternary Science Reviews*, **19**(1-5), 439–457.

Knox, J. C. (2006). Floodplain sedimentation in the Upper Mississippi Valley: Natural versus human accelerated. *Geomorphology*, **79**, 286–310.

Lal, R. (2004). Managing soil carbon. *Science*, **304**, 393.

Lal, R. (2005). Soil erosion and carbon dynamics. *Soil & Tillage Research*, **81**(2), 137–142.

Lal, R. & Kimble, J. (1999). Pedogenic carbonates and the global carbon cycle. In R. Lal, J. Kimble, H. Eswaran, & B. Stewart (Hrsg.), *Global climate change and pedogenic carbonates*, pp. 1–14. Lewis, Boca Raton, London, New York, Washington D.C.

Lane, S. N. & Richards, K. S. (1997). Linking river channel form and process: Time, space and causality revisited. *Earth Surface Processes and Landforms*, **22**(3), 249–260.

Lang, A. (2002). Phases of soil erosion-derived colluviation in the loess hills of South Germany. *Catena*, **51**, 209–221.

Lang, A. & Honscheidt, S. (1999). Age and source of colluvial sediments at Vaihingen-Enz, Germany. *Catena*, **38**(2), 89–107.

Lang, A., Bork, H.-R., Mäckel, R., Preston, N., Wunderlich, J., & Dikau, R. (2003). Changes in sediment flux and storage within a fluvial system: some examples from the Rhine chatchment. *Hydrological Processes*, **17**, 3321–3334.

Lawler, D. (1993). The measurement of river bank erosion and lateral channel change, a review. *Earth Surface Processes and Landforms*, **18**, 777–821.

Leigh, D. S. (2006). Terminal Pleistocene braided to meandering transition in rivers of the Southeastern USA. *Catena*, **66**(1-2), 155–160.

Leopold, L. & Wolman, M. G. (1957). River channel pattern: braided, meandering and straight. *United States Geological Survey Professional Paper*, **282-B**, 85 pp.

Leopold, L. B., Wolman, M. G., & Miller, J. (1964). *Fluvial Processes in Geomorphology*. Freemann and Company, San Francisco.

Lewin, J. & Brewer, P. A. (2001). Predicting channel patterns. *Geomorphology*, **40**(3-4), 329–339.

Lewin, J. & Macklin, M. G. (2003). Preservation potential for Late Quaternary river alluvium. *Quaternary Science Reviews*, **18**(2), 107–120.

Lewin, J., Macklin, M. G., & Johnstone, E. (2005). Interpreting alluvial archives: sedimentological factors in the British Holocene fluvial record. *Quaternary Science Reviews*, **24**, 1973–1889.

Litt, T., Brauer, A., Goslar, T., Merkt, J., Balaga, K., Muller, H., Ralska-Jasiewiczowa, M., Stebich, M., & Negendank, J. F. W. (2001). Correlation and synchronisation of Lateglacial continental sequences in northern central Europe based on annually laminated lacustrine sediments. *Quaternary Science Reviews*, **20**(11), 1233–1249.

Litt, T., Schmincke, H.-U., & Kromer, B. (2003). Environmental response to climatic and volcanic events in central Europe during the Weichselian Lateglacial. *Quaternary Science Reviews*, **22**, 7–32.

Ludwig, W., Probst, J. L., & Kempe, S. (1996). Predicting the oceanic input of organic carbon by continental erosion. *Global Biogeochemical Cycles*, **10**(1), 23–41.

Macaire, J. J., Bernard, J., Di-Giovanni, C., Hinschberger, F., Limondin-Lozouet, N., & Visset, L. (2006). Quantification and regulation of organic and mineral sedimentation in a late-Holocene floodplain as a result of climatic and human impacts (Taligny marsh, Parisian Basin, France). *Holocene*, **16**(5), 647–660.

Mäckel, R., Schneider, R., & Seidel, J. (2003). Anthropogenic impact on the landscape of the southern Badenia (Germany) during the Holocene - documented by colluvial and alluvial sediments. *Archaeometry*, **45**(3), 497–511.

Macklin, M. G. (1999). Holocene river environments in prehistoric Britain: Human interaction and impact. *Quaternary Proceedings*, **7**, 521–530.

Macklin, M. G. & Lewin, J. (2003). River sediments, great floods and centennial-scale Holocene climate change. *Journal of Quaternary Science*, **18**(2), 101–105.

Macklin, M. G., HudsonEdwards, K. A., & Dawson, E. J. (1997). The significance of pollution from historic metal mining in the Pennine orefields on river sediment contaminant fluxes to the North Sea. *Science of the Total Environment*, **194**, 391–397.

Macklin, M. G., Fuller, I., Lewin, J., Maas, G., Passmore, D., Rose, J., Woodward, J., Black, S., Hamlin, R., & Rowan, J. (2002). Correlation of fluvial sequences in the Mediterranean basin over the last 200 ka and their relationship to climate change. *Quaternary Science Reviews*, **21**, 1633â1641.

Macklin, M. G., Johnstone, E., & Lewin, J. (2005). Pervasive and long-term forcing of Holocene river stability and flooding in Greate Britian by centennial-scale climate change. *The Holocene*, **15**(7), 937–943.

Macklin, M. G., Benito, G., Gregory, K., Johnstone, E., Lewin, J., Michczynska, D., Soja, R., Starkel, L., & Thorndycraft, V. R. (2006). Past hydrological events reflected in the Holocene fluvial record of Europe. *Catena*, **66**, 145–154.

Magny, M. (2001). Palaeohydrological changes as reflected by lake-level fluctuations in the Swiss Plateau, the Jura Mountains and the northern French

Pre-Alps during the Last Glacial-Holocene transition: a regional synthesis. *Global and Planetary Change*, **30**(1-2), 85–101.

Magny, M. (2003). Holocene climatic variability as reflected by mid-European lake-level fluctuations, and its probable impact on prehistoric human settlements. *Quaternary International*, **113**(1), 65–79.

Makaske, B. (2001). Anastomosing rivers: a review of their classification, origin and sedimentary products. *Earth-Science Reviews*, **53**(3-4), 149–196.

Mann, M., Bradley, R., & Hughes, M. (1999). Northern hemisphere temperatures during the past millennium: inferences, uncertainties and limitations. *Geophysical Research Letters*, **26**, 759–762.

Martin, C. W. (2000). Heavy metal trends in floodplain sediments and valley fill, River Lahn, Germany. *Catena*, **39**(1), 53–68.

Matthews, J. A. & Briffa, K. (2005). The 'Little Ice Age': re-evaluation of an evolving concept. *Geografiska Annaler*, **87A**, 17–36.

Mayorga, E., Aufdenkampe, A. K., Masiello, C. A., Krusche, A. V., Hedges, J. I., Quay, P. D., Richey, J. E., & Brown, T. A. (2005). Young organic matter as a source of carbon dioxide outgassing from Amazonian rivers. *Nature*, **436**(7050), 538–541.

Messerli, B., Grosjean, M., Hofer, T., Nunez, L., & Pfister, C. (2000). From nature-dominated to human-dominated environmental changes. *Quaternary Science Reviews*, **19**(1-5), 459–479.

Meybeck, M. (1993). C, N, P and S in rivers: from sources to global inputs. In R. Wollast, F. Mackenzie, & L. Chou (Hrsg.), *Interactions of C, N, P and S: biogeochemical cycles and global change.*, pp. 163–193. Springer, Berlin, Heidelberg, New York.

Meybeck, M. (2003). Global analysis of river systems: from Earth system controls to Anthropocene syndromes. *Philosophical Transactions of the Royal Society of London Series B-Biological Sciences*, **358**(1440), 1935–1955.

Meybeck, M., Laroche, L., Durr, H. H., & Syvitski, J. P. M. (2003). Global variability of daily total suspended solids and their fluxes in rivers. *Global and Planetary Change*, **39**(1-2), 65–93.

Middelkoop, H., Thonon, I., & Van der Perk, M. (2002). Effective discharge for heavy metal deposition on lower River Rhine flood plains. In *The structure, function and managemant of fluvial sedimentary systems. IAHS Publ.*, **276**, pp. 151–159, Alice Springs, Australia.

Milliman, J. & Syvistki, J. P. (1992). Geomorphic / tectonic control of sediment discharge to the ocean: the importance of small mountainous rivers. *The Journal of Geology*, **100**, 525–544.

Mol, J. (1997). Fluvial response to Weichselian climate changes in the Niederlausitz (Germany). *Journal of Quaternary Science*, **12**(1), 43–60.

Molnar, P. (2001). Climate change, flooding in arid environments, and erosion rates. *Geology*, **29**(12), 1071–1074.

Morehead, M. D., Syvitski, J. P., Hutton, E. W. H., & Peckham, S. D. (2003). Modeling the temporal variability in the flux of sediment from ungauged river basins. *Global and Planetary Change*, **39**(1-2), 95–110.

Morgan, R. P. C. (1986). *Soil erosion and conservation*. Longman, Harlow.

Nanson, G. (1986). Episodes of vertical accretion and catastrophic stripping: a model of disequilibrium flood-plain development. *Geological Society of America Bulletin*, **97**, 1467–1475.

Nanson, G. C. & Croke, J. (1992). A genetic classification of floodplains. *Geomorphology*, **4**, 459–486.

Nanson, G. C. & Knighton, A. D. (1996). Anabranching rivers: Their cause, character and classification. *Earth Surface Processes and Landforms*, **21**(3), 217–239.

Negendank, J. F. W. (2004). The Holocene: Considerations with regard to its climate and climate archives. In H. Fischer, T. Kumke, G. Lohmann, G. Flösser, H. Miller, H. von Storch, & J. F. W. Negendank (Hrsg.), *The Climate in Histroical Times. Towards a Synthesis of Holocene Data and Climate Models.*, pp. 1–12. Springer, Berlin.

Nicholas, A. P. & Walling, D. E. (1997). Modelling flood hydraulics and overbank deposition on river floodplains. *Earth Surface Processes and Landforms*, **22**(1), 59–77.

Niller, H. (1998). *Prähistorische Landschaften im Lösgebiet bei Regensburg. Kolluvien, Auenlehme und Böden als Archive der Paläoumwelt. Regensburger Geographische Schriften*, **31**. Regensburg.

Niller, H. (2001). Wandel prähistorischer Landschaften. Kolluvien, Auenlehme und Böden: Archive zur Rekonstruktion vorgeschichtlicher anthropogener Landschaftsveränderungen in Lösgebiet bei Regensburg. *Erdkunde*, **55**, 32–48.

Noe, G. B. & Hupp, C. R. (2005). Carbon, nitrogen, and phosphorus accumulation in floodplains of Atlantic Coastal Plain rivers, USA. *Ecological Applications*, **15**(4), 1178–1190.

Nolte, S. (1999). *Auensedimente der Wetter als Indikatoren für die spätglaziale und holozäne fluviale Morphodynamik in der nördlichen Wetterau*. Dissertation, Friedrich Wilhelm.

Oldfield, F. & Alverson, K. (2003). The societal relevance of paleoenvironmental research. In K. Alverson, R. Bradley, & T. Pedersen (Hrsg.), *Paleoclimate, global change and the future*, pp. 1–11. Springer, Berlin.

Oldfield, F. & Dearing, J. A. (2003). The role of human activities in past environmental change. In K. Alverson, R. Bradley, & T. Pedersen (Hrsg.), *Paleoclimate, global change and the future*, pp. 143–162. Springer, Berlin.

Olley, J. M. & Wasson, R. (2003). Changes in the flux of sediment in the Upper Murrumbidgee catchment, Southeastern Australia, since European settlement. *Hydrological Processes*, **17**, 3307–3320.

Owens, P. N. & Walling, D. E. (2003). Temporal changes in the metal and phosphorus content of suspended sediment transported by Yorkshire rivers, UK over the last 100 years, as recorded by overbank floodplain deposits. *Hydrobiologia*, **494**(1-3), 185–191.

Panin, A. (2004). Landâocean sediment transfer in palaeotimes, and implications for present-day natural fluvial fluxes. *IAHS Publ.*, **288**, 115–124.

Parton, W. J., Scurlock, J. M. O., Ojima, D. S., Gilmanov, T. G., Scholes, R. J., Schimel, D. S., Kirchner, T., Menaut, J. C., Seastedt, T., Moya, E. G., Kamnalrut, A., & Kinyamario, J. I. (1993). Observations and Modeling of Biomass and Soil Organic-Matter Dynamics for the Grassland Biome Worldwide. *Global Biogeochemical Cycles*, **7**(4), 785–809.

Petit, J., Jouzel, J., Raynaud, D., Barkov, N., Barnola, J.-M., Basile, I., Benders, M., Chappellaz, J., Davis, M., Delayque, G., Delmotte, M., Kotlyakov, V., Legrand, M., Lipenkov, V., Lorius, C., Ppin, L., Ritz, C., Saltzman, E., & Stievenard, M. (1999). Climate and atmospheric history

of the past 420,000 years from the Vostok ice core, Antarctica. *Nature*, **399**, 429–436.

Pfister, L., Kwadijk, J., Musy, A., Bronstert, A., & Hoffmann, L. (2004). Climate change, land use change and runoff prediction in the Rhine-Meuse basins. *River Research and Applications*, **20**(3), 229–241.

Phillips, J. D. (1999). *Earth Surface Systems. Complexity, Order, and Scale.* Blackwell, Oxford.

Phillips, J. D. (2003). Sources of nonlinearity and complexity in geomorphic systems. *Progress in Physical Geography*, **27**(1), 1–23.

Phillips, J. D. (2006). Deterministic chaos and historical geomorphology: a review and look forward. *Geomorphology*, **76**, 109–121.

Pinter, N., van der Ploeg, R., Schweigert, P., & Hoefer, G. (2006). Flood magnification on the River Rhine. *Hydrological Processes*, **20**, 147–164.

Pizzuto, J. (1987). Sediment diffusion during overbank flows. *Sedimentology*, **34**, 301–317.

Poesen, J., Nachtergaele, J., Verstraeten, G., & Valentin, C. (2003). Gully erosion and environmental change: importance and research needs. *Catena*, **50**, 91–133.

Powlson, D. (2005). Will soil amplify climate change? *Nature*, **433**, 204–205.

Prasad, S., Brauer, A., Rein, B., & Negendank, J. F. W. (2006). Rapid climate change during the early Holocene in western Europe and Greenland. *Holocene*, **16**(2), 153–158.

Preston, N. J. (2001). *Geomorphic response to environmental change: the inprint to deforestation and agricultural land-use on the contemporary landscape of the Pleiser Hügelland, Bonn, Germany.* Dissertation, Rheinische Friedrichs-Wilhelms-University.

Quinton, J. N., Catt, J. A., Wood, G. A., & Steer, J. (2006). Soil carbon losses by water erosion: Experimentation and modeling at field and national scales in the UK. *Agriculture Ecosystems & Environment*, **112**(1), 87–102.

Rasmussen, C., Torn, M. S., & Southard, R. J. (2005). Mineral assemblage and aggregates control carbon dynamics in a California conifer forest. *Soil Science Society of America Journal*, **69**(6), 1711–1721.

Rasmussen, S. O., Andersen, K. K., Svensson, A. M., Steffensen, J. P., Vinther, B. M., Clausen, H. B., Siggaard-Andersen, M.-L., Johnsen, S. J., Larsen, L. B., Dahl-Jensen, D., Bigler, M., Röthlisberger, R., Fischer, H., Goto-Azuma, K., Hansson, M. E., & Ruth, U. (2006). A new Greenland ice core chronology for the last glacial termination. *Journal of Geophysical Research*, **111**, D06102.

Redman, C. (1999). *Human Impact on Ancient Environments*. The University of Arizona Press, Tuscon.

Reid, L. & Dunne, T. (1996). *Rapid evaluation of sediment budgets*. GeoEcology paperback. Catena, Reiskirchen.

Reimer, P., Baillie, M., Bard, E., Bayliss, A., Beck, J., Bertrand, C., Blackwell, P., Buck, C., Burr, G., Cutler, K., Damon, P., Edwards, R., Fairbanks, R., Friedrich, M., Guilderson, T., Hughen, K., Kromer, B., McCormac, F., Manning, S., Bronk Ramsey, C., Reimer, R., Remmele, S., Southon, J., Stuiver, M., Talamo, S., Taylor, F., van der Plicht, J., & Weyhenmeyer, C. (2004). INTCAL04 Terrestrial radiocarbon age calibration, 0-26 cal kyr BP. *Radiocarbon*, **46**, 1029–1058.

Richards, K. S. (2002). Drainage basin structure, sediment delivery and the response to environmental change. In S. Jones & L. Frostick (Hrsg.), *Sediment flux to basins: causes, controls and conseqoences.. Special Publications*, **191**, pp. 149–160. Geological Society, London.

Roberts, N. (1998). *The Holocene: An Environmental History*. Blackwell, 2 edition.

Rohdenburg, H. (1970). Morphodynamische Aktivitäts- und Stabilitätszeit statt Pluvial- und Interpluvialzeiten. *Eiszeitalter und Gegenwart*, **21**, 81–96.

Rohling, E. J. & Palike, H. (2005). Centennial-scale climate cooling with a sudden cold event around 8,200 years ago. *Nature*, **434**(7036), 975–979.

Rommens, T., Verstraeten, G., Poesen, J., Govers, G., Van Rompaey, A., Peeters, I., & A., L. (2005). Soil erosion and sediment deposition in th Belgian loess belt during the Holocene: establishing a sediment budget for a small agricultural catchment. *The Holocene*, **15**(7), 1032–1043.

Rommens, T., Verstraeten, G., Bogman, P., Peeters, I., Poesen, J., Govers, G., Van Rompaey, A., & Lang, A. (2006). Holocene alluvial sediment

storage in a small river catchment in the loess area of central Belgium. *Geomorphology*, **77**(1-2), 187–201.

Ruddiman, W. F. (2003). The anthropogenic greenhouse era began thousands of years ago. *Climatic Change*, **61**(3), 261–293.

Rumsby, B. (2000). Vertical accretion rates in fluvial systems: A comparison of volumetric and depth-based estimates. *Earth Surface Processes and Landforms*, **25**(6), 617–631.

Rumsby, B. & Macklin, M. G. (1996). River response to the last neoglacial (the Little Ice Age) in northern, western and central Europe. In J. Branson, A. G. Brown, & K. J. Gregory (Hrsg.), *Global Continental Change: the context of Palaeohydrology*, pp. 217–233. Geological Society Special Publication.

Sarmiento, J. & Gruber, N. (2002). Sinks for anthropogenic carbon. *Physics today*, **55**(8), 30–36.

Schaller, M., von Blanckenburg, F., Hovius, N., & Kubik, P. W. (2001). Large-scale erosion rates from in situ-produced cosmogenic nuclides in European river sediments. *Earth and Planetary Science Letters*, **188**(3-4), 441–458.

Schellmann, G. (1990). Fluviale Geomorphodynamik im jüngeren Quartär des unteren Isar- und angrenzenden Donautales. *Düsseldorfer Geographische Schriften*, **29**.

Schiefer, E., Slaymaker, O., & Klinkenberg, B. (2001). Physiographically controlled allometry of specific sediment yield in the Canadian Cordillera: A lake sediment-based approach. *Geografiska Annaler*, **83A**(1-2), 55–65.

Schimel, D. S., Braswell, B. H., Holland, E. A., McKeown, R., Ojima, D. S., Painter, T. H., Parton, W. J., & Townsend, A. R. (1994). Climatic, Edaphic, and Biotic Controls over Storage and Turnover of Carbon in Soils. *Global Biogeochemical Cycles*, **8**(3), 279–293.

Schirmer, W. (1983). Symposium "Franken": Ergebnisse zur holozänen Talentwicklung und Ausblick. *Geologisches Jahrbuch*, **A71**, 355–370.

Schirmer, W. (1995). Valley bottoms in the late Quaternary. *Zeitschrift für Geomorphologie N.F., Suppl.-Bd.*, **100**, 27–51.

Schirmer, W., Bos, J., Dambeck, R., Hinderer, M., Preston, N., Schulte, A., Schwalb, A., & Wessels, M. (2005). Holocene fluviatile processes and valley history in the river Rhine catchment. *Erdkunde*, **59**(3/4), 199–215.

Schlichting, E., Blume, H., & Stahr, K. (1995). *Bodenkundliches Praktikum.* Blackwell Wissenschafts-Verlag, Berlin, Wien.

Schlünz, B. & Schneider, R. (2000). Transport of terrestrial organic carbon to the oceans by rivers: re-estimating lux- and burial rates. *International Journal of Earth Sciences*, **88**, 599–606.

Schmidtchen, G. (2003). Hang- und Moorentwicklung in der Knicklandschaft Ostholtsteins - das Profil Kiel-Schlüsbeck. *Forschungen zur Deutschen Landeskunde*, **253**, 251–268.

Schmidtchen, G., Liese, C., & Bork, H. (2003). Boden- und Reliefentwicklung am Woseriner See in Mecklenburg-Vorpommern. *Forschungen zur Deutschen Landeskunde*, **253**, 213–228.

Schumm, S. (1977). *The fluvial system.* John Wiley & Sons Ltd., New York.

Schumm, S. (1979). Geomorphic thresholds: the concept and ist application. *Transactions Institute of British Geographers (New Series)*, **4**(4), 485–515.

Schumm, S. (1991). *To interpret the Earth. Ten ways to be wrong.* Cambridg University Press, Cambridge.

Schumm, S. (2005). *River variability and complexity.* Cambridge, University Press.

Seidel, J. (2004). *Massenbilanzen holozäner Sedimente am südlichen und mittleren Oberrhein.* Dissertation, Albert-Ludwigs-Universität.

Shala, B. (2001). *Jungquartäre Talgeschichte des Rheins zwischen Krefeld und Dinslaken.* Dissertation, Heinrich-Heine-Universität.

Sidorchuk, A. Y. & Golosov, V. N. (2003). Erosion and sedimentation on the Russian Plain, II: the history of erosion and sedimentation during the period of intensive agriculture. *Hydrological Processes*, **17**(16), 3347–3358.

Slattery, M. C., Gares, P. A., & Phillips, J. D. (2002). Slope-channel linkage and sediment delivery on North Carolina coastal plain Cropland. *Earth Surface Processes and Landforms*, **27**(13), 1377–1387.

Slaymaker, O. (2006). Towards the identification of scaling relations in drainage basin sediment budgets. *Geomorphology*, **80**, 8–19.

Slaymaker, O. & Spencer, T. (1998). *Physical Geography and Global Environmental Change*. Addison Wesley Longman, Essex.

Spreafico, M. (1996). Hydrology of the Rhine basin. In IHP/OHP (Hrsg.), *The River Rhine - Developement and Management*, pp. 13–25. Koblenz.

Starkel, L. (2002a). Change in the frequency of extreme events as the indicator of climatic change in the Holocene (in fluvial systems). *Quaternary International*, **91**, 25–32.

Starkel, L. (2002b). Younger Dryas - Preboreal transition documented in the fluvial environment of Polish rivers. *Global and Planetary Change*, **2002**, 157–167.

Starkel, L., Soja, R., & Michczynska, D. (2006). Past hydrological events reflected in the Holocene history of Polish rivers. *Catena*, **66**, 24–33.

Stolum, H. (1996). River meandering as a self-organisation process. *Science*, **271**, 1710–1713.

Syvitski, J. P. M. (2003). Supply and flux of sediment along hydrological pathways: research for the 21st century. *Global and Planetary Change*, **39**(1-2), 1–11.

Taylor, M. P. (1996). The variability of heavy metals in floodplain sediments: A case study from mid Wales. *Catena*, **28**(1-2), 71–87.

Tebbens, L., Veldkamp, A., Westerhoff, W., & Kroonenberg, S. (1999). Fluvial incision and channel downcuttingas a response to Late-glacial and Early Holocene climate change: the lower reach of the River Meuse (Maas), The Netherlands. *Journal of Quaternary Science*, **14**(1), 59â75.

Ten Brinke, W. (2005). *The Dutch Rhine: A restrained river*. Veen Magazines, Diemen.

Thiemeyer, H., Blümel, W., Dambeck, R., Dieckmann, B., Eberle, J., Glade, T., Hecht, S., Houben, P., Moldenhauer, K.-M., Schrott, L., Schulte, A., Vogt, R., & Wunderlich, J. (2005). Soils, sediments and slope porcesses and their effects on sediment fluxes into the river Rhine. *Erdkunde*, **59**(3/4), 184–198.

Thorndycraft, V. & Benito, G. (2006a). Late Holocene fluvial chronolgy of Spain: The role of climate variability and human impact. *Catena*, **66**, 34–41.

Thorndycraft, V. R. & Benito, G. (2006b). The Holocene fluvial chronology of Spain: evidence from a newly compiled radiocarbon database. *Quaternary Science Reviews*, **25**, 223–234.

Trimble, S. W. (1999). Decreased rates of alluvial sediment storage in the Coon Creek Basin, Wisconsin, 1975-93. *Science*, **285**(5431), 1244–1246.

Tucker, G. E., Lancaster, S., Gasparini, N., & Bras, R. L. (2001). The Channel-Hillslope Integrated Landscape Development Model (CHILD). In R. Harmon & W. Doe III (Hrsg.), *Landscape Erosion and Evolution Modeling*, pp. 349–388. Kluwer Academic/Plenum Publishers, New York.

van den Berg, J. (1995). Prediction of alluvial channel pattern of perennial rivers. *Geomorphology*, **12**, 259–279.

van der Lee, G. E. M., Venterink, H. O., & Asselman, N. E. M. (2004). Nutrient retention in floodplains of the Rhine distributaries in The Netherlands. *River Research and Applications*, **20**(3), 315–325.

Van Geel, B., Van der Plicht, J., Kilian, M. R., Klaver, E. R., Kouwenberg, J. H. M., Renssen, H., Reynaud-Farrera, I., & Waterbolk, H. T. (1998). The sharp rise of Delta C-14 ca. 800 cal BC: Possible causes, related climatic teleconnections and the impact on human environments. *Radiocarbon*, **40**(1), 535–550.

van Rompaey, A. J. J., Govers, G., & Puttemans, C. (2002). Modelling land use changes and their impact on soil erosion and sediment supply to rivers. *Earth Surface Processes and Landforms*, **27**(5), 481–494.

Vandenberghe, J. & Maddy, D. (2001). The response of river systems to climate change. *Quaternary International*, **79**, 1–3.

Verstraeten, G., Van Rompaey, A., Poesen, J., Van Oost, K., & Govers, G. (2003). Evaluating the impact of watershed management scenarios on changes in sediment delivery to rivers? *Hydrobiologia*, **494**(1-3), 153–158.

von Blanckenburg, F. (2005). The control mechanisms of erosion and weathering at basin scale from cosmogenic nuclides in river sediment. *Earth and Planetary Science Letters*, **237**(3-4), 462–479.

von Blanckenburg, F. (2006). The control mechanisms of erosion and weathering at basin scale from cosmogenic nuclides in river sediment (vol 237, pg 462, 2005). *Earth and Planetary Science Letters*, **242**(3-4), 223–239.

Vörösmarty, C. J., Meybeck, M., Fekete, B., Sharma, K., Green, P., & Syvitski, J. P. M. (2003). Anthropogenic sediment retention: major global impact from registered river impoundments. *Global and Planetary Change*, **39**(1-2), 169–190.

Walling, D. E. (1983). The sediment delivery problem. *Journal of Hydrology*, **65**, 209–237.

Walling, D. E. (1999). Linking land use, erosion and sediment yields in river basins. *Hydrobiologia*, **410**, 223–240.

Walling, D. E. & Fang, D. (2003). Recent trends in the suspended sediment loads of the world's rivers. *Global and Planetary Change*, **39**(1-2), 111–126.

Walling, D. E. & Webb, B. (1996). Erosion and sediment yield: a global overview. *IAHS Publ.*, **236**, 3–19.

Walling, D. E., He, Q. P., & Nicholas, A. P. (1996). Flooplains as Suspended Sediment Sinks. In M. G. Anderson, D. E. Walling, & P. Bates (Hrsg.), *Floodplain Processes*, pp. 399–440. John WIley & Sons Ltd., Chichester.

Walling, D. E., Owens, P. N., & Leeks, G. J. L. (1998). The role of channel and floodplain storage in the suspended sediment budget of the River Ouse, Yorkshire, UK. *Geomorphology*, **22**(3-4), 225–242.

Walling, D. E., Fang, D., Nicholas, A. P., & Sweet, R. J. (2006). River floodplains as carbon sinks. *IAHS Publ.*, **306**, 460–470.

Wallinga, J., Murray, A. S., Duller, G. A. T., & Tornqvist, T. E. (2001). Testing optically stimulated luminescence dating of sand-sized quartz and feldspar from fluvial deposits. *Earth and Planetary Science Letters*, **193**(3-4), 617–630.

Wasson, R. (1996). *Land use and climate impacts on fluvial systems during the period of agriculture. Recommendations for a research porject and its implementation.. PAGES Workshop Report*, **Series 96-2**.

Wasson, R. (2002). Sediment budgets, dynamics, and variability: new approaches and techniques. *IAHS Publ.*, **276**, 471–478.

Wetzel, V. (1996). The River Rhine - Navigation and water power, engineering works, economical and ecological aspects, management. In IHP/OHP (Hrsg.), *The River Rhine - Developement and Management*, pp. 63–77. Koblenz.

Wilson, R., Drury, S., & Chapman, J. (1999). *The Greate Ice Age. Climate change and life*. Routledge.

Wohl, E. (2005). Disconnected rivers: Human impacts to rivers in the United States. In J. Ehlen, W. Haneberg, & R. Larson (Hrsg.), *Humans as Geologic Agents. Reviews in Engineering Geology*, **XVI**, pp. 19–34. Geological Society of America, Boulder, Colorado.

Wolman, M. & Miller, J. (1960). Magnitude and frequency of forces on geomorphic processes. *Journal of Geology*, **68**(1), 54–74.

Wolman, M. G. & Leopold, l. B. (1957). River flood plains: some observations on their formation. *United States Geological Survey Professional Paper*, **282C**, 87–107.

Wunderlich, J. (1998). *Paläoökologische Untersuchungen zur spätglazialen und holozänen Entwicklung im Bereich der Hessischen Senke. Ein Beitrag zur internationalen Global Change-Forschung.* Habilitationsschrift, Philipps-Universität Marburg.

Xu, J. X. (1998). Naturally and anthropogenically accelerated sedimentation in the Lower Yellow River, China, over the past 13,000 years. *Geografiska Annaler*, **80 A**, 67–78.

Zepp, H. (2004). *Geomorphologie. Grundriß Allgemeine Geographie*. UTB, Stuttgart.

Zimmermann, A. (1996). Zur Bevölkerungsdichte in der Urgeschichte Mitteleuropas. In I. Campen, J. Hahn, & M. Uerpmann (Hrsg.), *Festschrift Müller-Beck. Spuren der Jagd - Die Jagd nach Spuren. Tübinger Monographien zur Urgeschichte*, **11**, pp. 46–61.

Zimmermann, A. (2003). Der Beginn der Landwirtschaft in Mitteleuropa. Evolution oder Revolution? In W. Menghin & D. Planck (Hrsg.), *Menschen, Zeiten, Räume - Archäologie in Deutschland*, pp. 133–134. Konrad Theiss Verlag, Stuttgart.

Zimmermann, A., Richter, J., Frank, T., & Wendt, K.-P. (2004). Landschaftarchäologie 2. überlegungen zu Prinzipien einer Landschaftsarchäologie. *Berichte der Römisch-Germanischen Kommission*, **85**, 37–95.

Zolitschka, B., Behre, K.-E., & Schneider, J. (2003). Human and climatic impact on the environment as derived from colluvial, fluvial and lacustrine archives - examples from the Bronze Age to the Migration period, Germany. *Quaternary Science Reviews*, **22**, 81–100.